

**Institut für Hydrologie
der Albert-Ludwigs-Universität Freiburg i. Br.**

Ingo Heidbüchel

**Recharge Processes in Ephemeral Streams Derived from a
Coupled Stream Flow Routing / Groundwater Model -
Application to the Lower Kuiseb (Namibia)**



Diplomarbeit unter Leitung von Prof. Dr. Chr. Leibundgut
Freiburg i. Br., Mai 2007

**Institut für Hydrologie
der Albert-Ludwigs-Universität Freiburg i. Br.**

Ingo Heidbüchel

**Recharge Processes in Ephemeral Streams Derived from a
Coupled Stream Flow Routing / Groundwater Model -
Application to the Lower Kuiseb (Namibia)**

Referent: Prof. Dr. Chr. Leibundgut

Koreferent: Dr. Chr. Külls

Diplomarbeit unter Leitung von Prof. Dr. Chr. Leibundgut
Freiburg i. Br., Mai 2007

Table of Contents

List of Figures	III
List of Tables	VII
List of Tables in the Annex	VII
Acknowledgements	VIII
Summary	IX
Zusammenfassung	XI
1 Introduction	1
1.1 Motivation	1
1.2 Scope	3
1.3 Objectives	4
1.4 Conclusion	5
2 Study Area	6
2.1 Topography	7
2.2 Climate	9
2.3 Geology	10
2.4 Stream flow characteristics	12
2.5 Conclusion	14
3 Methods	16
3.1 Modelling	19
3.1.1 Stream flow routing with DAFLOW	19
3.1.2 Groundwater flow with MODFLOW	21
3.1.3 Flow interactions between stream and aquifer	23
3.2 Sensitivity analysis	24
3.3 Conclusion	27
4 Process Identification	28
4.1 Qualitative observations	28
4.1.1 Depth to water table	29
4.1.2 Aquifer thickness	39
4.1.3 Hydraulic conductivity	43

4.1.4	Hydraulic gradient.....	46
4.1.5	Multiple flood waves	47
4.2	Quantitative budget calculations.....	51
4.3	Conclusion	53
5	Application to the Kuiseb River.....	55
5.1	Input to the groundwater model.....	55
5.1.1	Model area.....	56
5.1.2	Boundary conditions	57
5.1.3	Geology.....	58
5.1.4	Recharge.....	60
5.1.5	Pump wells.....	60
5.1.6	Drain.....	61
5.1.7	Initial conditions	61
5.2	Input to the hydraulic model	61
5.2.1	Cross-sections	62
5.2.2	Input hydrographs	63
5.3	Conclusion	65
6	Results	66
6.1	Natural steady-state.....	66
6.2	Pumped steady-state.....	70
6.3	Pumped transient.....	71
6.4	Conclusion	77
7	Validation and Uncertainty.....	78
8	Overall Conclusions	80
	Bibliography	83
	Annex	86

List of Figures

Figure 0.0: <i>Front of a flash flood in the Kuiseb River (A. Schmitz, 2004)</i>	Cover
Figure 1.1: <i>The modified hydrological cycle of arid regions.</i>	2
Figure 1.2: <i>The drop of average water tables in the aquifer between Swartbank and Rooibank in the years from 1987 to 1999.</i>	3
Figure 1.3: <i>Possible groundwater scenarios.</i>	4
Figure 2.1: <i>Location of the Kuiseb River catchment.</i>	6
Figure 2.2: <i>Satellite image of the study area.</i>	7
Figure 2.3: <i>Aerial photograph of a Kuiseb tributary.</i>	8
Figure 2.4: <i>Longitudinal profile of the Kuiseb in the model area downstream of Gobabeb.</i>	9
Figure 2.5: <i>Elevation information and isohyets for the Kuiseb catchment.</i>	10
Figure 2.6: <i>Geological map of the model area with settlements along the Kuiseb.</i>	11
Figure 2.7: <i>Geological transect through the model area.</i>	12
Figure 2.8: <i>Differences of flood discharge between Gobabeb, Swartbank and Rooibank at variable return periods</i>	13
Figure 2.9: <i>Return periods for discharge volumes and peak discharges at Gobabeb, Swartbank and Rooibank.</i>	14
Figure 3.1: <i>The basic principle of the flood routing routine.</i>	20
Figure 3.2: <i>Schematical illustration of the finite difference grid and the most common boundary conditions used by MODFLOW.</i>	23
Figure 3.3: <i>Streamwater – groundwater interaction in MODFLOW/DAFLOW.</i>	24
Figure 3.4: <i>Test aquifer with stream channel, boundary conditions, observation points and transect position.</i>	25
Figure 3.5: <i>Cross-sectional view of the test aquifer with variable depth to water table and variable aquifer thickness.</i>	26
Figure 3.6: <i>Hydrograph of the synthetic flood wave used as input to the hydraulic model.</i> ...	27
Figure 4.1: <i>Flood hydrographs at four points along the river. Aquifer thickness (100 m); depth to water table (1 m).</i>	29
Figure 4.2: <i>Inflow into and outflow from the storage. Aquifer thickness = 100 m; depth to water table = 1 m.</i>	30
Figure 4.3: <i>Flood hydrographs at four points along the river. Aquifer thickness (100 m); depth to water table (2 m).</i>	31

Figure 4.4: Inflow into and outflow from the storage. Aquifer thickness = 100 m; depth to water table = 2 m.	32
Figure 4.5: Flood hydrographs at four points along the river. Aquifer thickness (100 m); depth to water table (6 m).	32
Figure 4.6: Steepening of the flood wave front due to decreasing infiltration rate.	33
Figure 4.7: Groundwater heads along a transect perpendicular to the stream channel after 50, 100, 200, 400 and 700 hours. Aquifer thickness = 100 m; depth to water table = 6 m; hydraulic conductivity = $1 \cdot 10^{-5}$ m/s.	34
Figure 4.8: Inflow into and outflow from the storage. Aquifer thickness = 100 m; depth to water table = 6 m.	35
Figure 4.9: Flood hydrographs at four points along the river. Aquifer thickness (100 m); depth to water table (10 m).	35
Figure 4.10: Inflow into and outflow from the storage. Aquifer thickness = 100 m; depth to water table = 10 m.	36
Figure 4.11: Flood hydrographs at four points along the river. Aquifer thickness (100 m); depth to water table (20 m).	37
Figure 4.12: Inflow into and outflow from the storage. Aquifer thickness = 100 m; depth to water table = 20 m.	37
Figure 4.13: Flood hydrographs at four points along the river. Aquifer thickness (100 m); depth to water table (35 m).	38
Figure 4.14: Flood hydrographs at four points along the river. Aquifer thickness (100 m); depth to water table (60 m).	39
Figure 4.15: Influence of aquifer thickness on groundwater recharge. Flood hydrographs at different aquifer thicknesses, ranging from 20 to 1000 m. Depth to water table is constantly 10 m.	40
Figure 4.16: Volume of water from identical flood waves that is transported out of the aquifer through the porous matrix after it infiltrated into the saturated storage zone. Comparison of different aquifer thicknesses.	41
Figure 4.17: Comparison of different aquifer thicknesses.	42
Figure 4.18: In- and outflow behaviour at two different aquifer thicknesses ($AqTh = 100$ m compared to $AqTh = 1000$ m). The depth to water table is both times 6 m.	43
Figure 4.19: Flood hydrographs at four points along the river. Aquifer thickness = 100 m; depth to water table = 10 m; hydraulic conductivity = $1 \cdot 10^{-5}$ m/s.	43

Figure 4.20: Hydraulic conductivity of the aquifer changed to $1 \cdot 10^{-2}$ m/s. No steepening of the rising limb anymore. Flood wave does not reach the second kilometer.	44
Figure 4.21: Different groundwater recharge behaviour due to varying hydraulic conductivities.	45
Figure 4.22: Rise of water tables in the immediate vicinity of the stream channel. Aquifer thickness = 100 m; depth to water table (60 m); hydraulic conductivity ($1 \cdot 10^{-5}$ m/s).	45
Figure 4.23: Relative stability of water tables at higher hydraulic conductivities. Aquifer thickness = 100 m; depth to water table (60 m); hydraulic conductivity ($1 \cdot 10^{-2}$ m/s).	46
Figure 4.24: The impact of higher slope on flood waves.	47
Figure 4.25: Double flood wave input to the hydraulic model. Flood hydrographs at four points along the river. Aquifer thickness (60 m); depth to water table (20 m).	48
Figure 4.26: Inflow into and outflow from the storage of two successive flood waves. Aquifer thickness = 60 m; depth to water table = 20 m.	49
Figure 4.27: The process of rapidly mounting groundwater caused by flash floods.	50
Figure 4.28: Hydrological conveyor belt.	50
Figure 4.29: Interdependencies of infiltrated water volume, depth to water table and aquifer thickness. The linear equations for the straight lines are added.	51
Figure 4.30: Linear dependencies of slope and axis intercept for different aquifer thicknesses.	52
Figure 5.1: Dimensions of the model area.	56
Figure 5.2: Elevation distribution in the model area.	56
Figure 5.3: Boundary conditions for the groundwater model.	58
Figure 5.4: Geological subdivisions of the model area.	58
Figure 5.5: The three main groundwater abstraction areas of the Active Kuiseb aquifer: Dorob South, Rooibank A and Swartbank. Location of the pump wells.	61
Figure 5.6: Cross-sections of the stream channel at the weirs of Gobabeb and Rooibank.	62
Figure 5.7: Derivation of the hydraulic geometry parameters at Rooibank. Discharge (Q) is plotted against the width (W) and the cross-sectional area (A) of the channel.	63
Figure 5.8: Synthetic hydrograph used as input to the routing routine.	64
Figure 5.9: Succession of flood waves in the course of the simulation.	64
Figure 6.1: Depth to water table in the alluvial aquifer of the Lower Kuiseb.	66
Figure 6.2: Longitudinal cross-section of the model area.	68
Figure 6.3: Starting point grid for the particle tracking.	68
Figure 6.4: Preferred flow paths in the Lower Kuiseb model area.	69

Figure 6.5: Flow paths originating in the alluvial aquifer.	70
Figure 6.6: Simulation of drawdowns caused by water abstraction from pump wells in the Kuiseb alluvial aquifer.	70
Figure 6.7: Total depletion of the aquifer downstream of Swartbank.	71
Figure 6.8: Rise of groundwater table after a flood event with a duration of 5 days.	72
Figure 6.9: Progression of the recharge front in the Active Kuiseb alluvium after 10, 20 and 46 days. Rise of water tables in meters.	73
Figure 6.10: Flood hydrographs from the transient flood routing at 5 points along the river.	74
Figure 6.11: Behaviour of the aquifer after the flooding ended. Redistribution of infiltrated water. Rise of water tables in meters.	75
Figure 6.12: Comparison of three sets of hydrographs. A: very first floods from the beginning of the simulation; B: last of the 17 flood waves in straight succession; C: flood wave after 9 months of no-flow in the channel.	76

List of Tables

<i>Table 3.1: Comparison of different modelling approaches to groundwater-surface water interaction.....</i>	18
<i>Table 4.1: Slope and axis intercept for the recharge equations at different aquifer thicknesses.</i>	51
<i>Table 5.1: Hydraulic properties of the model area.....</i>	59

List of Tables in the Annex

<i>Annex I: List of abbreviations and symbols.....</i>	86
<i>Annex II: Pump rates of the wells for groundwater abstraction in the Kuiseb alluvium.....</i>	87

Acknowledgements

Mein größter Dank gebührt sicherlich dem Betreuer meiner Diplomarbeit, Christoph Külls. Er hatte immer ein offenes Ohr für meine Fragen und viele gute Ideen, wenn ich mal nicht weiter wusste. Außerdem hat er sich jedes Mal viel Zeit für mich genommen, obwohl er eigentlich überhaupt keine hatte. Danke dafür.

An Herrn Prof. Dr. Leibundgut geht ebenfalls ein Dankeschön für die Vergabe der Diplomarbeit.

Andrea Schmitz war die Kuiseb-Expertin, die immer wusste, woher man fehlende Daten, Karten, Fotos bekommen konnte. Das hat mir sehr weitergeholfen.

Anne Gunkel hat nicht nur einen Großteil meiner Kommafehler korrigiert, sondern mir auch ihr gesamtes, imposantes Informatikfachwissen zur Verfügung gestellt.

Cindy Hugenschmidt danke ich für die positive Kritik und die Ermunterung, die sie mir im Endspurt der Arbeit zuteil werden ließ.

Hannes Leistert konnte mir wertvolle Informationen zu den Fluten im Kuiseb geben, Julian Klaus wusste Bescheid über den Grundwasserzustrom in das Modellgebiet.

Natürlich dürfen meine Mutter und mein Vater hier auch nicht fehlen. Die beiden haben mich nämlich das ganze Studium über rückhaltlos und uneingeschränkt unterstützt.

Deshalb: vielen, vielen Dank!

Summary

This thesis served the purpose of examining the processes that regulate groundwater recharge from ephemeral streams. Infiltrating stream water can contribute a considerable volume of recharge to the aquifer. And since groundwater is often the only source of water in arid regions, it is of vital importance to identify the main controls regulating the infiltration behaviour of flash floods.

A special focus was set on the influence that shallow groundwater tables have on groundwater-surface water interaction.

A coupled modelling approach was chosen to determine the parameters that affect groundwater recharge the most. The selected model consists of a 1-dimensional diffusion wave routing routine for surface water (DAFLOW) and a 3-dimensional finite-differences groundwater model (MODFLOW). The two parts are linked via a leakage term which mainly depends on the gradient from aquifer head to the stage in the stream channel and on the hydraulic conductivity of the riverbed.

Within the scope of a sensitivity analysis, the following parameters were tested:

- Depth to water table
- Aquifer thickness
- Hydraulic conductivity
- Hydraulic gradient

It proved that both **depth to water table** and **aquifer thickness** are linearly related to the volume of groundwater recharge. However, the recharge volume is approximately 100 times more sensitive to a change of depth to water table than to a change of aquifer thickness.

An equation was derived combining the influences of depth to water table and aquifer thickness. With this equation, it is possible to calculate recharge volumes for any combination of the two parameters given certain boundary conditions (such as a constant distribution of hydraulic conductivities).

Two distinct recharge processes that dominate during the passage of a flash flood were identified. The **hydraulic conductivity** determines which one of those two processes takes place:

- In case, the hydraulic conductivity of the riverbed is smaller than the hydraulic conductivity of the aquifer, the infiltration is only restricted by the riverbed and water can disperse freely within the aquifer. That leads to a comparatively uniform rise of the groundwater table throughout the whole aquifer.
- In case, the hydraulic conductivity of the aquifer is smaller than the hydraulic conductivity of the riverbed, only the water tables in close vicinity to the stream

channel tend to rise, whereas aquifer sections further away stay unaffected. This behaviour intensifies if the hydraulic conductivity continues decreasing with distance from the stream channel.

The influence of the **hydraulic gradient** is negligible since it does neither affect the flood duration nor the discharge at a certain point along the river.

Successive flood waves may exhibit a totally different recharge behaviour. If the first flood wave raises the groundwater tables directly below the stream up to the channel elevation, the second flood may not have the possibility to infiltrate anymore. That way, it can occur that flood waves flow on a rather narrow strip of mounted groundwater without infiltrating, leaving large parts of the aquifer uninfluenced.

The Lower Kuiseb area is located in Namibia, in the hyperarid coastal strip next to the Atlantic Ocean. MODFLOW/DAFLOW was set up for this region to simulate groundwater flow and the reaction of the groundwater to flash floods.

- The first step was to simulate the steady-state conditions of the system without artificial water abstraction from pump wells. From this simulation, the natural groundwater levels and the main flow paths of the system were derived. The findings supported the assumption that the paleochannels serve as preferred flow paths under the dune field to the south of the Kuiseb River. However, water that infiltrates into the alluvial aquifer of the Active Kuiseb channel is more likely to move down the alluvium, instead of diverging into one of the paleochannels.
- The second step was the inclusion of pump wells and the observation of the changes to the natural system. It was found that maintaining the current pump rates will eventually deplete the alluvial aquifer downstream of Swartbank completely.
- The third step was to add the stream flow routing routine and to simulate the reaction of the groundwater system to a series of flash floods with median flood properties. The simulation showed that the alluvium reacts quickly and groundwater levels rise until the aquifer is filled completely. However, after the floods have passed, the groundwater levels drop only very slowly and diffusion seems to be the predominant process.

Keywords: Groundwater Recharge – Indirect – Ephemeral Stream– Coupled Model – Stream Flow Routing – Namibia – Kuiseb – Arid

Zusammenfassung

Das Ziel dieser Arbeit war es, den Prozess der indirekten Grundwasserneubildung in Trockengebieten genauer zu untersuchen. Dabei sollte ein spezielles Augenmerk auf Schwallabflüsse gelegt werden, da diese einen großen Anteil an der Grundwasserneubildung arider Gebiete haben können. Schwallabflüsse sind plötzlich auftretende, teils sehr große Abflussereignisse in ansonsten trockenen Flussbetten. Das Infiltrationsverhalten dieser Abflüsse kann stark variieren, je nachdem welche Voraussetzungen im Aquifer herrschen.

Ein gekoppeltes Modell wurde angewandt, um Aussagen darüber zu treffen, welche Parameter die Intensität der Grundwasserneubildung am stärksten beeinflussen. Das Modell besteht aus dem 1-dimensionalen Wellenablaufmodell DAFLOW (basierend auf dem Diffusionswellenansatz) und dem 3-dimensionalen Grundwassermodell MODFLOW. Die beiden Teilmodelle sind verbunden über einen Infiltrationsterm, der hauptsächlich vom Gradienten zwischen Grundwasserspiegel im Aquifer und Wasserstand im Gerinne, sowie von der hydraulischen Leitfähigkeit des Flussbettes abhängt.

Im Rahmen einer Sensitivitätsanalyse, durchgeführt in einem vereinfachten Modellaquifer, wurden folgende Parameter getestet:

- Flurabstand
- Aquifermächtigkeit
- Hydraulische Leitfähigkeit
- Hydraulischer Gradient

Es stellte sich heraus, dass sowohl der **Flurabstand** als auch die **Aquifermächtigkeit** in linearem Zusammenhang zum neugebildeten Grundwasservolumen stehen. Jedoch reagiert das Neubildungs-Volumen ungefähr 100 mal stärker auf eine Veränderung des Flurabstandes, als auf eine Veränderung der Aquifermächtigkeit.

Basierend auf diesen Erkenntnissen konnte eine Gleichung abgeleitet werden, welche für beliebige Flurabstände und Aquifermächtigkeiten die Grundwasserneubildung berechnen kann, wenn bestimmte Randbedingungen gegeben sind (z.B. eine konstante Verteilung der hydraulischen Leitfähigkeiten im Aquifer).

Zwei Arten der Grundwasserneubildung in ephemeren Flüssen konnten unterschieden werden. Dabei bestimmt die **hydraulische Leitfähigkeit** des Aquifers, welche der beiden dominiert:

- Falls die hydraulische Leitfähigkeit des Flussbettes kleiner ist, als die des Aquifers, wird die Infiltration nur durch das Flussbett begrenzt. Dann kann sich das infiltrierte Wasser im Aquifer frei verteilen und der Wasserstand im gesamten Aquifer steigt relativ gleichmäßig an.
- Falls die hydraulische Leitfähigkeit des Aquifers kleiner ist, als die des Flussbettes, so steigen oftmals nur die Wasserstände in der direkten Umgebung des Flusslaufs an, wohingegen weiter entfernte Aquiferkompartimente unbeeinflusst bleiben. Dieses Verhalten verstärkt sich noch, wenn die hydraulische Leitfähigkeit mit zunehmendem Abstand vom Flussbett weiter abnimmt.

Der Einfluss des **hydraulischen Gradienten** auf die Grundwasserneubildung ist unbedeutend, da eine Änderung des Gradienten sich weder auf die Flutdauer noch auf den Abfluss an einem bestimmten Punkt entlang des Flusses auswirkt.

Kurz aufeinanderfolgende Flutwellen können sich unter Umständen völlig verschieden verhalten. Wenn bereits die erste Welle die Grundwasserstände weit angehoben hat, dann ist die Infiltrationsrate der zweiten schon von Beginn an deutlich herabgesetzt. So kann es sein, dass Flutwellen auf einem relativ schmalen Grat deutlich erhöhten Grundwassers fließen, ohne intensiv zur Neubildung beizutragen.

Das Gebiet des unteren Kuiseb befindet sich in Namibia, in einem schmalen, hyperariden Küstenstreifen am Atlantik. Das Modell MODFLOW/DAFLOW wurde für dieses Gebiet eingerichtet, um die dortige Grundwassersituation besser einschätzen zu können, im Besonderen die Reaktion des Grundwassers auf Schwallabflüsse.

- Der erste Schritt bestand aus der Simulation der stationären Situation, wie sie sich ohne künstliche Grundwasserentnahme darstellen würde. Als Ergebnis wurden die natürlichen Wasserstände im Gebiet erhalten, sowie dessen Hauptfließwege. Dadurch konnte die Annahme bestätigt werden, dass die Paläokanäle unter dem Dünenfeld als bevorzugte Fließwege dienen. Jedoch wird Wasser, welches in das Alluvium des Kuiseb infiltriert, mit hoher Wahrscheinlichkeit auch dort bleiben auf seinem Weg stromabwärts. Nur ein Bruchteil des neugebildeten Grundwassers zweigt vom Hauptkanal in einen der Paläokanäle ab.
- Im zweiten Schritt wurden die Entnahmehäuser im Alluvium aktiviert. Im Anschluss wurde beobachtet, welche Auswirkungen die Brunnen auf das natürliche System

haben. Das Resultat sagt die völlige Erschöpfung des alluvialen Aquifers von Swartbank bis zum Meer voraus, falls mit den aktuellen Pumpraten weitergefördert wird.

- Im dritten Schritt wurden schließlich mehrere Flutwellen (mit medianen Fluteigenschaften) durch das Gebiet geleitet. Es zeigte sich, dass das Grundwasser sehr schnell reagiert und bis kurz unter die Oberfläche des Alluviums ansteigt. Nachdem die Fluten allerdings aufhören, verhält sich der nun zum Großteil gesättigte Aquifer äußerst passiv. Die hohen Wasserstände sinken nur sehr langsam wieder ab, wobei sie ebenso zu den Seiten, in die Paläokanäle, wie auch stromabwärts im Alluvium diffundieren.

Schlüsselwörter: Grundwasserneubildung – Indirekt – Periodischer Fluss – Gekoppeltes Modell – Wellenablauf – Namibia – Kuiseb – Arid

1 Introduction

Groundwater is a valuable resource. Especially porous aquifers, like sandy or gravelly alluvial deposits, exhibit certain properties that favour groundwater storage compared to surface water storage in lakes, rivers or artificial reservoirs. On the one hand, the porous aquifer matrix acts as a filter improving the quality of the water flowing through. On the other hand, the storage capacity of aquifers generally exceeds the one of surface water bodies. Moreover, groundwater is more protected from evaporation. Therefore, groundwater often is not subject to major changes in availability throughout the course of one year.

Especially in arid environments, groundwater is the most reliable natural source of drinking water for the population.

1.1 Motivation

Groundwater resources in arid regions tend to be overexploited when either the population itself grows or the population's demands for water grow. If sustainable water use is neglected, the aquifer is often pumped until depletion. Once depleted, aquifers in dry regions require much longer periods of time to fill up again. Under humid conditions one "good" spring might suffice to refill the storage, whereas desert aquifers may need 10,000s of years to reach again initial water levels.

How is it possible to achieve sustainability in water extraction? First of all, to operate sustainably, it is essential to know the recharge rate to the aquifer, for this will equal the maximum average rate of groundwater abstraction.

It is widely accepted that in arid regions, recharge occurs mainly indirectly (HENDRICKS & WALKER 1997), i.e. via the leakage from ephemeral streams. Originating in neighbouring, more humid areas, flash floods enter arid environments and infiltrate into the ground. These so-called transmission losses form the bulk of inflow to the aquifer, often exceeding direct recharge from precipitation. However, it should be noted that subsurface inflow (originally formed by direct recharge) can also make a considerable contribution to groundwater recharge (*Figure 1.1*).

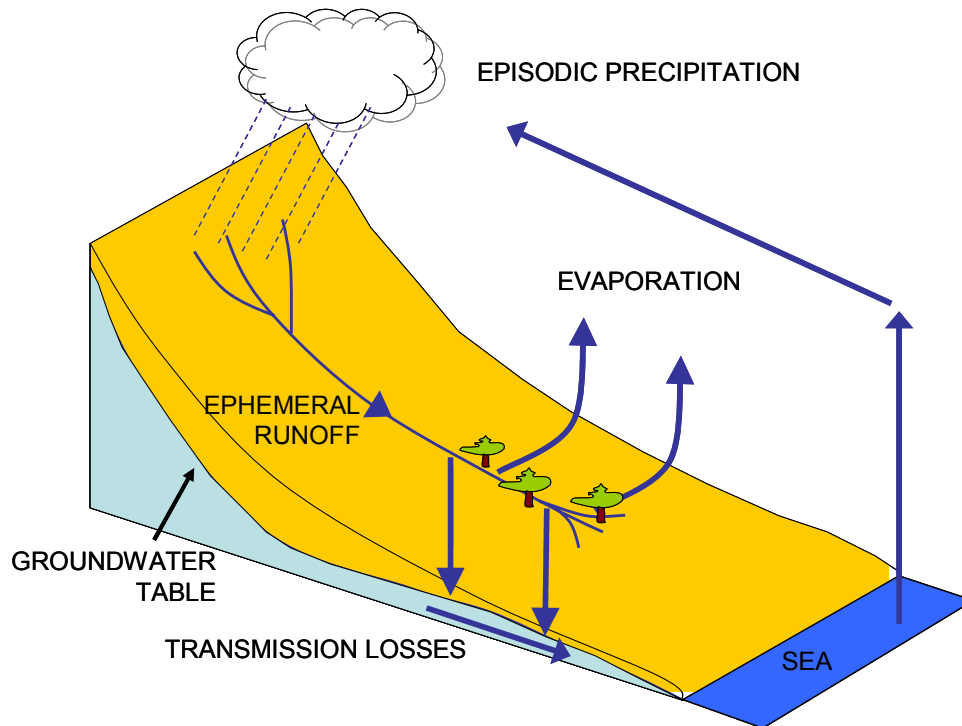


Figure 1.1: *The modified hydrological cycle of arid regions.*

The Lower Kuiseb area is situated at the arid coastal strip of the Namib Desert. Although there is almost no rainfall, the town of Walvis Bay developed just at the outlet of the ephemeral Kuiseb River. The city's supply with drinking water is therefore completely provided by the alluvial aquifers of the Kuiseb. Additionally, the township of Swakopmund and the uranium mine in Rössing receive their water from the Kuiseb aquifer. Around 60,000 people are dependent on this water (MUIÑO 1998). In recent years, a significant drop in groundwater levels was observed (*Figure 1.2*), whereas the demands for water are still growing. It is necessary to alter the groundwater abstraction policy to still be able to use this resource in the future.

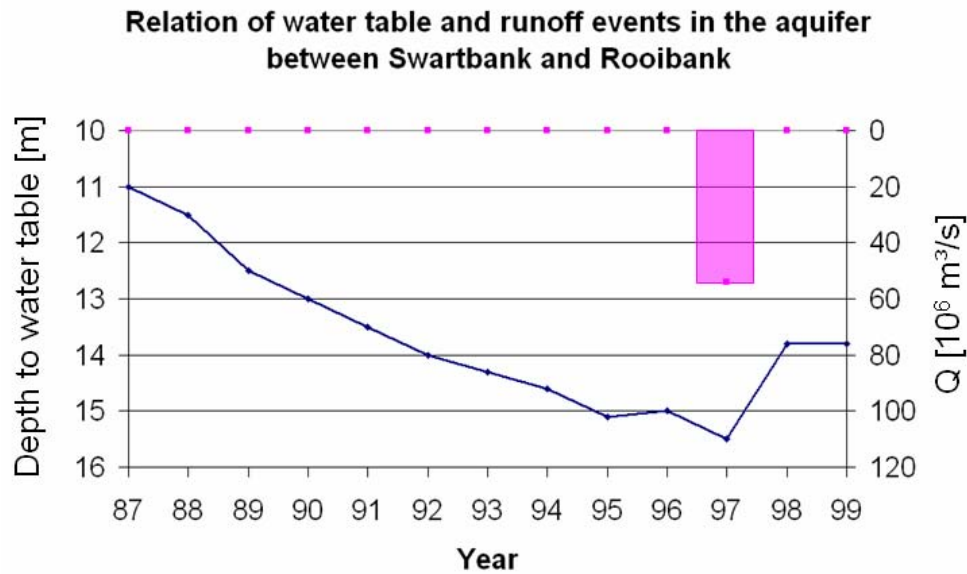


Figure 1.2: The drop of average water tables in the aquifer between Swartbank and Rooibank in the years from 1987 to 1999 (blue line). The influence of a single flood event (pink column) on the groundwater levels is obvious. Modified after NAMWATER (1998).

This thesis intends to make a contribution to solving the water problems in the Lower Kuseb area insofar as it provides new information on the groundwater flow and groundwater recharge processes in the Kuseb channel and in the whole Lower Kuseb area. It also aims at enhancing the general knowledge on the process dynamics of indirect recharge to alluvial aquifers.

1.2 Scope

The alluvial fill of the Kuseb River is rather shallow. Its thickness hardly anywhere exceeds 30 m. Moreover, the Kuseb channel is quite narrow and surrounded by bedrock aquifers on both sides which exhibit hydraulic conductivities some orders of magnitude lower. This leads to a situation, where the depth to water table is small under natural conditions (5 to 15 m in average). Shallow groundwater tables may restrict the recharge from flash floods since the aquifer may fill up rapidly, leaving no more storage space for further infiltration.

This thesis will concentrate on the groundwater - surface water interaction in arid regions with a special focus on the influence of shallow groundwater tables on infiltration. *Figure 1.3* presents three possible scenarios.

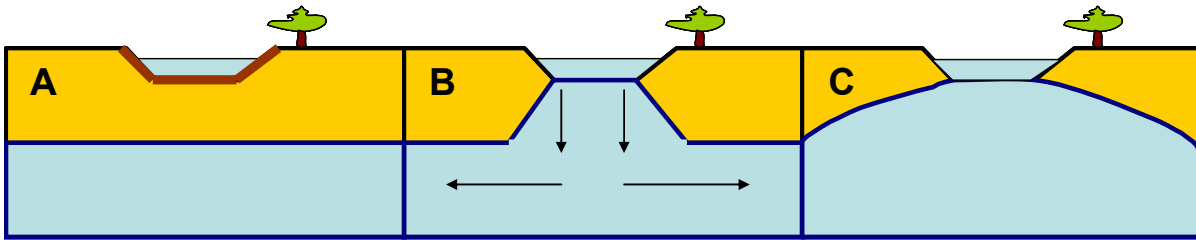


Figure 1.3: A: no infiltration due to low hydraulic conductivity of riverbed, B: high infiltration in highly conductive aquifers, C: impaired infiltration in less conductive aquifers and groundwater mounding below the channel.

1.3 Objectives

The main objectives of this thesis will be:

- to contribute to the understanding of indirect groundwater recharge in general and
- to improve knowledge on the groundwater system of the Lower Kuiseb area.

To examine the special interactions of groundwater and surface water, a coupled model was chosen that combines a stream flow routing routine (DAFLOW) with a groundwater model (MODFLOW). This model offers some advantages over both mere routing and mere groundwater models:

- a) It accounts for changes in groundwater levels that influence the rate of recharge to the aquifer.
 - High water levels may reduce infiltration.
- b) It considers the varying amount of available water for recharge over time and space by routing the flood.
 - Floods can simply “rush by” without infiltrating.

There are also some restrictions to the model. Since it does not include the unsaturated zone between the riverbed and the groundwater surface, all the water that infiltrates into the aquifer is directly added to the groundwater storage. That means the water passes through the unsaturated zone without any time delay and without considering the changing hydraulic conductivity at different saturation levels. However, the lack of the unsaturated zone is not considered to be a big disadvantage, for the aim of this study is to examine the effect of *high* groundwater tables on groundwater recharge.

1.4 Conclusion

The motivation of this study is the fact that groundwater plays a vital role in arid regions and that there is still much room for improvement of the knowledge on recharge processes. Especially the indirect recharge from ephemeral streams is worth to be examined in more detail since it is able to deliver big volumes of water in very short periods of time.

This study will concentrate on groundwater – surface water interaction with a special focus on shallow groundwater tables.

The objectives of this study will be to contribute to the general understanding of indirect groundwater recharge and to improve knowledge on the groundwater system of the Lower Kuiseb area.

2 Study Area

The study area, the Lower Kuiseb, is situated at the Atlantic Coast in the western part of Namibia in the Namib Desert. The catchment of the Kuiseb ranges from the sea, south of the town of Swakopmund, up to the Khomas Highland, near Namibia's capital Windhoek (*Figure 2.1*).

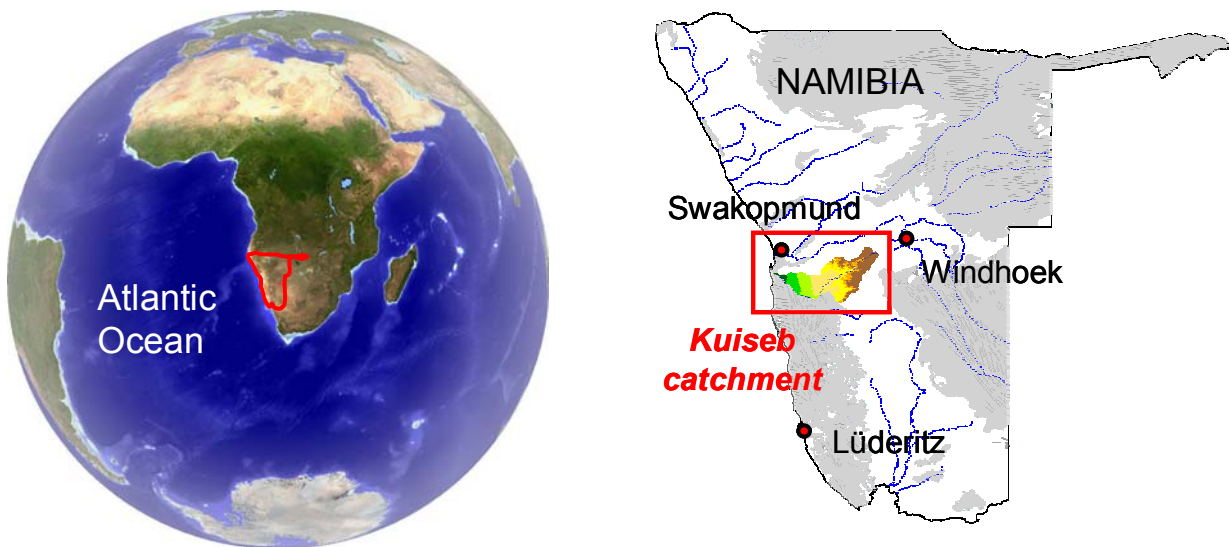


Figure 2.1: Location of the Kuiseb River catchment. It drains into the Atlantic Ocean at the Namibian West Coast.

The study area comprises the last 80 km of the Kuiseb River. The township of Walfish Bay is located at the north-western corner of the area (450,000 E; 7,420,000 N; 5 m a.s.l.), the settlement of Gobabeb at the south-eastern corner (505,000 E; 7,394,000 N; 408 m a.s.l.), (*Figure 2.2*).

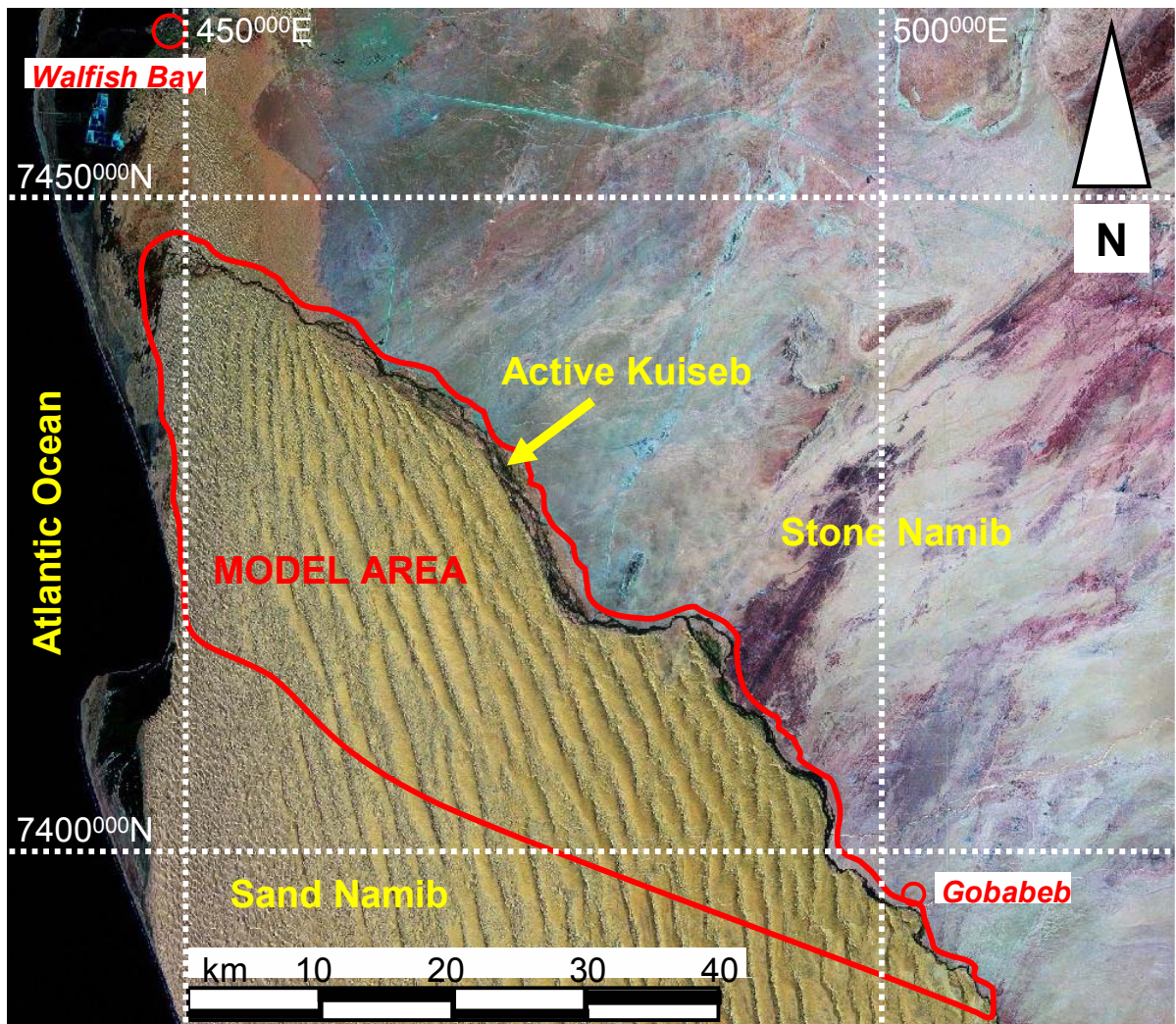


Figure 2.2: Satellite image of the study area. The Lower Kuseib constitutes the border between the Stone Namib to the north-east and the Sand Namib to the south-west.

2.1 Topography

The Kuseib River originates in the mountainous area of the Khomas Highland (up to 2,000 m), to the west of Namibia's capital Windhoek. The whole catchment has a size of approximately 14,700 km², the Kuseib River a length of 560 km. On its way to the sea, the Kuseib crosses an escarpment which separates the interior plateau from the coastal plain. In the middle parts, it incised into the basement rock a deep and narrow canyon with an average width of 20 m and a depth of up to 200 m. The gradient is comparatively steep (0.003 – 0.004 m/m), resulting in the total lack of alluvium at some sections of the channel.



Figure 2.3: Aerial photograph of a Kuiseb tributary. In the background the green belt of the Kuiseb is visible as well as the dunes of the Sand Namib. Picture taken by A. Schmitz, January 2004.

Entering the study area, the slope of the alluvial channel decreases considerably. The floodplain is only slightly inclined towards the sea (1 – 2 m/km) and the channel widens up to 2500 m at some points. Interestingly, the channel of the Kuiseb constitutes the border between the Sand Namib (extensive dune fields) in the south and the Stone Namib (gravel plains, sometimes referred to as Plain Namib) in the north (*Figure 2.3*). This is mainly due to the fact that during flood events, the Kuiseb washes out all the sand that was blown into its channel from the dune area before. For the last 1.8 million years, the Kuiseb prevented the sand Namib to move further northwards. The Stone Namib exhibits low hills of hardrock, partly capped by gravel layers. The sand dunes on the opposite side are mostly of longitudinal type and rise up to 100 m with interdune valleys that can be as wide as 2 km. In the channel there is tree and scrub vegetation forming a green belt in the middle of the surrounding desert, a so-called linear oasis. The vegetation is dependent on the groundwater supply from the alluvial aquifer and it is reported to recede in recent years because of the drop of the groundwater table (MUIÑO 1998).

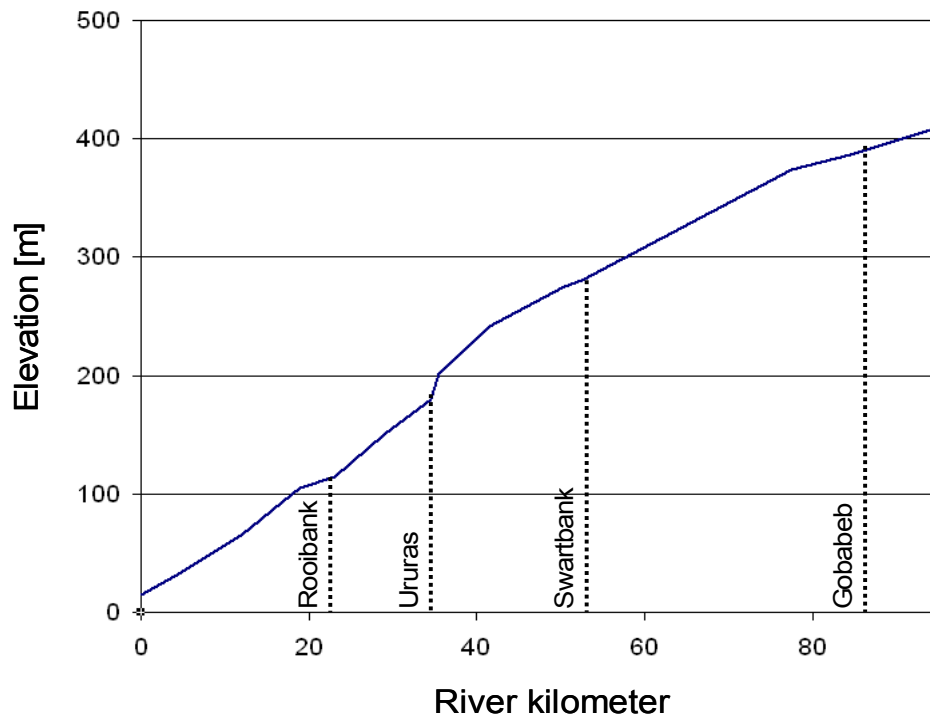


Figure 2.4: Longitudinal profile of the Kuiseb in the model area downstream of Gobabeb. Modified after BLOM (1978).

Approaching the sea, the inclination again rises to ~ 4 m/km, giving the Lower Kuiseb a slightly convex profile (Figure 2.4). In former times, the river split up into two branches downstream of Haob. One branch led to the north to the township of Walfish Bay, the other one drained towards the sea. Because of the flooding danger of Walfish Bay, a flood protection wall was built that nowadays cuts off the northern branch (BLOM 1978). About 5 km from the sea the river channel loses its defined shape. In this area, the floods in recent years were not strong enough to remove the dune sands so that the dunes made their way into the channel. Behind the dune belt, next to the sea, lies a flat, hummocky wetland area with extensive tracts of reeds and salt marshes (MUIÑO 1998).

2.2 Climate

The rainfall at Gobabeb averages 21 mm per year decreasing towards the sea (Figure 2.5). At the coast it has only an average of 14 mm/a. That means that the climate in the study area is hyperarid. The coastal strip of the Namib is the driest part of the country because of the cold Benguela current which flows northwards and parallel to the coast, delivering cold water from the south. This leads to the cooling and consequentially to the subsidence of the air mass in

the whole region. The coastal desert is a temperate desert with annual mean temperatures below 18°C. The relatively low temperatures are caused by the cooling sea breeze.

Another feature of coastal deserts is the high amount of fog precipitation. Especially in the morning hours, the fog can extend inland for more than 100 km and leaves Rooibank with 80 mm and Gobabeb with 31 mm of extra precipitation per year (MUIÑO 1998).

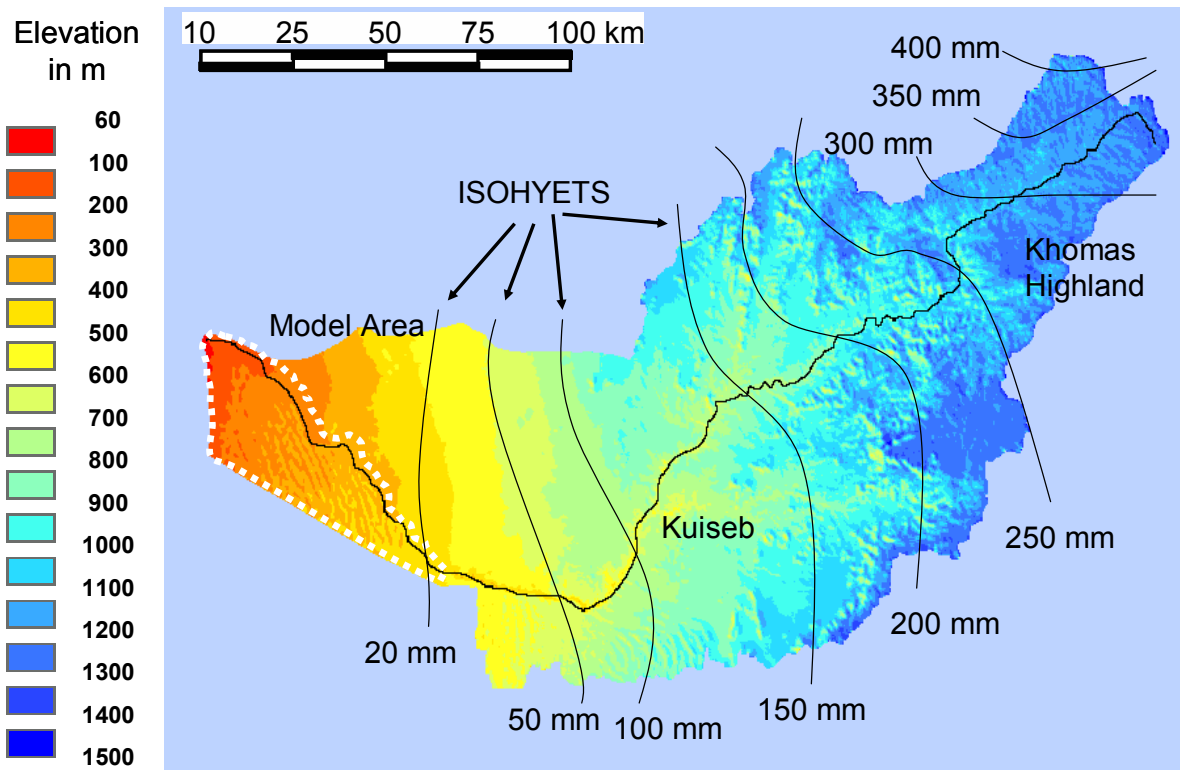


Figure 2.5: Elevation information and isohyets for the Kuiseb catchment. Modified after DWA (1987).

Since the evaporation in the Lower Kuiseb area is extremely high (>3000 mm/a), neither the fog precipitation nor the rare rainfalls contribute to the groundwater recharge. They only satisfy the needs of the specialized flora and fauna (SCHMIDT & PLÖTHNER 1999)

2.3 Geology

Most of the Namib Desert is underlain by Precambrian bedrock (granites, gneisses and schists). To the north of the Kuiseb River, the gravel plains exhibit a deflation surface that is partly covered by a thin layer of coarse gravel.

To the south of the Kuiseb, wide stretches of the Sand Namib basement are formed by Tertiary deposits, the Tsondab sandstone. It was deposited some 20 to 50 thousand years ago under arid conditions on top of the Precambrian bedrock (AIN 1999 in SCHMITZ 2004).

The study area's basement consists mainly of this Precambrian bedrock. However, in some parts (predominantly in the middle between Swartbank and Rooibank) the Tsondab sandstone forms the basement (*Figure 2.6*). This can be explained by the faulting and subsidence of the sandstone into the underlying Precambrian bedrock.

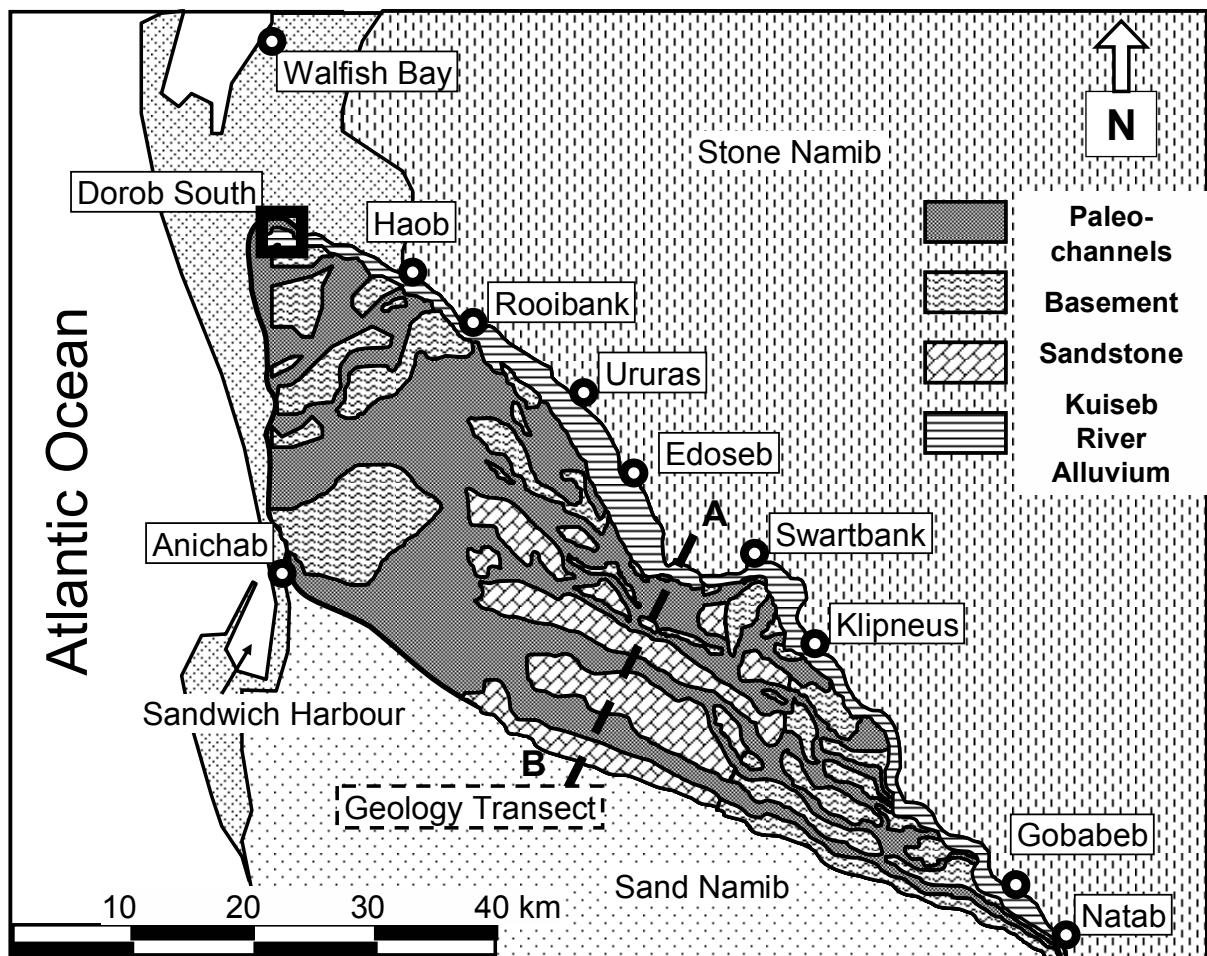


Figure 2.6: Geological map of the model area with settlements along the Kuiseb. Modified after LENZ (1995).

The Kuiseb did not always follow its present course. Starting from Natab and splitting off the active river, it incised a channel network into the respective underlying basement rock. These erosional processes probably took place between the Pliocene and the Pleistocene. Afterwards, this part of the drainage system was filled again with dune sands, gravel, calcareous muds and silts. Today, the former riverbeds are called paleochannels and they are completely covered by dune sands of the Sand Namib. They are expected to be important for

the groundwater movement and storage of the area since the hydraulic conductivities and the porosities of their fillings are much higher than the ones of the surrounding hardrock barriers (*Figure 2.7*).

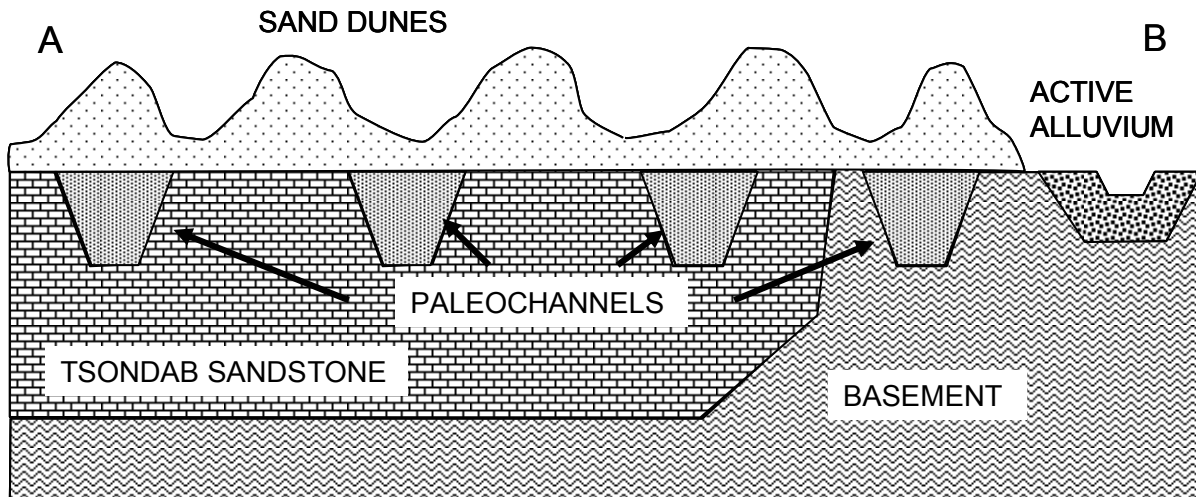


Figure 2.7: Geological transect through the model area. Its location is indicated in Figure 2.6.

The alluvium of the Active Kuiseb has an average thickness of 20 m, at some point up to 50 m. Hardrock outcrops occur at Gobabeb, Narob, Swartbank, Rooibank, Haob and upstream of Klipneus for more than 10 km regularly. These outcrops form barriers for the groundwater and divide the alluvium into several aquifer units. At the same time, they narrow the riverbed to some 100 m or even less (MUIÑO 1998).

2.4 Stream flow characteristics

The Kuiseb River is an ephemeral stream that is dry for most of the year and sometimes even for whole years. Runoff is only generated in the upper parts of the catchment, where there falls enough precipitation. Only if the volume of runoff generated is large enough, it also reaches the Lower Kuiseb area without completely evaporating or infiltrating into the ground before. These so-called flash floods are relatively short-lived and highly variable in size, duration and occurrence. Between the years 1836 and 2007 only 16 flash floods reached the sea (the last time during the rainy season 1962/63). Since 1963 all floods suffered that much transmission losses on their way that they went no further than Rooibank (WNNR 1984 in SCHMITZ 2004).

The transmission losses are highest in the upper part of the area between Gobabeb and Swartbank, as can be derived from *Figure 2.8* (KÜLLS & LEISTERT 2006). However, this is most probably only due to the higher amounts of runoff that reach the stream section between Gobabeb and Swartbank.

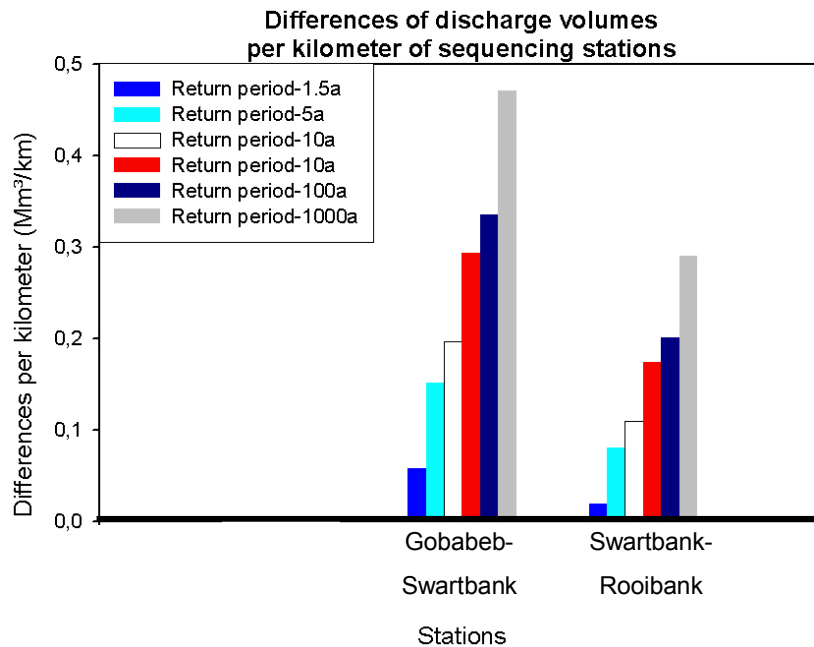


Figure 2.8: Differences of flood discharge between Gobabeb, Swartbank and Rooibank at variable return periods (serves also as a measure for transmission losses). Modified after KÜLLS & LEISTERT (2006).

The annualities of discharge volumes and peak discharges vary considerably between the gauging stations, especially in the Lower Kuiseb area where most of the transmission losses occur. *Figure 2.9* gives examples. Both the discharge volumes and the peak discharges decrease in downstream direction. At Gobabeb the volume of an event that statistically occurs every tenth year is 10 million m³, at Swartbank 3 million m³ and at Rooibank only 0.15 million m³. The same applies to the peak discharges: Gobabeb – 90 m³/s, Swartbank 25 m³/s, Rooibank – 0.9 m³/s (for a ten year event).

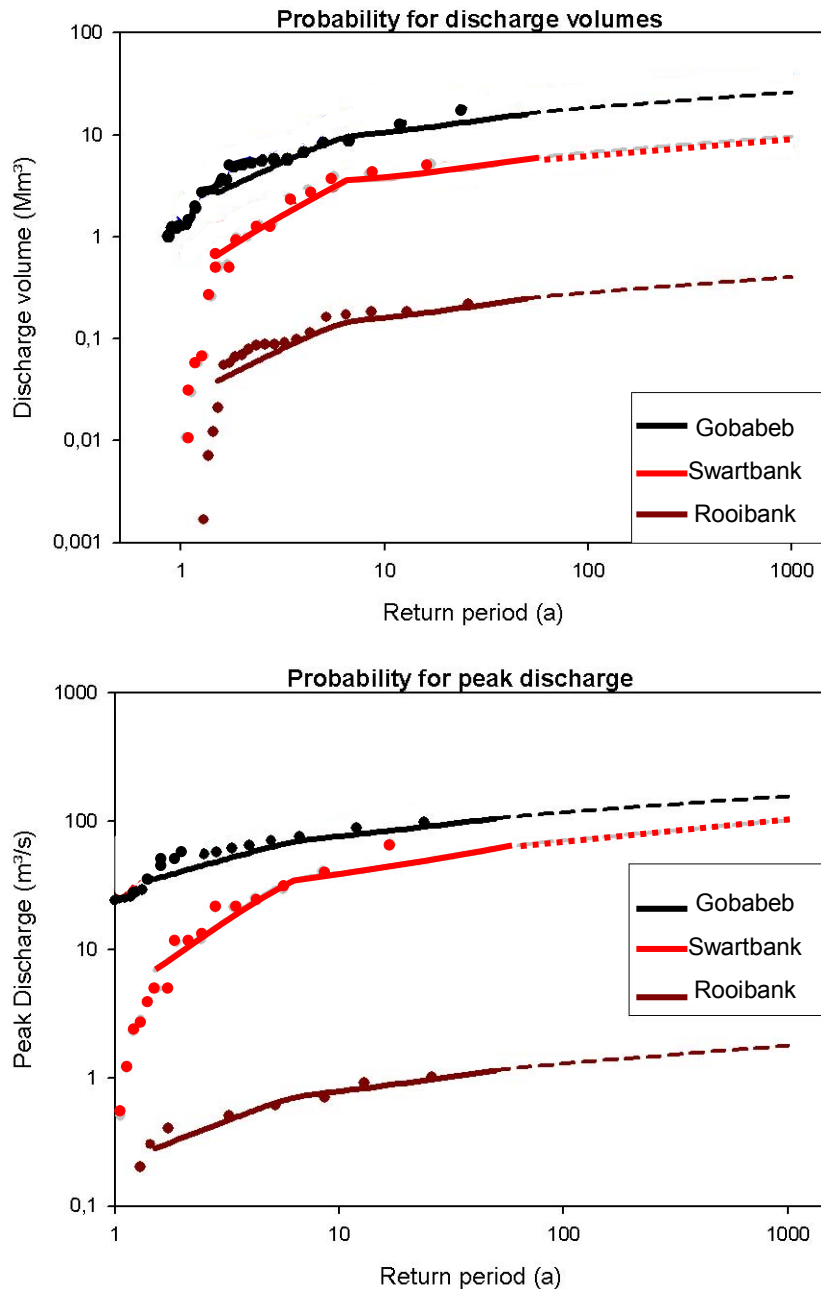


Figure 2.9: Return periods for discharge volumes and peak discharges at Gobabeb, Swartbank and Rooibank. Modified after KÜLLS & LEISTERT (2006).

2.5 Conclusion

The study area is situated at the West Coast of Namibia in the narrow hyperarid strip close to the city of Walfish Bay. The area is approximately 80 km long and 25 km wide. The southern part of the area is covered by dune sands, on the northern boundary lies the channel of the Active Kuiseb. The dune sands cover former, now abandoned paleochannels that are filled with material of relatively high hydraulic conductivity compared to the underlying gneissic

and granitic bedrock. The Kuiseb River is an ephemeral stream that originates in the highlands to the east of the area. Flash floods cause transmission losses in the alluvium of the river. The highest losses occur between Gobabeb and Swartbank. The alluvial aquifer is rather shallow, rarely exceeding 20 m.

3 Methods

Different approaches exist to model streamwater-groundwater interaction. Most of them combine a stream flow routing routine with a groundwater model and link the two via a leakage term.

FREEZE (1972) was one of the first to link a one-dimensional (1-D) stream flow routing model to a three-dimensional (3-D) groundwater model. The stream flow part solved the full shallow water equations; the groundwater routine used the 3-D Richards equation for variably saturated flow. The two parts were linked by a linear time-delay algorithm, not considering the hydraulic conductivity of the riverbed. The main goal of this work was to better understand the influence of subsurface flow on surface runoff.

ABBOTT ET AL. (1986) developed the *Système Hydrologique Européenne* (SHE). This model is highly physically-based and includes modules for the modelling of different hydrological processes: interception, evapotranspiration, snowmelt, channel flow, overland flow, flow in the unsaturated zone and flow in the saturated zone. Channel and overland flow are not modelled the same way. For the channel flow, a 1-D diffusion wave approach is used, the overland flow is modelled with a 2-D diffusion wave approach. The subsurface is also divided into two compartments, the unsaturated zone (1-D Richards equation) and the saturated zone (2-D Bossinesq equation). That means, in the unsaturated zone water can only move vertically up or down, and the saturated zone consists of a single layer that must be unconfined. The leakage to and from the aquifer can be restricted by the introduction of a variable riverbed conductivity.

The modular 3-D finite-difference groundwater model MODFLOW was developed by MCDONALD & HARBAUGH in 1988. It is mainly designed to model the saturated zone. Therefore, it does not include the unsaturated zone and applies the 3-D Bossinesq equation for the saturated groundwater flow. A stream flow routing package is also included, but it is no true surface water flow model and limited to steady flow in rectangular, prismatic channels. Consequently, it does not calculate the flood wave propagation properly.

PERKINS & KOUSSIS (1996) aimed at enhancing the surface-groundwater interaction of MODFLOW by replacing the STREAM package with a 1-D diffusive wave routing scheme. This model uses the Muskingum-Cunge method to solve the equations for the flood routing. The leakage from the river is dependent on the head difference and on the hydraulic conductivity of the riverbed.

SWAIN & WEXLER (1996) also replaced the STREAM package with a 1-D diffusion wave model, BRANCH. This stream flow routing routine allows the river to run dry and rewet again; a feature that is necessary for the modelling of ephemeral streams. NEMETH ET AL. (2003) introduced an alternate leakage expression to MODBRANCH, the reach transmissivity. Instead of calculating the amount of leakage from the hydraulic conductivity and the thickness of the riverbed, two new parameters are used: the transmissivity of the underlying aquifer and the length of the affected river section. This allows for uneven riverbed geometry.

In 1999 VANDERKWAAK integrated surface and subsurface flow processes (and solute transport) into one coherent framework. Within the Integrated Hydrology Model (InHM) a 2-D diffusion wave accounts for the surface water flow, whereas the saturated and the unsaturated zones are both modelled with a 3-D Richards equation approach. The subsurface space is divided into two continua – the first one representing the soil matrix and the second one describing the macropores. Both continua run parallelly. The linkage from subsurface to surface flow is managed by a 1-D variation of the Darcy equation for unsaturated conditions. The advantage of this approach is that it takes into account the variable saturation of the aquifer (i.e. the changing hydraulic conductivity of the riverbed) and not only the hydraulic head difference. It also eliminates the iterative coupling of surfacewater and groundwater by the assembling and solving of one system of discrete algebraic equations, so that water and solute fluxes between continua are determined as part of the solution.

THOMS (2003) modified MODFLOW to simulate 3-D variably saturated flow using the Richards equation. The overland flow is also modelled within MODFLOW by using the uppermost layer as a 2-D “routing” layer. This is achieved by treating it like a saturated soil layer with no storage properties. Its governing equations are converted into the kinematic flow approximation for overland flow. The vertical hydraulic conductivity is constant and equal to the saturated conductivity of the cell below. The horizontal hydraulic conductivity is derived from the Darcy-Weisbach equation for steady-uniform surface flow. Water will be conducted vertically until the hydraulic head exceeds the ground surface elevation, then the horizontal conductance parameters will be activated.

NISWONGER & PRUDIC (2004) aimed to enhance the MODFLOW model by adding a vadose zone that links the surface routing package (STR1) to the groundwater routine. The flow through the vadose zone is calculated by a 1-D kinematic wave solution to the Richards equation. The advantage of this approach is that flow through and storage in the vadose zone are explicitly considered. However, the STR1 package is only able to model steady, uniform

flow in the stream, i.e. the volume of water in the surface channel will not be modified during the simulation. The leakage from the stream to the vadose zone is dependent on the aquifer head, the saturation in the vadose zone, the streambed conductivity and the river stage.

For this study a model was chosen that combines a 1-D diffusion wave routine (DAFLOW) with the 3-D groundwater model MODFLOW. The linkage is done via a simple hydraulic head gradient / riverbed conductivity relation. The model is discussed in more detail in the next section. *Table 3.1* resumes the important features of the introduced modelling approaches.

Table 3.1: Comparison of different modelling approaches to groundwater-surface water interaction.

Name of Model / Name of Author	Surface	Leakage	Unsaturated Zone	Saturated Zone
Freeze, 1972	1-D full shallow water equations	Head gradient with linear time-delay algorithm	3-D Richards	3-D Richards
SHE, 1986	Overland: 2-D diffusion wave, Channel: 1-D diffusion wave	Head gradient with riverbed conductivity	1-D Richards	2-D Bossinesq
Perkins, 1996	1-D diffusion wave, Muskingum-Cunge	Head gradient with riverbed conductivity	-	3-D Bossinesq (MODFLOW)
MODBRANCH, 1996	1-D diffusion wave (BRANCH)	Reach transmissivity	-	3-D Bossinesq (MODFLOW)
InHM, 1999	2-D diffusion wave	1-D Darcy, variably saturated	3-D Richards, dual continua	3-D Richards, dual continua
Thoms, 2003	2-D kinematic wave	Head gradient, soil properties	3-D Richards	3-D Richards
Niswonger, 2004	Steady, uniform flow (STR1 package)	Head gradient with riverbed conductivity, saturation of vadose zone	1-D kinematic wave	3-D Bossinesq (MODFLOW)
MODFLOW / DAFLOW, 1999	1-D diffusion wave (DAFLOW)	Head gradient with riverbed conductivity	-	3-D Bossinesq (MODFLOW)

3.1 Modelling

The stream flow routing - groundwater model MODFLOW/DAFLOW was developed by JOBSON & HARBAUGH in 1999. It consists of the DAFLOW model (designed by JOBSON in 1989) and the MODFLOW model (designed by McDONALD & HARBAUGH in 1988). The coupling of the two models was accomplished by splitting the DAFLOW code into subroutines that are consistent with the modular structure of MODFLOW. This was done in such a way that multiple DAFLOW steps can be run iteratively within a MODFLOW time step.

MODFLOW/DAFLOW was chosen to model the groundwater situation in the Lower Kuseb area because of the following reasons:

- It is based on the accepted and well-tested groundwater model MODFLOW.
- It is able to route a flood wave.
- It allows the riverbed to run dry.
- It does not require too explicit data for the river geometry.
- It is not necessary to model the unsaturated zone in the Lower Kuseb area because the groundwater table is naturally high and the focus of this work is to evaluate the influence of high water tables on groundwater recharge (and especially on its restriction).

3.1.1 Stream flow routing with DAFLOW

The Saint-Venant equations are differential equations for modelling the stream flow of 1-D unsteady flow in open channels. They form the basis for the diffusion analogy method used by DAFLOW and consist of the continuity of mass equation (1) and the continuity of momentum equation (2):

$$\frac{\partial Q}{\partial X} + \frac{\partial A}{\partial t} = 0 \quad (1)$$

$$\frac{1}{g} \frac{\partial U}{\partial t} + \frac{U}{g} \frac{\partial U}{\partial X} + \frac{\partial Y}{\partial X} + S_f - S_o = 0 \quad (2)$$

Q is discharge, X is distance along the channel, A is cross-sectional area of flow, t is time, g is acceleration of gravity, U is velocity, Y is depth, S_f is friction slope and S_o is streambed slope. The diffusion wave approach disregards the two inertia terms of the continuity of momentum equation and leaves us with equation (3)

$$\frac{\partial Y}{\partial X} + S_f - S_o = 0 \quad (3)$$

After the introduction of a wave diffusion coefficient D_f , the rearrangement of equation (3) (for details see JOBSON & HARBAUGH 1999) and its substitution into the continuity of mass equation (1), the diffusive wave form of the flow equation is derived (4):

$$\frac{\partial Q_s}{\partial t} + C \frac{\partial Q_s}{\partial X} - D_f \frac{\partial^2 Q_s}{\partial X^2} = 0 \quad (4)$$

where Q_s is the flow under steady uniform flow conditions and C is the translation coefficient (or celerity) that determines the speed of the moving wave. Each time step, DAFLOW calculates the advection of the wave and its diffusion subdividing the stream into reaches of steady uniform flow separated by transitions of unsteady flow (*Figure 3.1*).

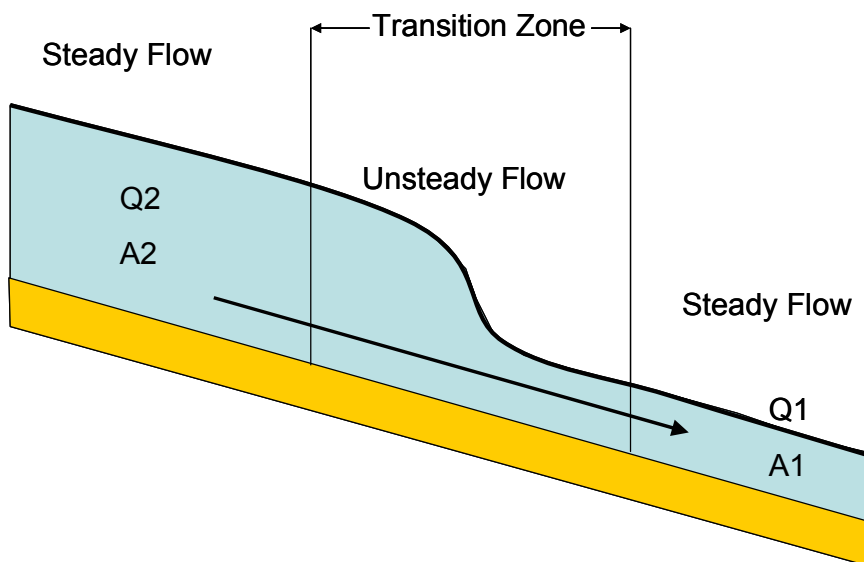


Figure 3.1: The basic principle of the flood routing routine – steady uniform flow subreaches connected by a transition of uniformly progressive flow. Modified after JOBSON & HARBAUGH (1999).

DAFLOW uses a special approach to include the channel geometry into its calculations. It is not necessary to specify cross sections of the channel in the input files. Channel geometry is expressed by two empirical equations (5) and (6) that were found to define the shape of the riverbed:

$$A = A0 + A1 * Q_s^{A2} \quad (5)$$

A is the cross-sectional area of natural channels, A1 and A2 are constants called the hydraulic-geometry coefficient and exponent for area and A0 is the average cross-sectional area at zero flow.

For the width of the channel:

$$W = W1 * Q_s^{W2} \quad (6)$$

W is the top width of natural channels, W1 and W2 are constants called the hydraulic-geometry coefficient and exponent for width.

Hydraulic-geometry exponents have been found to maintain relatively consistent values both along a stream and between streams (JOBSON 1989, BEVEN & KIRKBY 1993). The average values for A2 and W2 are 0.66 and 0.26 respectively (LEOPOLD & MADDOCK 1953, STALL & YANG 1970, JOBSON 1989).

DAFLOW yields the most accurate results in rivers, in which the slope is not too small. In general, the time step size must increase if flat terrain should be modelled. In case of one-hour time steps, a slope of 0.0003 m/m or higher is appropriate.

3.1.2 Groundwater flow with MODFLOW

MODFLOW is based on the 3-D groundwater-flow equation (9) that consists of the continuity equation (7) and the Darcy equation for saturated conditions (8):

$$\frac{\partial q_x}{\partial x} + \frac{\partial q_y}{\partial y} + \frac{\partial q_z}{\partial z} = -S_s \frac{\partial h}{\partial t} + R \quad (7)$$

$\partial q / \partial x$ is the change of flow rate in the respective direction in space (x, y, z), $\partial h / \partial t$ is the change of hydraulic head with time, S_s is the specific storage and R stands for all other sources and sinks.

$$\frac{Q}{A} = K * \frac{\partial h}{\partial x} \quad (8)$$

Q is the flow through the cross-sectional area A, K_{aq} is the hydraulic conductivity of the aquifer and $\partial h / \partial x$ the hydraulic gradient.

$$\frac{\partial}{\partial x} \left(K_x \frac{\partial h}{\partial x} \right) + \frac{\partial}{\partial y} \left(K_y \frac{\partial h}{\partial y} \right) + \frac{\partial}{\partial z} \left(K_z \frac{\partial h}{\partial z} \right) = S_s \frac{\partial h}{\partial t} - R \quad (9)$$

MODFLOW uses finite differences and boundary conditions to solve this equation for groundwater flow in three dimensions. The aquifer is divided into rectangular cells and the hydraulic head is calculated in every single cell for each time step (*Figure 3.2*).

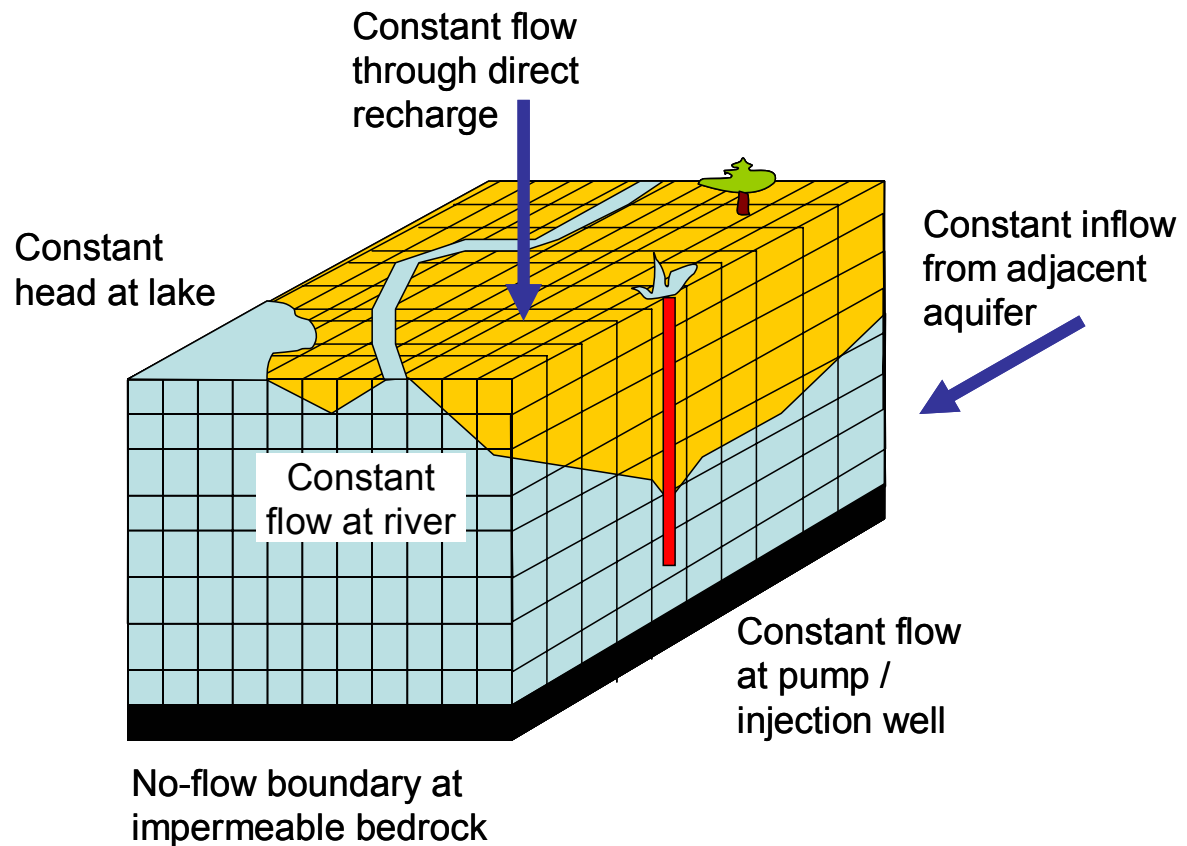


Figure 3.2: Schematical illustration of the finite difference grid and the most common boundary conditions used by MODFLOW. Modified after MCDONALD & HARBAUGH (1988).

3.1.3 Flow interactions between stream and aquifer

The leakage from or to the stream is calculated for each MODFLOW cell separately. The necessary parameters are (see *Figure 3.3*):

K_{be}	→	hydraulic conductivity of the riverbed
L	→	length of the stream reach in hydraulic connection with the aquifer cell
W	→	average width of the stream along the aquifer cell
H	→	head of the aquifer in the cell
Y	→	average depth of stream in the subreach crossing the aquifer cell
B_e	→	average elevation of the riverbed crossing the aquifer cell
B_t	→	thickness of the streambed

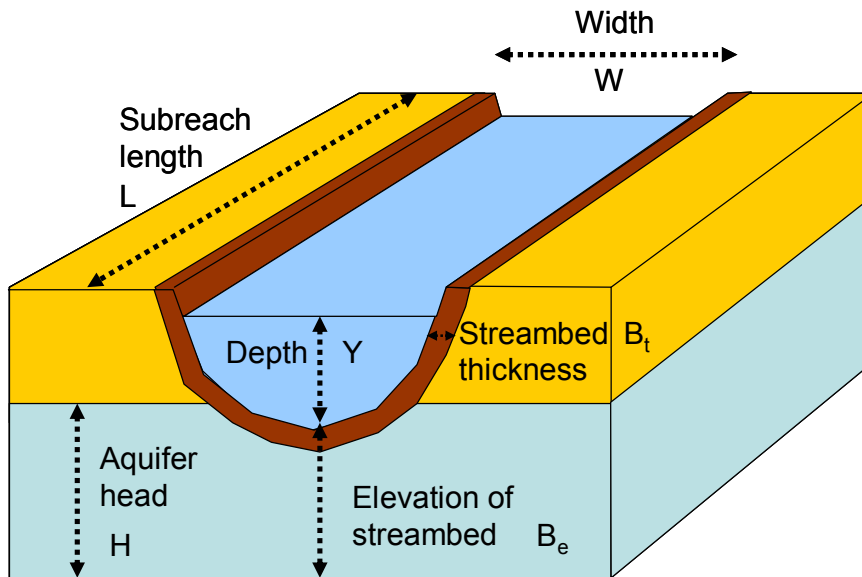


Figure 3.3: Streamwater – groundwater interaction in MODFLOW/DAFLOW. Modified after JOBSON & HARBAUGH (1999).

These parameters are either calculated by the model (W , H , Y) or directly entered into the input files (K_{be} , L , B_e , B_t) for each subreach.

The leakage equation (10) computes the seepage flow (S_{ep}) following Darcy's law:

$$S_{ep} = \frac{K_{be} * L * W (H - Y - B_e)}{B_t} \quad (10)$$

3.2 Sensitivity analysis

To gain a better understanding of the basic processes that affect groundwater recharge in arid environments, a sensitivity analysis was carried out. The coupled groundwater / surface water model MODFLOW/DAFLOW was applied to a test aquifer. The geometry of the hypothetical aquifer was chosen to be symmetrical and as simple as possible. The basic properties were as follows:

- Width: 2100 m, divided into 21 columns (each column 100 m)
- Length: 4100 m, divided into 41 rows (each row 100 m)
- Number of Layers: 1 layer (with variable thickness)
- Specific yield: 20 %

The river was a straight line, with a length of 4100 m, crossing the aquifer in the middle of column 11, e.g. exactly in the centre. The bed conductivity was supposed to be 0.0001 m/s and the bed thickness 1 m. The bottom of the riverbed lay 2 m below the aquifer surface (Figure 3.4).

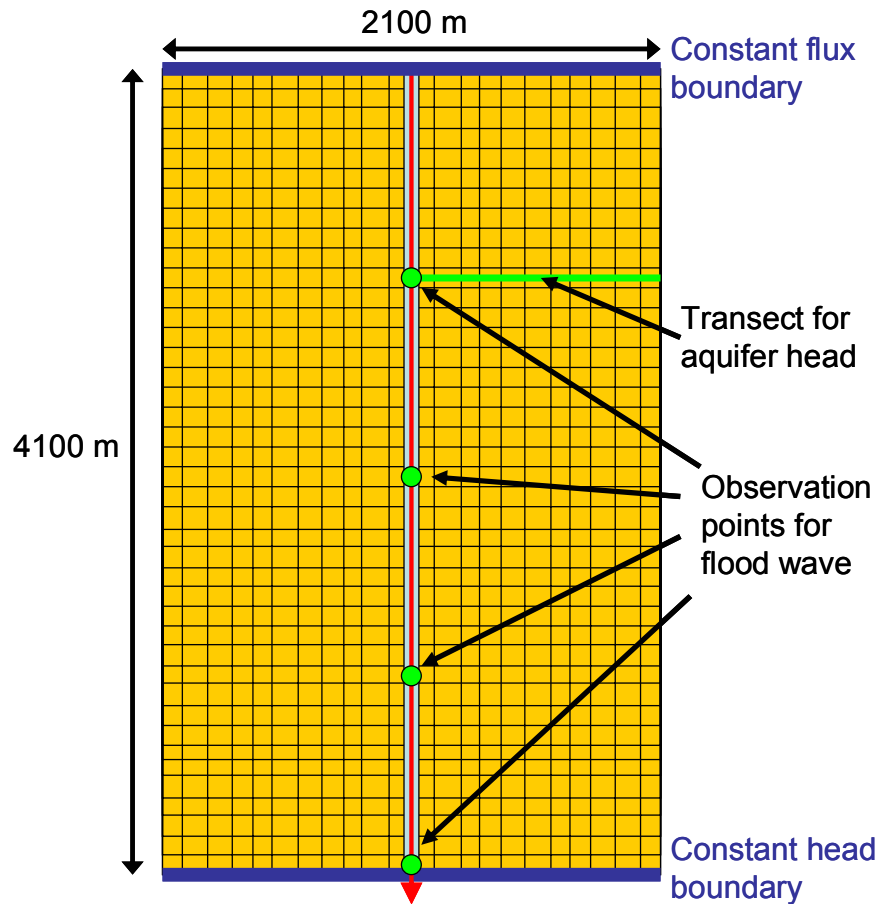


Figure 3.4: Test aquifer with stream channel, boundary conditions, observation points and transect position.

The hydraulic geometry coefficients were

$$A_0 = 0; \quad A_1 = 3.87; \quad A_2 = 0.66$$

$$\text{and} \quad W_1 = 26.6; \quad W_2 = 0.26.$$

The values of A_2 and W_2 are typical average values and the value 0 for A_0 indicates that no ponding occurs at no-flow conditions.

Variable parameters included (see also Figure 3.5):

- Depth to water table: 1 m; 2 m; 6 m; 10 m; 20 m; 60 m; 100 m
- Aquifer thickness: 2 m; 6 m; 10 m; 20 m; 35 m; 60 m; 100 m; 1000 m
- Hydraulic conductivity: 10^{-2} m/s; 10^{-5} m/s

- Hydraulic gradient: 0.0012 m/m; 0.025 m/m
- Flood wave input: single peak; double peak

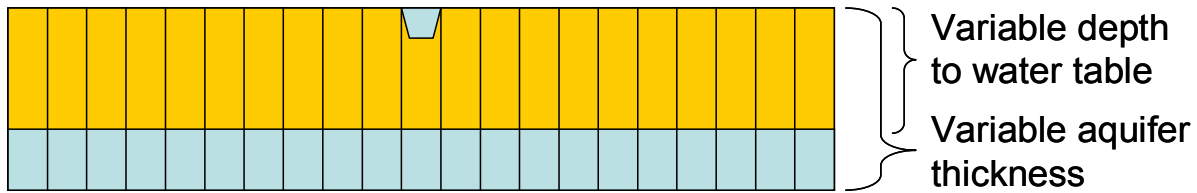


Figure 3.5: Cross-sectional view of the test aquifer with variable depth to water table and variable aquifer thickness.

To guarantee a constant water table in the inclined aquifer, a constant flux boundary was assigned to the first row of cells in the highest part of the aquifer. The volume of water entering through this boundary was calculated with the rearranged equation of Darcy (11):

$$Q = A * K * \frac{\partial h}{\partial x} \quad (11)$$

A is the cross-sectional area of the saturated aquifer equalling the width of the aquifer (a constant value: 2100 m) times the saturated thickness of the aquifer (being variable). K_{aq} is the saturated hydraulic conductivity of the aquifer and $\partial h / \partial x$ its hydraulic gradient. That means all the parameters in the equation are variable and a new inflow has to be calculated for any of the parameter combinations.

A constant head was assigned to the lower boundary of the aquifer. The head was set to the respective depth to water table of the particular simulation.

The flood wave input has a triangular form, where the rising limb of the wave captures one third of the hydrograph and the falling limb the other two thirds. The total volume of water amounts to 1.6 million m^3 (Figure 3.6). The peak discharge of the flood is $7.5 m^3/s$ and the total duration 5 days.

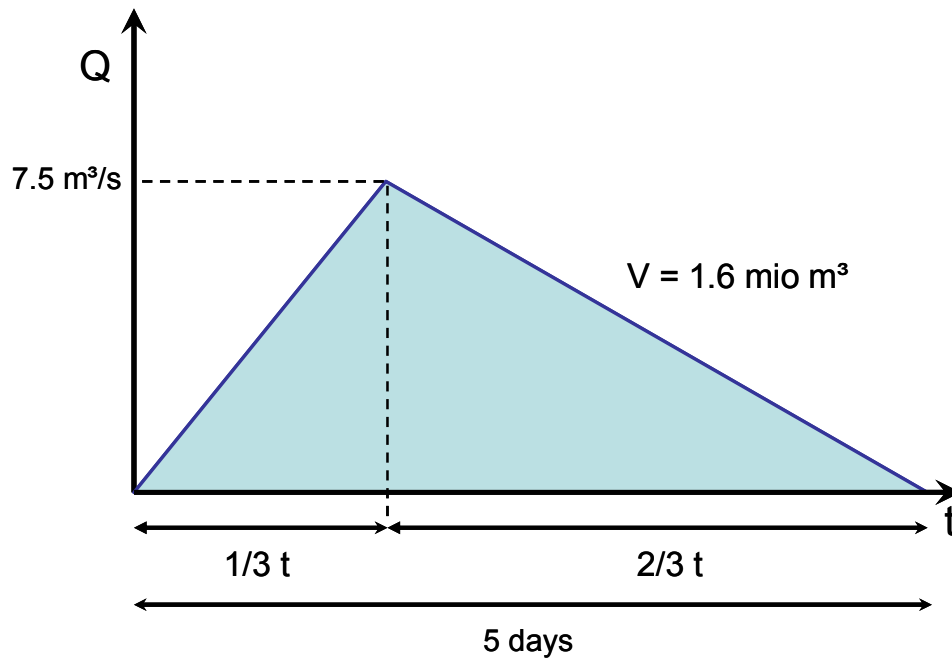


Figure 3.6: Hydrograph of the synthetic flood wave used as input to the hydraulic model.

A double wave input was created to examine the behaviour of the aquifer when confronted with multiple floods in quick succession. It consists of 2 of the above-named flood waves that pass the aquifer one after the other with only 3 hours of no-flow in between them. The accumulated volume of the flood rises to 3.2 million m³.

3.3 Conclusion

To model surface water – groundwater interaction the model MODFLOW/DAFLOW was selected. It combines the 1-dimensional diffusion wave routing routine for surface water (DAFLOW) and the 3-dimensional finite-differences groundwater model MODFLOW. The two parts are linked via a leakage term which mainly depends on the gradient from aquifer head to the stage in the stream channel and the hydraulic conductivity of the riverbed.

The model was chosen because it is able to route a flood wave and allows the riverbed to run dry. Moreover, it considers the influence of high water tables on the infiltration behaviour of flood waves.

Before applying the model to the Kuiseb area, a sensitivity analysis was conducted in a geometrically simple aquifer. This was done in order to gain some knowledge on which parameters influence recharge most. The parameters tested included depth to water table, aquifer thickness, hydraulic conductivity and slope.

4 Process Identification

To evaluate the impact of the variable input parameters on groundwater recharge, numerous model runs were conducted. Each run, all the parameters but one were held steady. Thus, the differing recharge behaviour could only be attributed to the changing parameter. The model was run 720 1-hour time steps, that equals 30 days in total. The findings are described for each parameter separately below.

4.1 Qualitative observations

To obtain a better understanding of the basic processes in the aquifer, the research was focussed on the analysis of 3 hydrological features:

1) *Flood wave propagation*

The shape of the flood wave was monitored at four points along the riverbed. They were positioned 1 km, 2 km, 3 km and 4 km downstream of the river inlet respectively.

2) *Profiles of aquifer head*

Transects that cut the aquifer perpendicular to the river were used to observe the change of groundwater head in time and space.

3) *Storage change*

The alternating infiltration and exfiltration rates tell something about the change of storage content in the aquifer. Finally, budget calculations should allow a quantitative analysis of the impact of the different parameters on groundwater recharge.

The first series of runs was conducted with a hydraulic conductivity of the aquifer of $1 \cdot 10^{-5}$ m/s and a slope of 0.0012 m/m. Afterwards, the hydraulic conductivity was changed to $1 \cdot 10^{-2}$ m/s and finally the gradient was set to 0.025 m/m.

4.1.1 Depth to water table

The depth from the aquifer surface to the water table is a measure for the empty storage space available for groundwater recharge. Therefore, it is supposed to have a rather big influence on how much water infiltrates during the passage of a flood wave. How do the flood hydrographs at different points along the river change their shape when the depth to water table rises?

Figure 4.1 shows the situation where the aquifer thickness is 100 m and the depth to water table is 1 m. The instantaneous and rapid rise of the hydrographs right at the beginning of the simulation is caused by the incision of the riverbed into the aquifer. It lies 2 m below the aquifer surface and hence 1 m below the groundwater table. Therefore, in the first hours the river acts as a drain lowering the water table in the bordering overbank area. Afterwards, nearly the whole flood wave is routed through the channel without infiltrating. The peak flow stays the same at every monitoring station. This is not surprising since the aquifer is saturated from the beginning.

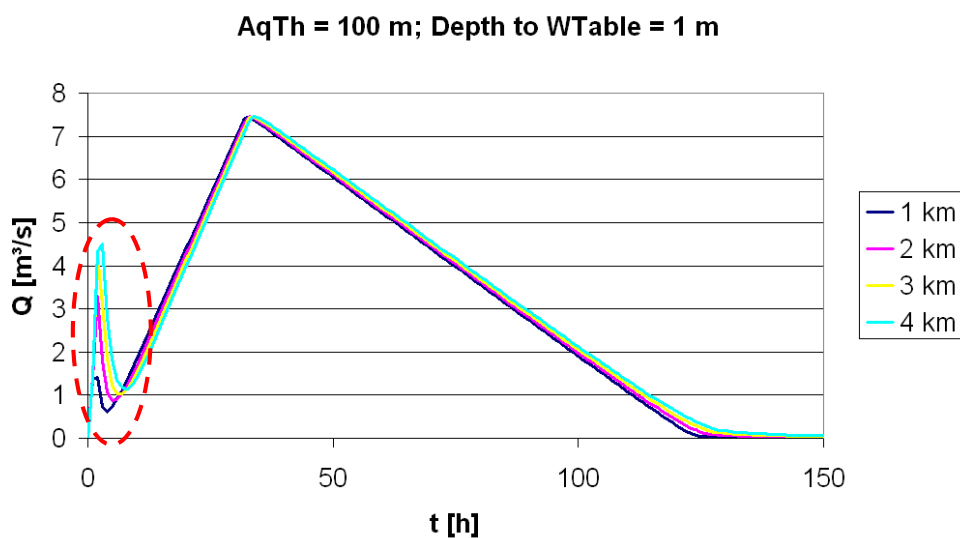


Figure 4.1: Flood hydrographs at four points along the river. *AqTh* = aquifer thickness (100 m); *Depth to WTable* = depth to water table (1 m).

Figure 4.2 is derived from the budget calculations of the groundwater model. It shows the temporal course of four budget terms. The rate of infiltration in 1000 m³/h is plotted against time. The first graph (turquoise) is the infiltration from the riverbed into the storage that lies either beneath or to the sides of the channel. The second one (blue) describes the inflow into the storage that can either result from direct infiltration from the riverbed or from inflow from

one aquifer cell to another. Then, there is the third term (yellow), the exfiltration into the riverbed which results in newly generated stream flow. The fourth graph (orange) depicts the outflow from storage (equivalent to the inflow into storage consisting of two terms: exfiltration into the riverbed and flow from one aquifer cell to the next).

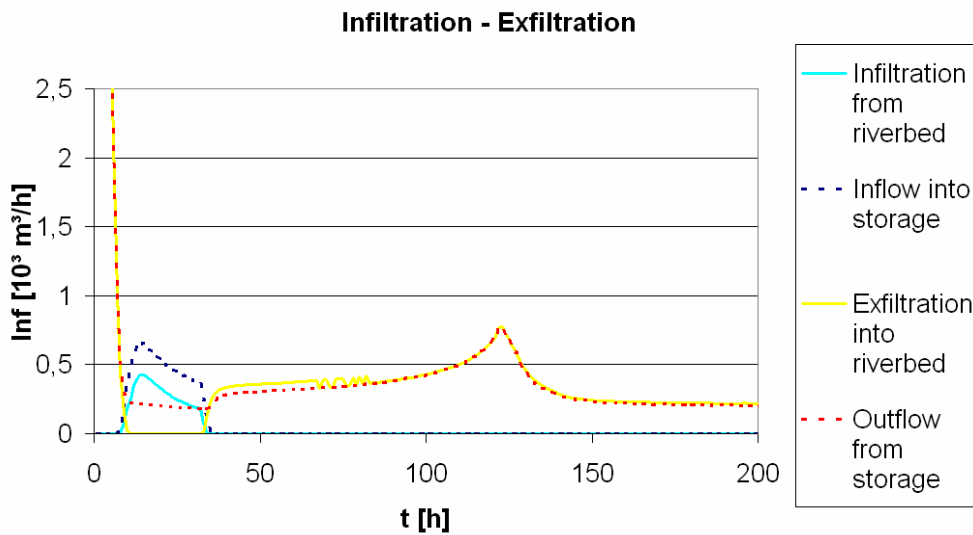


Figure 4.2: Inflow into and outflow from the storage. Aquifer thickness = 100 m; depth to water table = 1 m (Inf = Rate of infiltration / exfiltration).

Right from the beginning, the exfiltration from the aquifer into the dry riverbed dominates. The storage empties and generates runoff in the channel. The only time period where there is infiltration from the river to the aquifer is between the tenth and the 35th hour where the peak of the flood wave is actually higher than the aquifer head. Once the flood wave recedes water again starts to seep out of the aquifer. The small peak (at hour 120) results from the fact that at this point, no more water enters the river channel at the upper boundary. That way, the bank storage successively starts to discharge into the channel. From hour 150 on, the system reaches an equilibrium state with constant exfiltration from the aquifer into the channel.

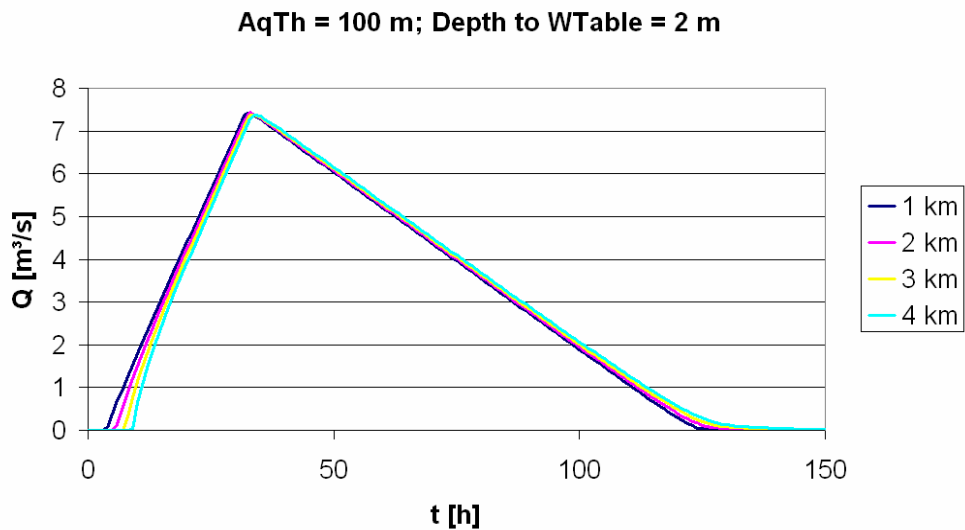


Figure 4.3: Flood hydrographs at four points along the river. *AqTh* = aquifer thickness (100 m); *Depth to WTable* = depth to water table (2 m).

The hydrographs in *Figure 4.3* resemble pretty much the input synthetic hydrograph. In this scenario the depth to water table is 2 m. The flood water can therefore only laterally enter the river bank without infiltrating downwards into the aquifer. Moreover, once the flood wave passed a river segment the bank storage seeps back into the river. All in all, the water cannot be stored in the aquifer for a longer time period but leaves the aquifer via the riverbed.

In this scenario the flood wave fills the empty storage right at the beginning. Already after 10 hours the storage is filled and the infiltration rate drops (*Figure 4.4*). There is still some infiltration going on because the flood wave rises until the 40th hour. After that, the water level in the channel lowers and exfiltration from the overbank begins. Exfiltration peaks after the flood wave passed the aquifer and stops, once the aquifer head in the overbank area dropped below the riverbed elevation.

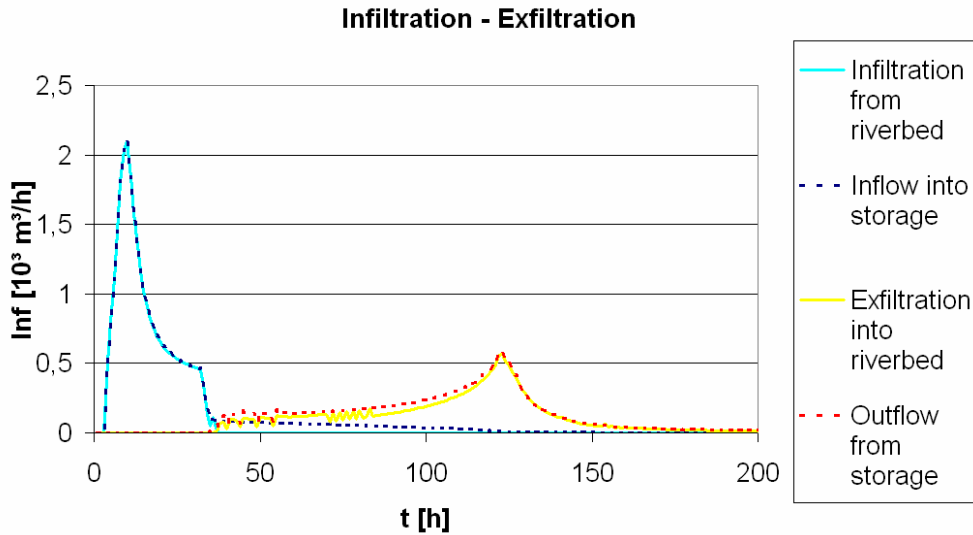


Figure 4.4: Inflow into and outflow from the storage. Aquifer thickness = 100 m; depth to water table = 2 m (Inf = Rate of infiltration / exfiltration).

In *Figure 4.5* for the first time it is possible to observe the influence of groundwater recharge on a passing flood wave. The rising limbs of the hydrographs at all observation points steepen considerably. This is a common feature of flash floods in arid regions and can be ascribed to the effects of infiltration into empty storage underneath the stream channel.

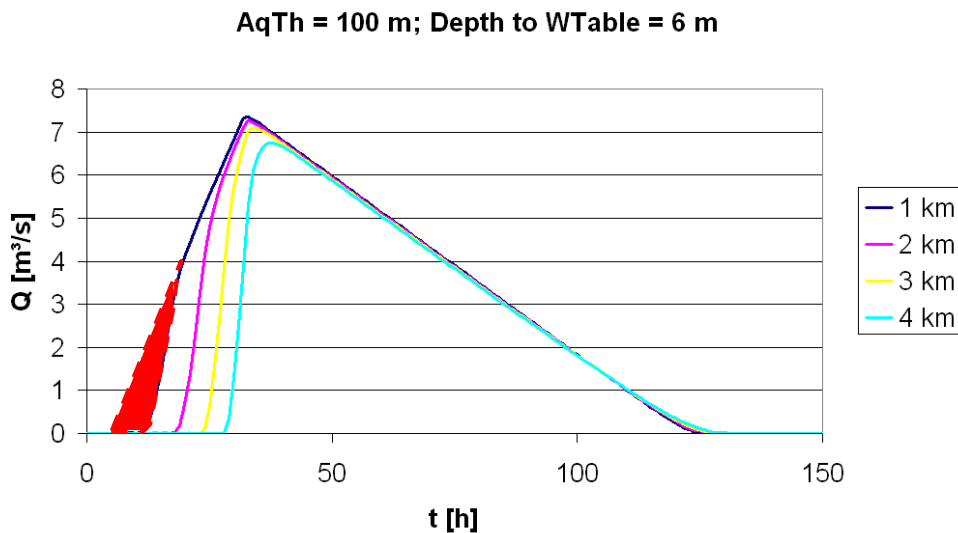


Figure 4.5: Flood hydrographs at four points along the river. $AqTh$ = aquifer thickness (100 m); Depth to $WTable$ = depth to water table (6 m).

The hydrograph becomes steeper because of the following processes:

- The flood wave arrives in a dry riverbed (there must not be silt or clay layers that restrict infiltration at the beginning).
- The water starts to infiltrate into the empty aquifer.

- When the flow in the riverbed exceeds the maximum infiltration rate, the water can flow on to the next river cell.
 - **This does not steepen the hydrograph; it just takes away a constant amount of water from the flood wave.**
- When the highly conductive alluvial deposits of the riverbed are completely filled, the infiltration rate recedes because the surrounding deposits normally have lower hydraulic conductivities.
 - **Only when the infiltration rate recedes the rising limb of the hydrograph steepens.**

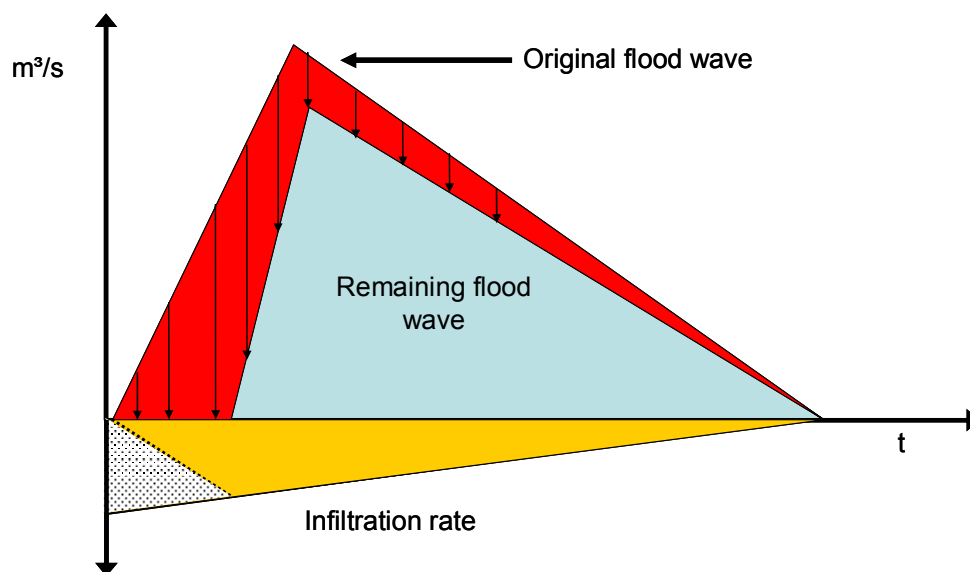


Figure 4.6: Steepening of the flood wave front due to decreasing infiltration rate.

The steepening of the hydrograph occurs because the infiltration process slows down or stops as soon as the aquifer is saturated (*Figure 4.6*). It can only be observed if the hydraulic conductivity of the aquifer is smaller than the one of the riverbed (as it is the case here). Only then, the water underneath the riverbed starts to mount up and has to flow away laterally before it is replaced by new water.

Figure 4.7 shows the mounting of the groundwater levels at a transect perpendicular to the river channel. Already after 50 time steps the groundwater level directly below the channel has risen up to the riverbed (yellow graph). This stands in contrast with the movement of the water levels in the cells further away from the channel since their rise takes some more time and does not reach the aquifer surface. After 100 hours, the groundwater surface below the channel already drops again, whereas the water tables further away are still on the rise

(compare the red graph at 200 hours with the blue one at 700 hours). Nevertheless, the storage space beyond 500 m is not used at all.

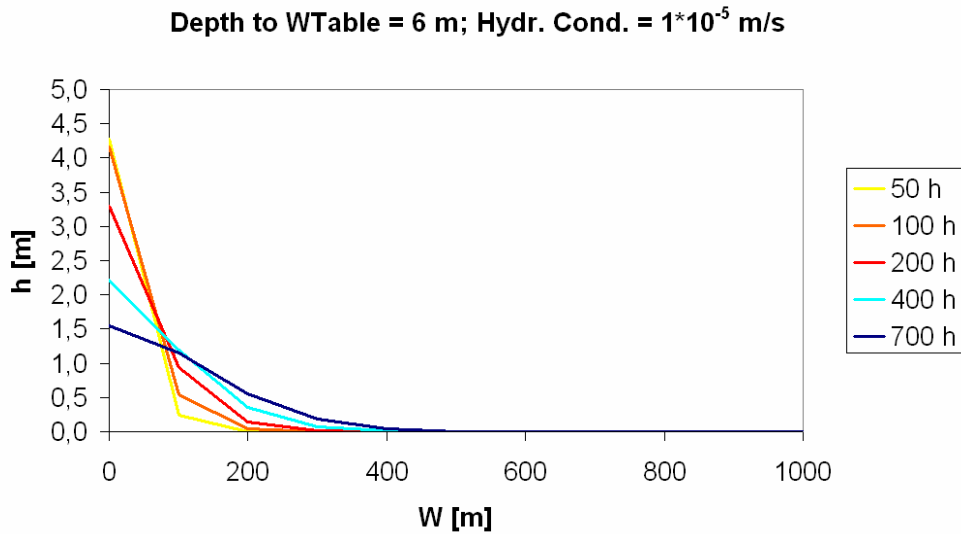


Figure 4.7: Groundwater heads along a transect perpendicular to the stream channel after 50, 100, 200, 400 and 700 hours. Aquifer thickness = 100 m; depth to water table = 6 m; hydraulic conductivity = $1 \cdot 10^{-5}$ m/s. W = width of aquifer in meters; h = groundwater head in meters.

Taking a look at *Figure 4.8* confirms the assumption that the whole storage space provided by the aquifer is filled after 40 hours. But there is still constant infiltration on a smaller scale. This infiltration is partly due to the slow lateral flow in the aquifer when the mounting groundwater extends into the surrounding cells. Noteworthy is also the fact that no exfiltration from the aquifer to the channels takes place anymore. This is not surprising since the groundwater levels never surpass the riverbed elevation.

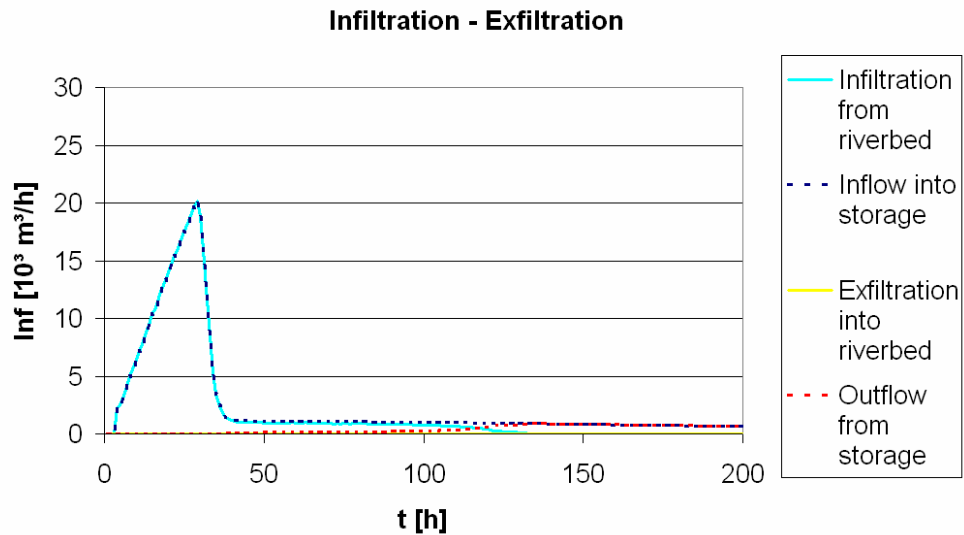


Figure 4.8: Inflow into and outflow from the storage. Aquifer thickness = 100 m; depth to water table = 6 m ($Inf = \text{Rate of infiltration} / \text{exfiltration}$).

The depth to water table is 10 m in *Figure 4.9*. It is clearly visible that the bigger storage space causes more recharge to the groundwater. If the hydrographs are considered to be integral volumes of the flood waves, it is rather simple to calculate the amount of recharge. This is done by subtracting the volume at km 4 from the volume of the original input hydrograph. The method of differences (to measure transmission losses) is based on this principle.

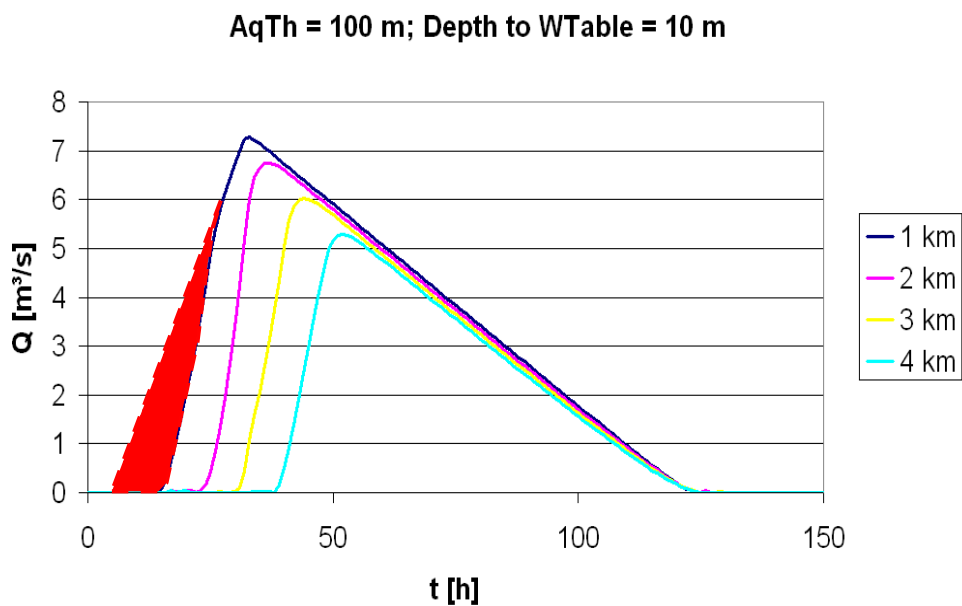


Figure 4.9: Flood hydrographs at four points along the river. $AqTh = \text{aquifer thickness}$ (100 m); $Depth\ to\ WTable = \text{depth to water table}$ (10 m).

The infiltration – exfiltration graph (*Figure 4.10*) supports the assumption that a greater proportion of the flood wave infiltrates before the aquifer is filled up to the riverbed elevation. After 50 hours, a small but constant infiltration rate remains until the flood wave completely passed the channel. Compared to the scenario where the depth to water table is only 6 m this time the infiltration rate is approximately twice as high. At 6 m it is around 1000 m³/h, at 10 m it already went up to 2000 m³/h. The hydraulic conductivity is still the same; the only parameter that changes is the depth to water table. This change causes the water beneath the channel to mount up further (almost twice as high) and therefore it provides more infiltration area to the sides for the inflowing water. Hence, more water can flow laterally into the dry aquifer.

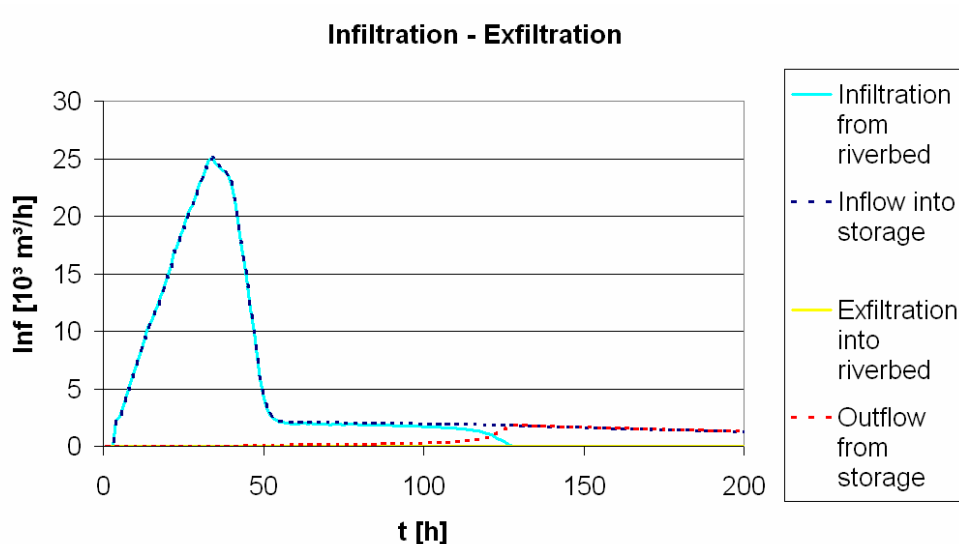


Figure 4.10: Inflow into and outflow from the storage. Aquifer thickness = 100 m; depth to water table = 10 m. (*Inf* = Rate of infiltration / exfiltration).

When the depth to water table rises up to 20 m, in our example no water reaches the outlet of the river anymore. That means, all the water infiltrates into the aquifer. The hydrograph at km 1 exhibits a new behaviour. Its beginning is again flatter than before and has the same slope as the input hydrograph (*Figure 4.11*). The new behaviour can be explained by the hydraulic conductivity of the riverbed that reaches its maximum. This can only happen now that the underlying cell is large enough to store all the infiltrating water at once without being dependent on the neighbouring cell's storage space. Like this, the infiltration is only restricted by the rate of leakage through the riverbed until the storage is filled up after approximately 25 h.

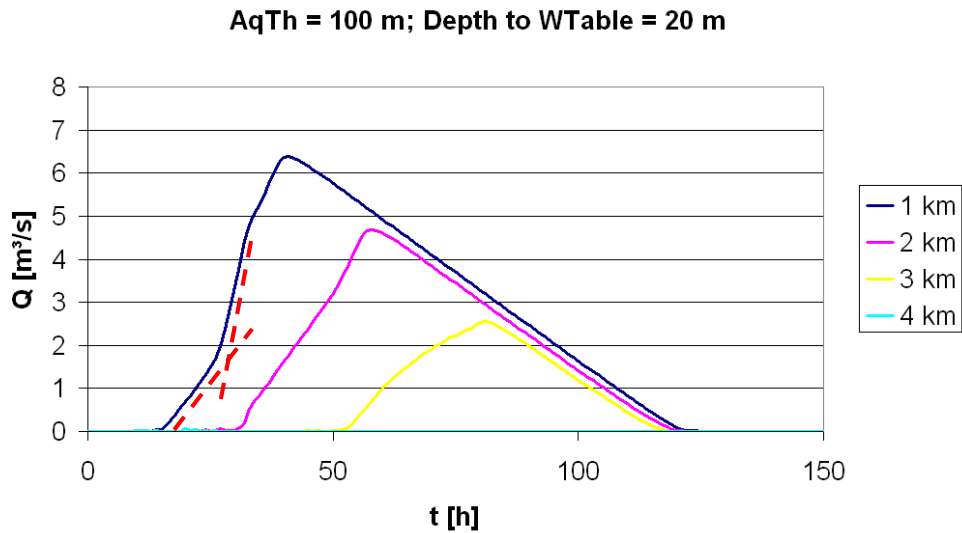


Figure 4.11: Flood hydrographs at four points along the river. *AqTh* = aquifer thickness (100 m); *Depth to WTable* = depth to water table (20 m).

This is an inherent behaviour to this kind of surface water - groundwater interaction models without an unsaturated zone. Since the unsaturated zone is non-existent, all the infiltrating water is directly added to the saturated zone without any time delay or hold up effects. The vertical hydraulic conductivity between the riverbed and the groundwater surface is therefore infinitely high. Under natural conditions, however, the flattening would only occur if the aquifer's hydraulic conductivity is higher than the one of the riverbed (which is not the case in this model run).

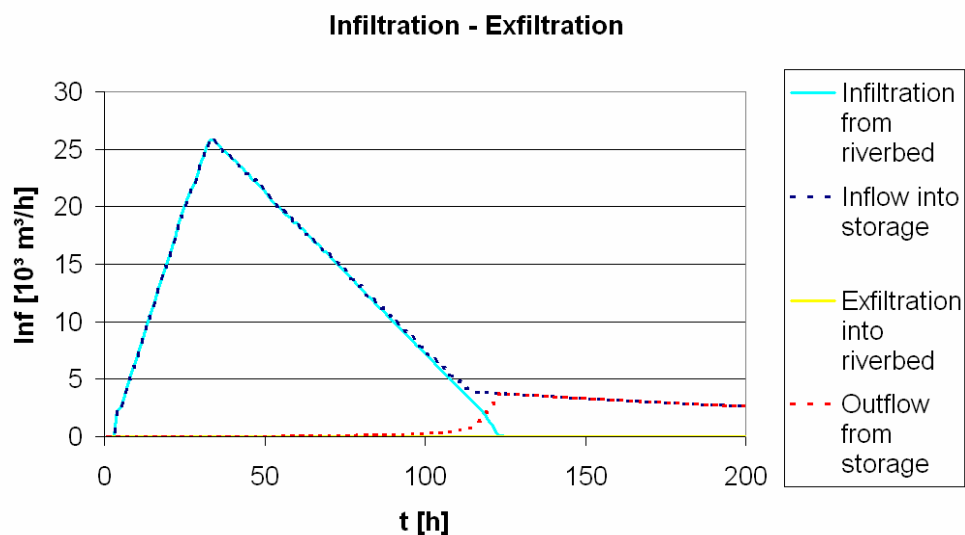


Figure 4.12: Inflow into and outflow from the storage. Aquifer thickness = 100 m; depth to water table = 20 m (*Inf* = Rate of infiltration / exfiltration).

Since all the water from the flood wave infiltrates into the aquifer, the integrated volume under the turquoise infiltration curve in *Figure 4.12* equals the input volume of 1.6 million m^3 . In this simulation, the empty storage space in the highly conductive alluvial channel is big enough to store all the water without being dependent on the less conductive bank storage space to the sides. This is why the infiltration curve looks that even, not exhibiting sudden reduction.

In *Figure 4.13*, the hydrograph at km 1 has 2 peaks. The first one resembles the input wave minus the constant maximum infiltration rate. The beginning of the second rise marks the point where the aquifer cell beneath the stream is filled up completely and the water has to flow laterally to the surrounding aquifer cells. The hydrograph at km 2 consists of the remaining water that could not infiltrate into the aquifer between km 1 and km 2. From km 3 on, no stream flow is observed anymore.

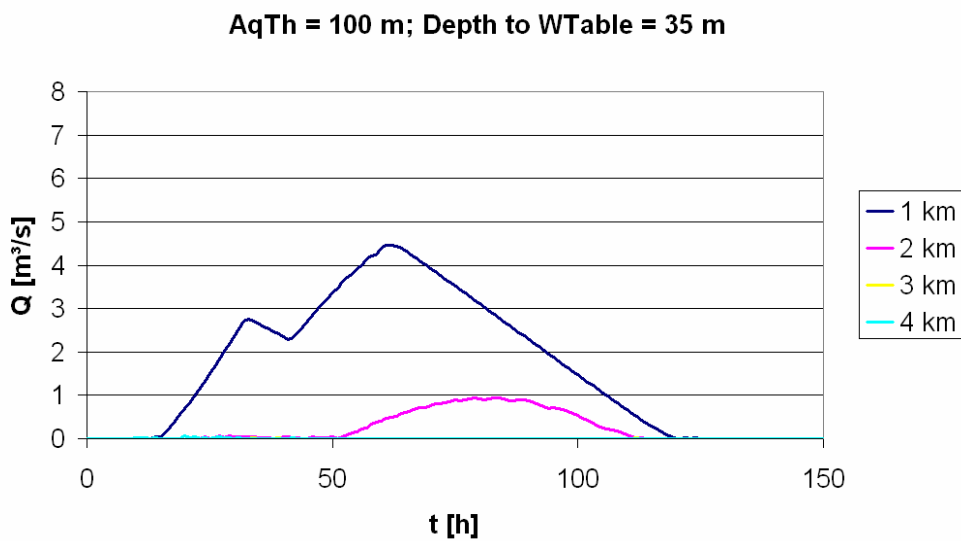


Figure 4.13: Flood hydrographs at four points along the river. *AqTh* = aquifer thickness (100 m); *Depth to WTable* = depth to water table (35 m).

In the last simulation of this series, where the depth to water table is 60 m, the flood wave only reaches km 1 before it completely seeps into the ground (*Figure 4.14*). Almost the whole hydrograph is determined by the maximum infiltration rate into an empty storage. Only from the 65th hour on the storage directly below the channel in the first river section is full. No stream flow is recorded at the lower observation points.

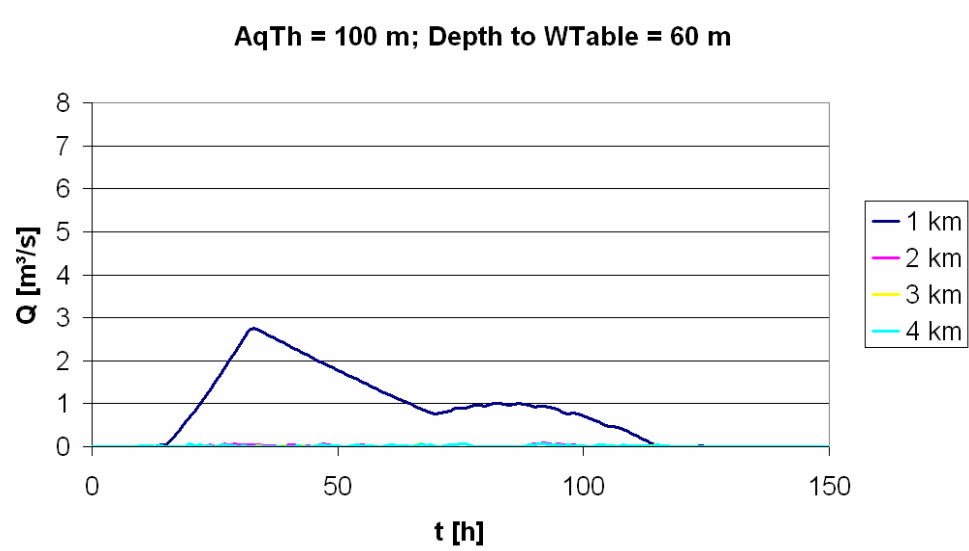


Figure 4.14: Flood hydrographs at four points along the river. *AqTh* = aquifer thickness (100 m); *Depth to WTable* = depth to water table (60 m).

4.1.2 Aquifer thickness

The simulations with variable aquifer thicknesses showed that higher thicknesses lead to higher groundwater recharge. This is not that obvious at smaller thicknesses below 100 m, but becomes significant when the thickness rises above 100 m (see *Figure 4.15*).

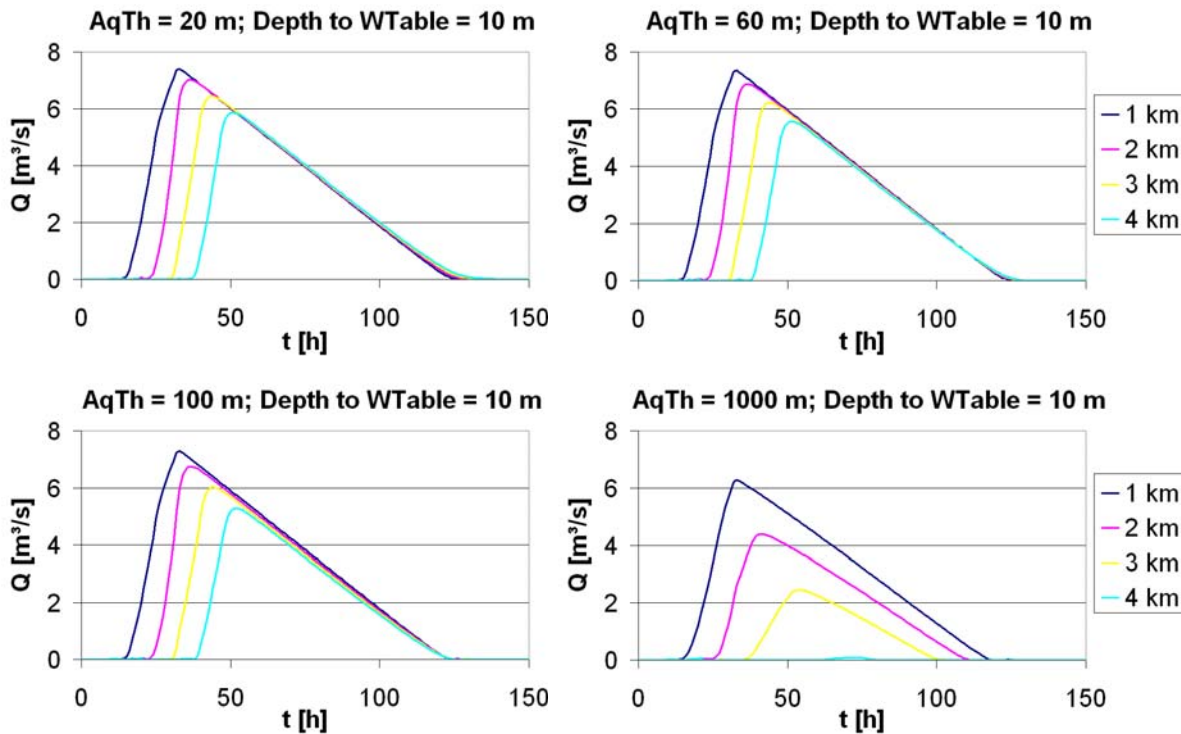


Figure 4.15: Influence of aquifer thickness on groundwater recharge. Flood hydrographs at different aquifer thicknesses, ranging from 20 to 1000 m. Depth to water table is constantly 10 m.

Figure 4.16 demonstrates that higher aquifer thicknesses allow a larger amount of the infiltrated water to be transported out of the system. The water fluxes through the upper and lower boundary of the aquifer are compared. The difference is plotted on the y-axis. If the volume is positive, the aquifer loses more water at the lower constant head boundary than it gains at the upper constant flux boundary. This additional water can only be provided by infiltration from the flood wave. The blue graph describes the additional water flow through the aquifer with a thickness of 1000 m. When the depth to water table is 6 m, 80,000 m³ of the infiltrating water are transported out of the system. An aquifer with a thickness of 100 m is able to transport 8,000 m³.

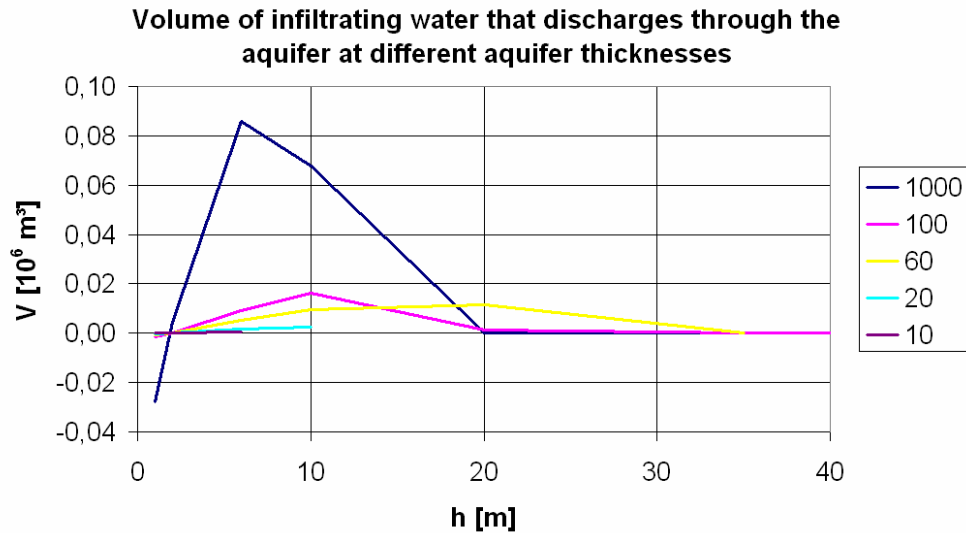


Figure 4.16: Volume of water from identical flood waves that is transported out of the aquifer through the porous matrix after it infiltrated into the saturated storage zone. Comparison of different aquifer thicknesses.

Obviously, higher thicknesses allow more water to be transported out of the system. The slightly higher hydraulic gradient which builds up when the wave is starting to infiltrate serves as an explanation for this behaviour. The change in gradient causes disproportionately more flow in the thicker aquifers than in the thinner ones. Applying the Darcy equation to two aquifers with differing thicknesses clarifies the situation. Two situations are compared:

- a) Normal aquifer situation without infiltrating flood wave. Constant in- and outflow.
- b) Situation where an infiltrating flood wave causes the groundwater surface to become slightly more inclined towards the outflow (since the flood wave starts to infiltrate in the upper part of the aquifer).

The extra inclination results in an additional flow, the amount of which is compared for different aquifer thicknesses with the help of a modified Darcy equation (12):

$$Q_F - Q_{NF} = A * K * \frac{\partial h + i}{\partial x} - A * K * \frac{\partial h}{\partial x} \quad (12)$$

With Q_F = flow at flood condition, Q_{NF} = flow at non flood condition, A = cross-sectional area, K_{aq} = hydraulic conductivity of the aquifer, ∂h = change in aquifer head, ∂x = length of aquifer, i = additional change in aquifer head.

$$\partial Q = A * K * \frac{i}{\partial x} \quad (13)$$

∂Q stands for additional flow caused by higher inclination.

Assuming two aquifers with similar parameters except the thickness:

- Hydraulic conductivity: 0.02 m/s
- Length: 4000 m
- Width: 2000 m
- Thickness: 100 m; 1000 m
- Cross-sectional area: 200,000 m²; 2,000,000 m²

In this case, a change in hydraulic gradient of 5 m leads to an additional outflow of 5 m³/s for the 100 m aquifer and to an additional outflow of 50 m³/s for the 1000 m aquifer (*Figure 4.17*).

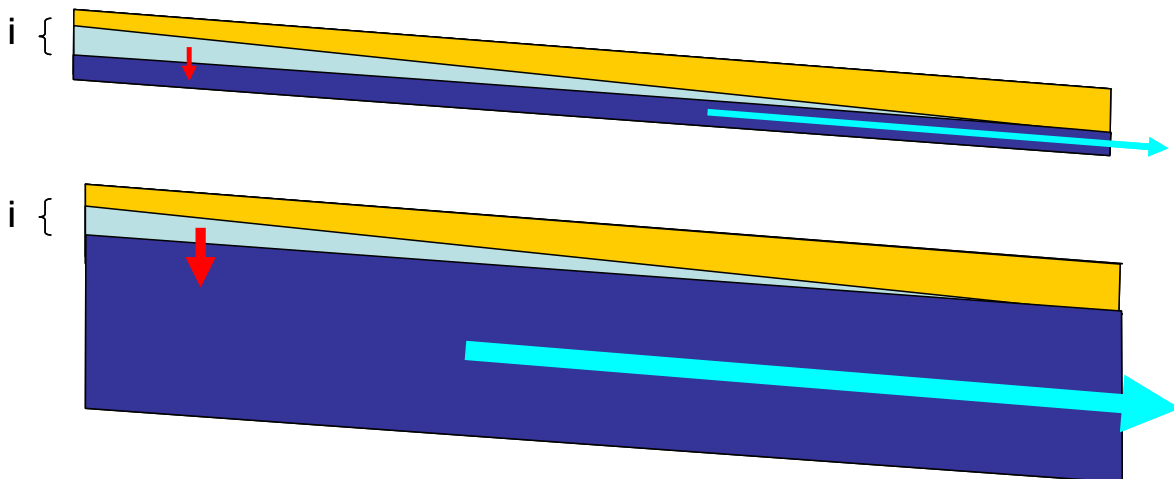


Figure 4.17: Higher aquifer thicknesses transport more water out of the system (blue arrow) and thus allow for more infiltration (red arrow).

To sum up, higher aquifer thickness allows for more groundwater recharge since a higher proportion of the infiltrating water can be transported away from the point of infiltration.

Figure 4.18 compares the infiltration-exfiltration situation for different aquifer thicknesses. The red area in the right figure marks the surplus infiltration that is made possible by the water being transported out of the model area through the aquifer. The infiltration rate in this period is not constant but recedes. This is due to the fact that after the flood wave went past, the aquifer heads fall again reducing the inclination.

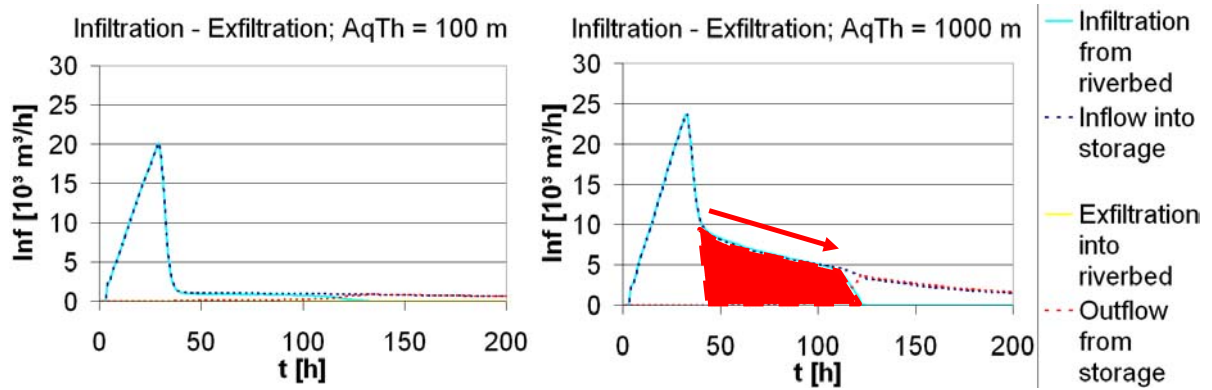


Figure 4.18: In- and outflow behaviour at two different aquifer thicknesses ($AqTh = 100\text{ m}$ compared to $AqTh = 1000\text{ m}$). The depth to water table is both times 6 m . The surplus infiltration is indicated (red area).

4.1.3 Hydraulic conductivity

In the second set of runs the hydraulic conductivity was changed to $1 \cdot 10^{-2}\text{ m/s}$ (from $1 \cdot 10^{-5}\text{ m/s}$ in the first ones). The most obvious difference occurred once the hydraulic conductivity of the aquifer was set to a higher value than the one of the riverbed. In this case, the infiltration is only limited by the riverbed's conductivity and no steepening of the hydrograph's rising limb occurs anymore (compare *Figure 4.19* with *Figure 4.20*). The result is a constant maximum abstraction rate from the flood wave until the whole storage space is filled (and not only the space directly beneath the stream).

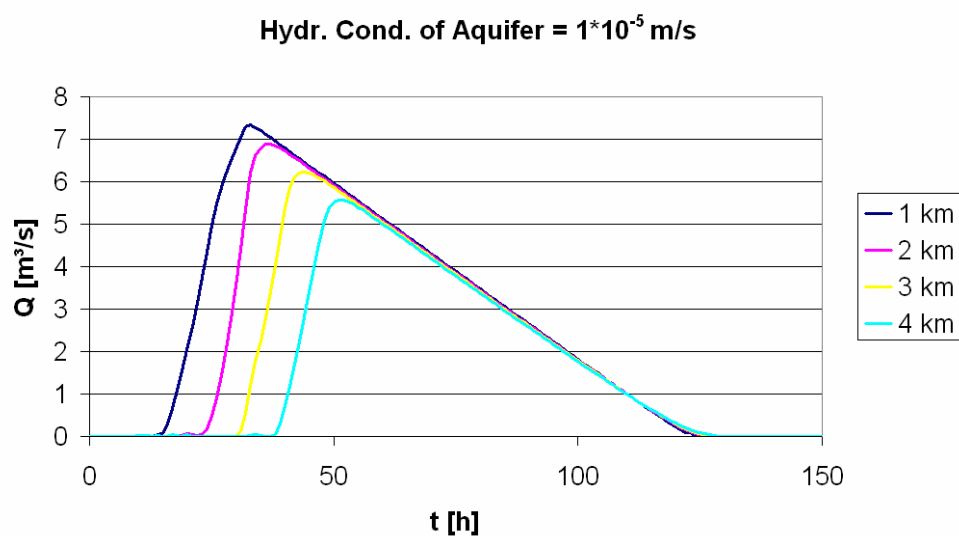


Figure 4.19: Flood hydrographs at four points along the river. Aquifer thickness = 100 m ; depth to water table = 10 m ; hydraulic conductivity = $1 \cdot 10^{-5}\text{ m/s}$. The rising limbs of the hydrographs steepen, the flood wave does not infiltrate completely into the aquifer.

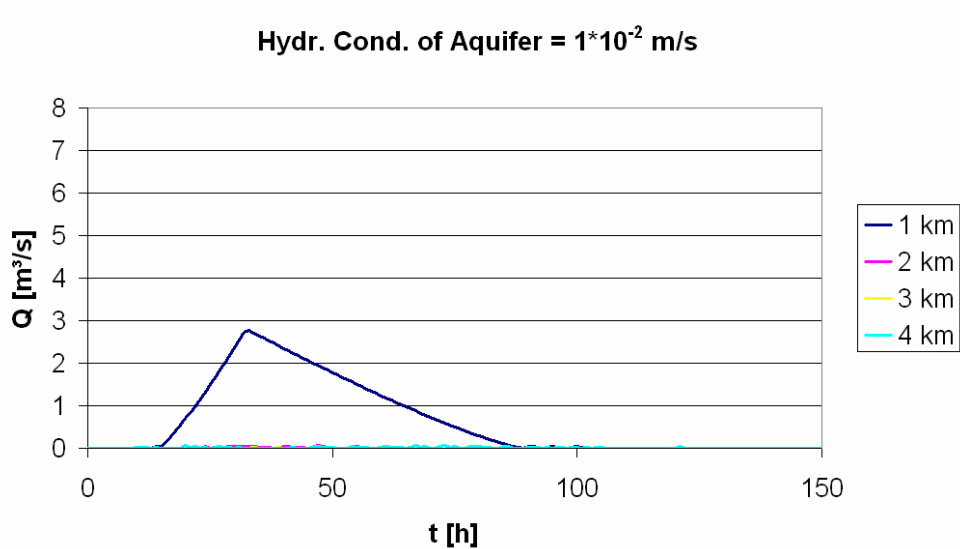


Figure 4.20: Hydraulic conductivity of the aquifer changed to $1 \cdot 10^{-2}$ m/s. The other parameters are the same as in Figure 4.19. No steepening of the rising limb anymore. Flood wave does not reach the second kilometer.

Figure 4.19 and Figure 4.20 point out the difference a variation in hydraulic conductivity can make. All the other parameters are constant (depth to water table = 10 m; aquifer thickness = 100 m, slope = 0.0012 m/m), just the hydraulic conductivities differ. Nevertheless, the recharge behaviour of the aquifer changes completely:

- If the hydraulic conductivity of the aquifer is lower than the one of the riverbed, the groundwater mounts below the channel and blocks (or at least hinders) infiltration (Figure 4.21, A).
- In case the hydraulic conductivity of the aquifer is higher than the one of the riverbed, all the infiltrating water can flow freely and disperse in the aquifer (Figure 4.21, B).

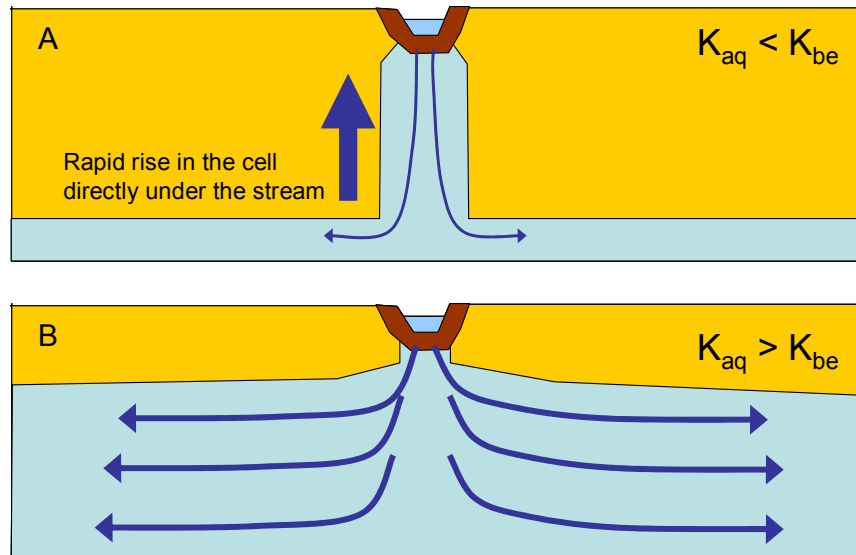


Figure 4.21: Different groundwater recharge behaviour due to varying hydraulic conductivities. A: Conductivity of aquifer is lower than conductivity of riverbed. B: Conductivity of aquifer is higher than conductivity of riverbed.

The change of behaviour can clearly be seen when comparing the transects of water levels in the test aquifer. *Figure 4.22* shows the mounting of the groundwater surface up to 45 m and the quick decline to the 400 m point, whereas the groundwater surface in *Figure 4.23* only rises 2.5 m, but fills the whole aquifer from the bottom up and from one side to the other.

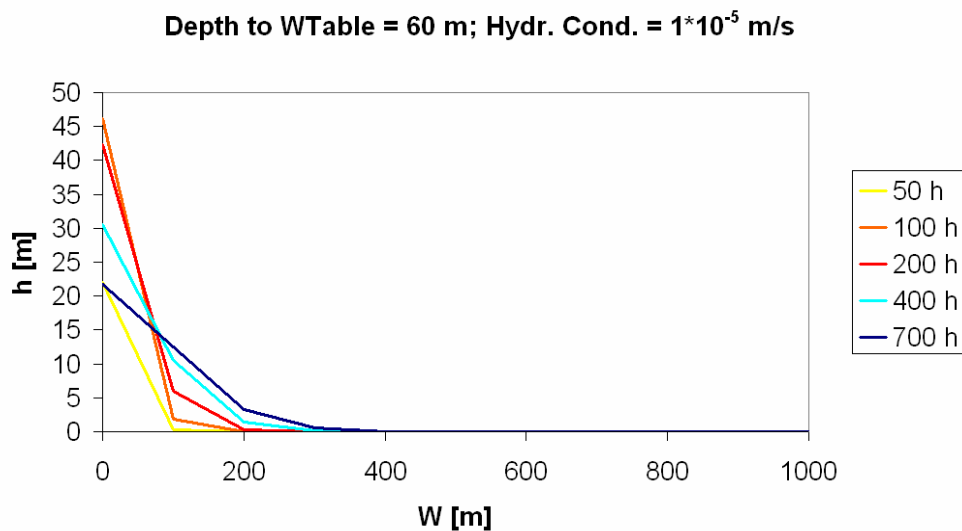


Figure 4.22: Rise of water tables in the immediate vicinity of the stream channel. Aquifer thickness = 100 m; Depth to WTable = depth to water table (60 m); Hydr. Cond. = hydraulic conductivity ($1 \cdot 10^{-5}$ m/s). W = width of aquifer in meters; h = groundwater head in meters.

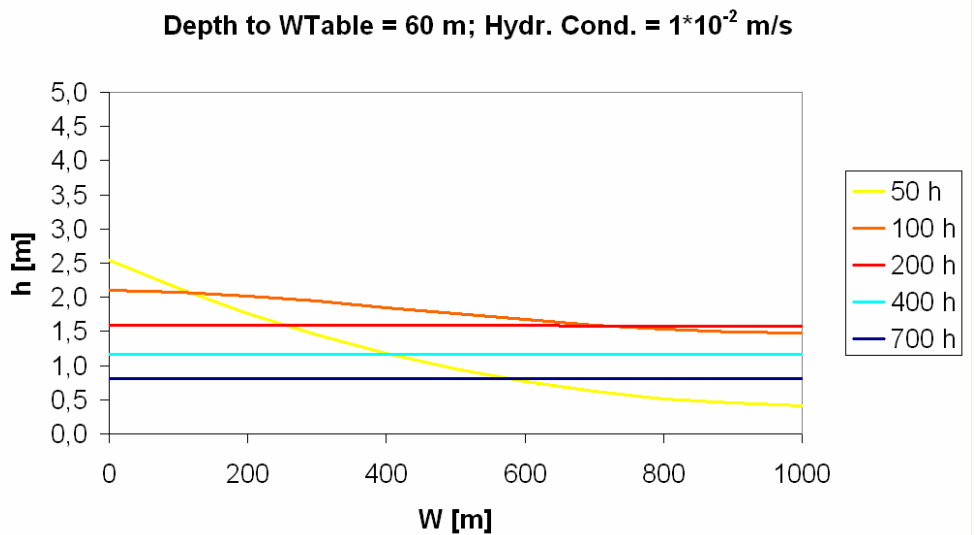


Figure 4.23: Relative stability of water tables at higher hydraulic conductivities. Aquifer thickness = 100 m; Depth to WTable = depth to water table (60 m); Hydr. Cond. = hydraulic conductivity ($1 \cdot 10^{-2}$ m/s). W = width of aquifer in meters; h = groundwater head in meters.

4.1.4 Hydraulic gradient

The hydraulic gradient determines the velocity of the flood wave as it traverses the aquifer. However, it does not influence the infiltration to a large extent since:

- The duration of the flood stays the same for each point along the river.
- The discharge that a flood wave delivers to a certain point along the river does not change with slope.

A higher gradient only implies a “spatial expansion” of the flood wave. Its length increases, if the slope increases. On the other hand, it also flows twice as fast, leaving the contact time between wave and aquifer the same (Figure 4.24). A change in gradient does not change the discharge at any point along the stream. Neither the peak flow nor the infiltration rate is changed. The only influence a higher slope may have on the infiltration process is that the cross-sectional area of the flood wave decreases (due to the higher velocity). This reduces the wetted perimeter and restricts the contact area between water body and aquifer to an extent that depends on the shape of the channel.

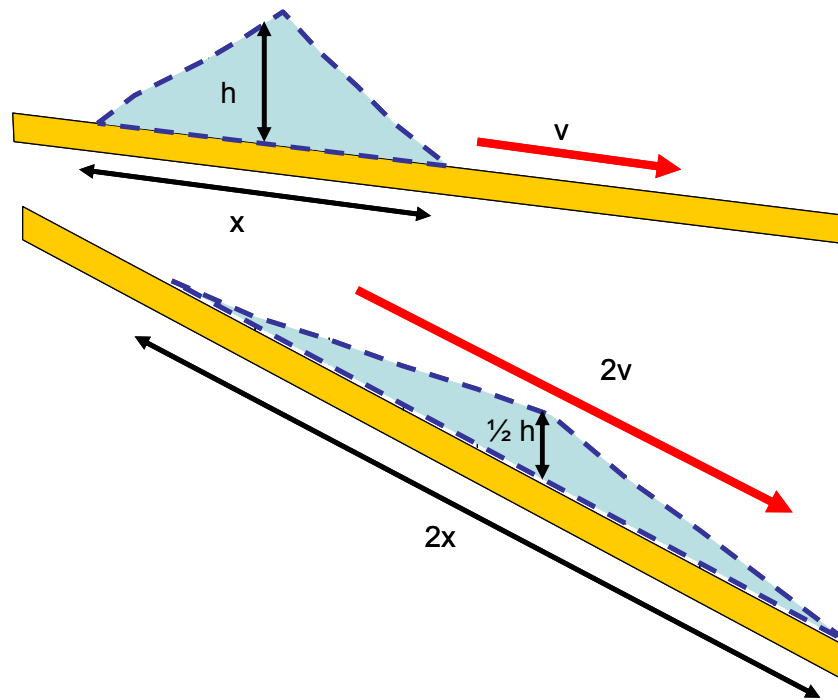


Figure 4.24: The impact of higher slope on flood waves. Velocity (v) increases, the wave stretches out and flattens. Duration of flooding and discharge stay the same at each point along the river.

All that leads to the conclusion that the slope has no big influence on groundwater recharge. The simulation results support this statement – they do not show differences of any kind between the particular runs, no matter whether the slope is 0.0012 m/m or 0.025 m/m.

4.1.5 Multiple flood waves

A double flood wave input was applied to the model to get an impression of how much one flood affects the aquifers response to successional floods. *Figure 4.25* displays the results of the simulation with an aquifer thickness of 60 m and a depth to water table of 20 m.

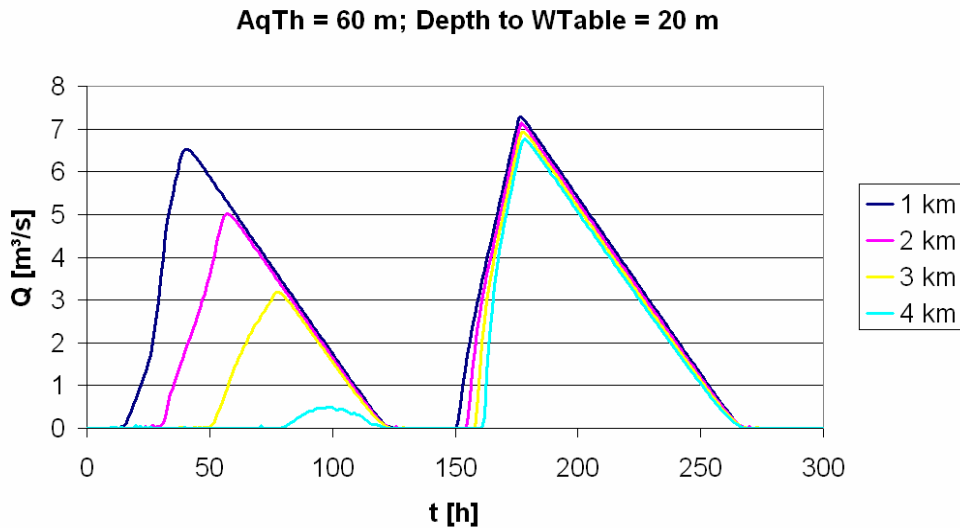


Figure 4.25: Double flood wave input to the hydraulic model. Flood hydrographs at four points along the river. $AqTh$ = aquifer thickness (60 m); $Depth\ to\ WTable$ = depth to water table (20 m).

In the lower parts of the test aquifer (around km 4), the wave arrives earlier during the second flood than during the first one. This could be interpreted as a higher velocity of the second wave. However, that is not the case since both waves flow with the same speed. That the second wave seems to arrive earlier is due to the fact that of the first wave only the very last part manages to flow that far downstream. The whole rising limb of the hydrograph infiltrated into the aquifer before. The less water gets lost to infiltration on the way, the faster a flood wave seems to progress down the channel. Since the first flood wave filled the aquifer below the stream channel completely, the second one cannot infiltrate anymore. The time in between the two waves is obviously not sufficient for the groundwater to be transported away laterally from underneath the stream channel. Consequently, the wave just “rushes by” without being diminished by infiltration to a large extent (*Figure 4.26*).

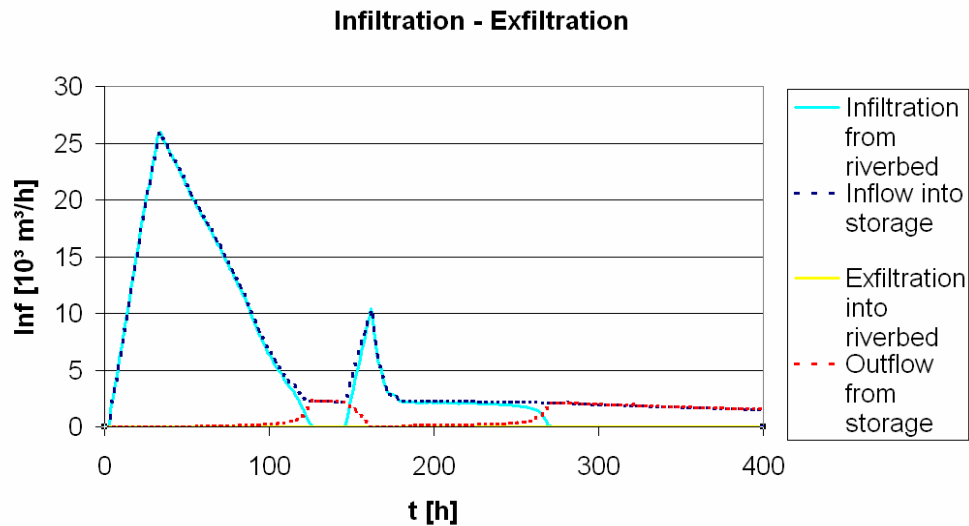


Figure 4.26: Inflow into and outflow from the storage of two successive flood waves. Aquifer thickness = 60 m; depth to water table = 20 m (Inf = Rate of infiltration / exfiltration).

This behaviour can have substantial effects on groundwater recharge:

- Large floods do not guarantee high quantities of recharge.
- It depends more on the **duration** of a flood wave how much water can (“has the time to”) infiltrate.
- Smaller floods with longer durations yield potentially more groundwater recharge than big but short-lived floods.
- The infiltration rate of consecutive flood waves decreases.

Flood waves can flow long distances on top of rather empty aquifers without losing big volumes of water. Then suddenly, infiltration rates may increase considerably once the wave reaches stream sections that were not flooded for a longer period of time. In these sections the volume of the flood waves decreases rapidly while the highly conductive riverbed sediments become saturated (*Figure 4.27*).

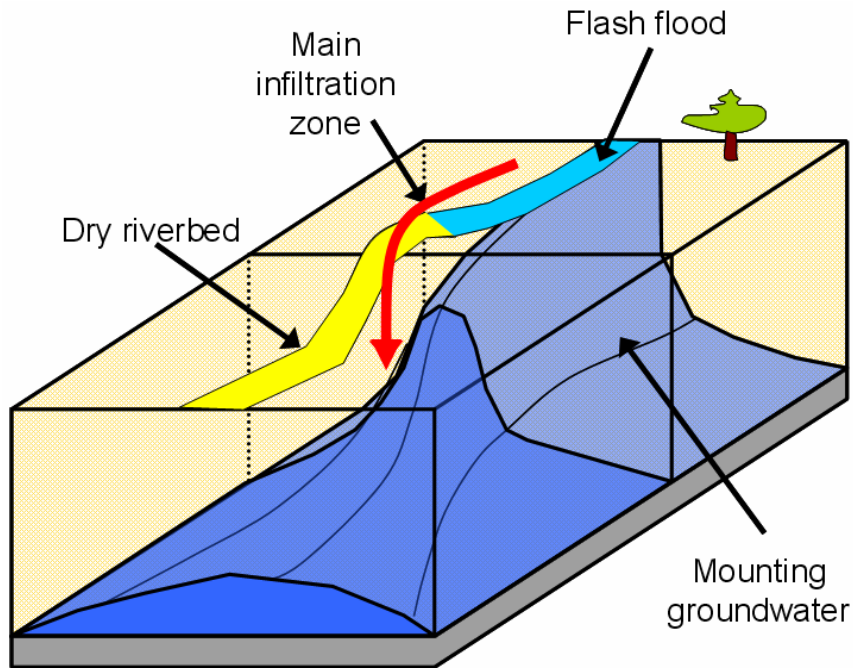


Figure 4.27: The process of rapidly mounting groundwater caused by flash floods.

The effect is comparable to a hydrological conveyor belt. Water is transported on top of a small strip of mounted groundwater until it is abruptly dropped when the strip ends.

In extreme cases flash floods can discharge into the sea leaving a “dry” aquifer behind (Figure 4.28).

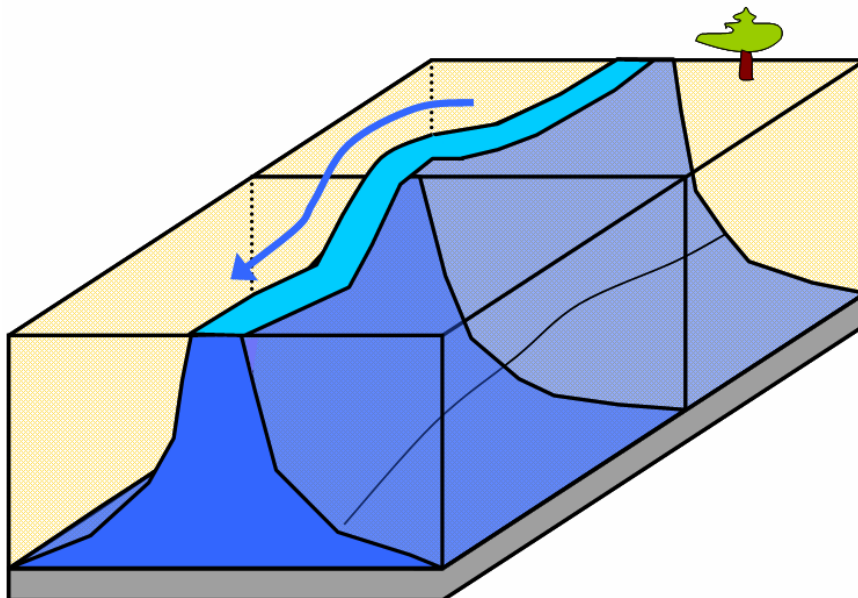


Figure 4.28: Very high groundwater tables directly beneath the stream channel restrict infiltration from flash floods considerably. Flash floods can „rush by“ leaving a rather dry aquifer behind them.

4.2 Quantitative budget calculations

For an aquifer with a certain hydraulic conductivity, it is possible to derive a simple equation to calculate the groundwater recharge dependent on the aquifer thickness and the initial depth to water table. This can be done because the volume of infiltrating water is linearly dependent both on the depth to water table and on the aquifer thickness. *Figure 4.29* illustrates the dependency.

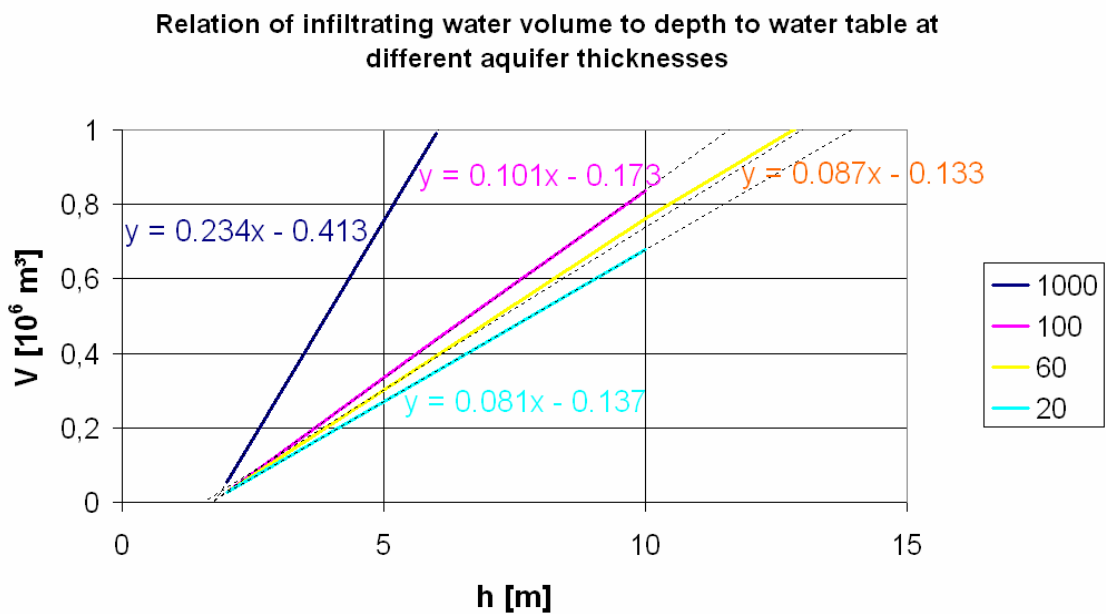


Figure 4.29: Interdependencies of infiltrated water volume (y-axis), depth to water table (x-axis) and aquifer thickness (variably coloured lines). The linear equations for the straight lines are added.

On the x-axis, the depth to water table is plotted against the infiltrating volume of water on the y-axis. For instance, the turquoise straight line visualises the linear relation of the two variables given an aquifer thickness of 20 m. If the thickness is changed to 60, 100 or 1000 m, the linear dependency remains but the line changes its slope and axis intercept (see *Table 4.1*).

Table 4.1: Slope and axis intercept for the recharge equations at different aquifer thicknesses.

AQUIFER THICKNESS	Slope	Axis intercept
20 m	0.081	-0.137
60 m	0.087	-0.133
100 m	0.101	-0.173
1000 m	0.234	-0.413

The change of slope is not random, but dependent on the change of aquifer thickness: the larger the aquifer thickness, the steeper the slope. The axis intercept also varies linearly with aquifer thickness. The change of slope and axis intercept is plotted against aquifer thickness in *Figure 4.30*. The linear dependency is obvious.

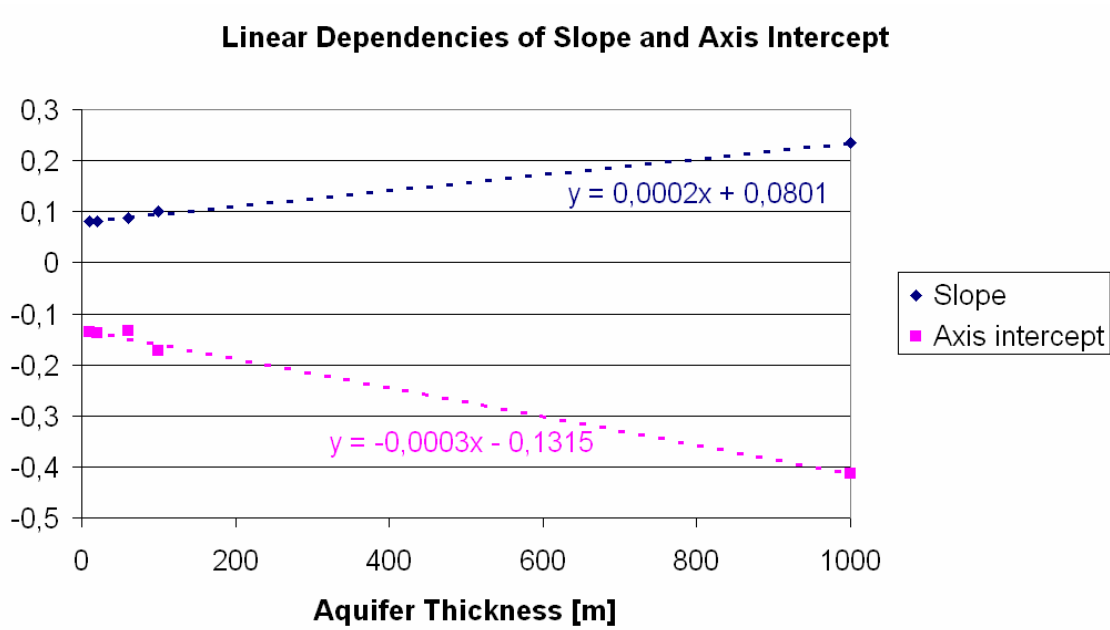


Figure 4.30: Linear dependencies of slope and axis intercept for different aquifer thicknesses.

The change of slope can be expressed by the following linear equation:

$$y = 0.0002 * AT + 0.0801 \quad (14)$$

y is the slope value and AT the aquifer thickness.

The same applies to the axis intercept:

$$y = -0.0003 * AT - 0.1315 \quad (15)$$

Substituting equations (14) and (15) into a linear equation with DWT as the depth to water table:

$$y = (0.0002 * AT + 0.0801) * DWT + (-0.0003 * AT - 0.1315) \quad (16)$$

In this case y stands for the infiltration volume in million m^3 and DWT for the depth to water table.

Rearranging equation (16) leads to:

$$y = 0.0002 * AT * DWT + 0.0801 * DWT - 0.0003 * AT - 0.1315 \quad (17)$$

From this equation, it can be derived that the recharge volume is approximately 100 times more sensitive to a change of the depth to water table than to a change of aquifer thickness. To get an equal increase of recharge, one has to either increase the depth to water table by 1 m or the aquifer thickness by 100 m.

With the equation it is possible to calculate the groundwater recharge for various aquifer thicknesses and depths to water table without setting up further model configurations. But note that the volume of the flood wave limits the maximum groundwater recharge.

Calibrating the equation for a certain aquifer is rather simple. The first step is to set up a simplified model with all the basic aquifer properties (hydraulic conductivity, width, length, effective porosity etc.) The slope can be any reasonable average value since it does not influence infiltration to a large extent. The input hydrograph should exhibit a typical shape for the area in question; its volume should range around the volume of average flood waves, rather exceeding it than falling short. After running the model with selected combinations of depths to water table and aquifer thicknesses, the relations can be plotted and the values of the equation can be derived.

4.3 Conclusion

The sensitivity analysis led to the following conclusions:

- The depth to water table has a major influence on groundwater recharge. It determines the space that is available for infiltrating water. The recharge volume is linearly dependent on the depth to water table.
- The aquifer thickness influences groundwater recharge insofar as thicker aquifers have the ability to transport more water in the saturated zone away from the point of infiltration. The recharge volume is also linearly dependent on aquifer thickness.

- An increase of depth to water table of 1 m has roughly the same effect on recharge volumes as an increase of aquifer thickness of 100 m.
- It is possible to derive a simple equation that describes the recharge volume of a certain aquifer depending on aquifer thickness and depth to water table
- The hydraulic conductivity of the aquifer is important for the recharge process as long as it does not exceed the hydraulic conductivity of the riverbed.
 - In most cases it restricts the velocity of water transport away from the point of infiltration.
 - However, it is of no importance if the riverbed conductivity restricts the infiltration.
- Two main recharge behaviours could be specified:
 - 1) In case the hydraulic conductivity of the riverbed is lower than the one of the aquifer:
 - Water infiltrates straight down to the groundwater table and is distributed evenly over the whole aquifer. Aquifer heads rise more or less simultaneously in the alluvial cross-section.
 - 2) In case the hydraulic conductivity decreases with distance from the channel:
 - The groundwater table mounts directly below the stream channel, restricting further infiltration. Large parts of the aquifer remain uninfluenced.
 - The front of a flash flood tends to steepen because infiltration rates decrease with time.
- The recharge volume depends more on the duration of a flood wave than on its peak discharge or volume.
- The influence of the hydraulic gradient is rather small, since both the flood duration and the discharge stay the same for all the points along the river.
- The recharge behaviour of successive flash floods can differ considerably. If the first flood raises the groundwater table in close vicinity of the stream channel, the second flood may not have the possibility to infiltrate anymore. That way, a flash flood can pass an aquifer which is dry in most parts on top of a small strip of mounted groundwater.

5 Application to the Kuiseb River

The area of the Lower Kuiseb is highly dependent on the groundwater recharge from flash floods. The alluvium of the river channel is relatively shallow, hardly exceeding 30 m. This restricts infiltration since under natural conditions the depth to water table is usually small. The paleochannels to the left side of the river may serve as a new source area for pumping wells. This model was set up to evaluate the reaction of the groundwater system to median-sized flash floods in the alluvium and in the paleochannels below the dune area.

Three different scenarios were examined in more detail:

- 1.) Natural steady-state:
 - The natural steady-state system without artificial pumping
- 2.) Pumping steady-state:
 - The steady-state system with current pumping rates
- 3.) Transient with flash flood:
 - 13 months of simulated aquifer behaviour with current pumping rates, the passage of multiple flood waves and a period of no-flow in the channel following the floods

5.1 Input to the groundwater model

Most of the data used for setting up the groundwater model was provided by the BGR (Bundesanstalt für Geowissenschaften und Rohstoffe, Germany) and the DWA (Department of Water Affairs, Namibia). Especially the hydraulic aquifer parameters derive from the “German-Namibian Groundwater Exploration Project” that took place from 1992 to 1995 (LENZ ET AL., SCHMIDT 1995). The input files for the MODFLOW model were created by means of the Processing MODFLOW program (CHIANG & KINZELBACH 1998). (On an important side note: when setting up the bas.-file with Processing MODFLOW it is necessary to add a simple INTERNAL in front of all the arrays. Only then, they can be read properly by the MODFLOW/DAFLOW program.)

5.1.1 Model area

The model area has an extent of 2116.5 km² (83 * 25.5 km) and is divided into 211650 cells with a side length of 100 m each. The grid is a finite difference grid (quadratic) consisting of 830 columns and 255 rows (*Figure 5.1*).

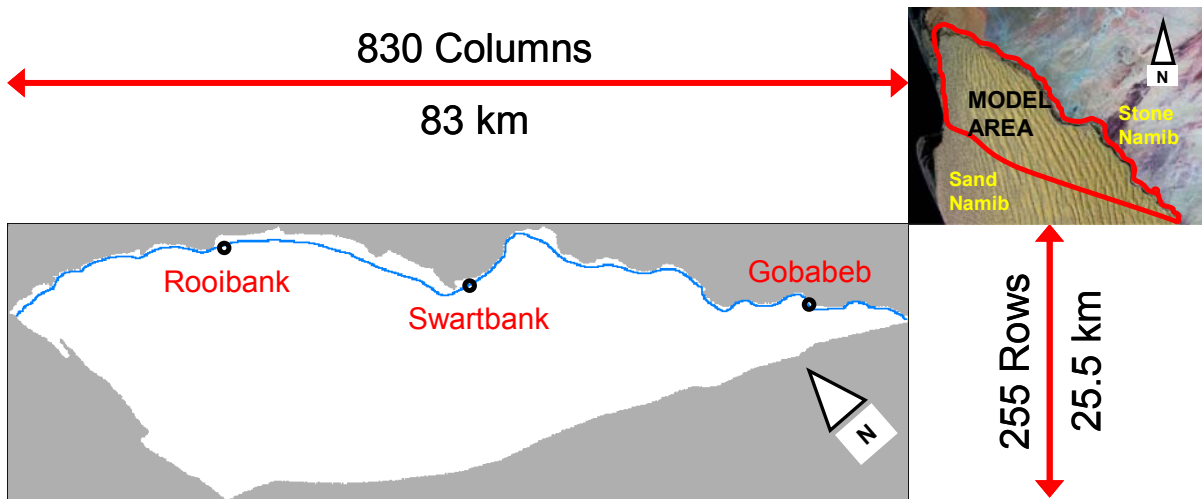


Figure 5.1: Dimensions of the model area.

The model has two layers with variable thicknesses. The surface elevation of the model area ranges from 80 m a.s.l. close to the sea up to 500 m a.s.l. in the upper catchment's dune field (*Figure 5.2*). The bottom elevation of the second layer is assumed to be at sea level. The bottom elevation of the first layer depends on the geological situation, which will be discussed in more detail in the next but one chapter.

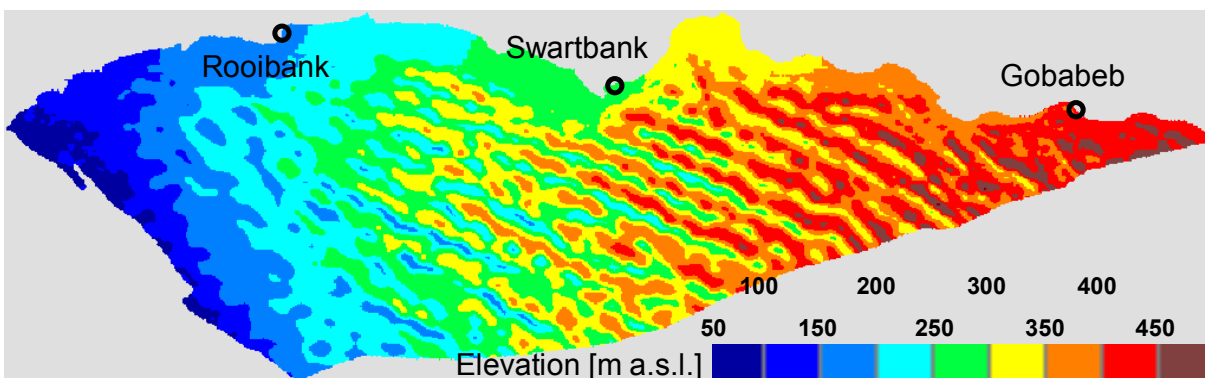


Figure 5.2: Elevation distribution in the model area.

5.1.2 Boundary conditions

One of the advantages in setting up a groundwater model for the whole Lower Kuiseb area is the fact that the boundary conditions surrounding it are well-known and easily implemented (*Figure 5.3*).

- b) The north-eastern boundary is a constant flux boundary.

Earlier surveys (applying the mixing-cell model) conducted by KLAUS (2007) imply that approximately 4 % of the inflow to the groundwater derive from the aquifer underneath the plateau of the Stone Namib. Given an approximate total recharge volume of 2 million m³ per year - 80,000 m³ of groundwater enter the model area from this direction.

- c) The western border is quite close to the sea and should remain relatively stable during the simulation. Therefore, it can be represented by a constant head boundary.

Considering that the surface elevation on the western border is close to 80 m a.s.l. and the average distance to the coast is 3 km, the constant head boundary was set to 50 m a.s.l.

- d) The south-western border can be considered a no-flow boundary out of two reasons:

- The streamlines should flow parallelly to the border due to the hydraulic gradient being steepest in this direction.
- The border also constitutes a geological fault line, cutting off the highly conductive aquifers of the model area from the surrounding basement rocks.

- e) The south-eastern corner of the model area is where the river enters. A general head boundary complies best with the requirements of this situation.

The general head's hydraulic conductivity equals the one of the channel alluvium ($4.17 \cdot 10^{-4}$ m/s).

The head on the boundary is 7 m below ground level, according to the average depth to water table in the alluvium.

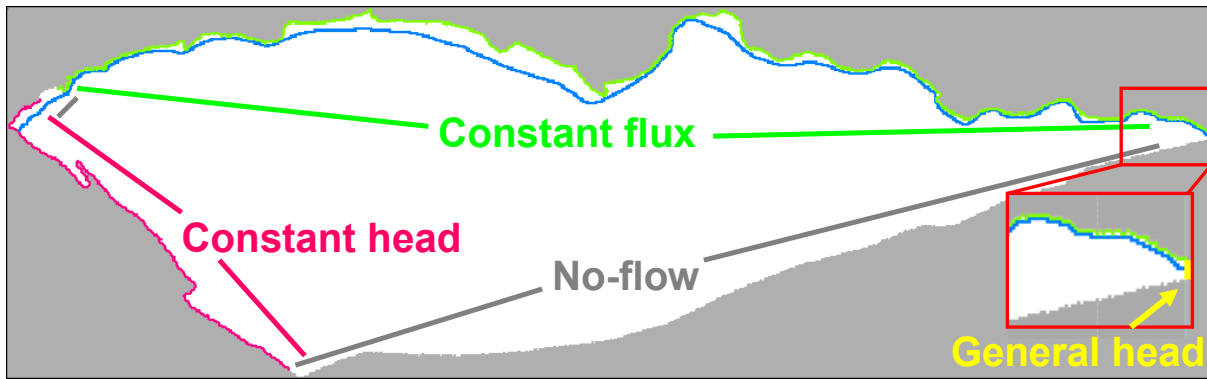


Figure 5.3: Boundary conditions for the groundwater model.

5.1.3 Geology

There are four major geological units in the model area. All of them exhibit different hydraulic properties (*Figure 5.4*).

- a) Basement: The granitic and gneissic basement rocks underlie the whole area and even crop out at some places (mainly in the lower and upper part of the area). Their hydraulic conductivity is comparatively small just like their effective porosity, specific storage and specific yield.
- b) Tsondab Sandstone: In the middle parts of the model area the upper model layer consists in large parts of sandstone. Due to faulting, the sandstone (which originally lay on top of the basement) broke into the basement. The sandstone conducts water more easily and is able to store more water than the basement. The average thickness of the sandstone formation is 100 m.

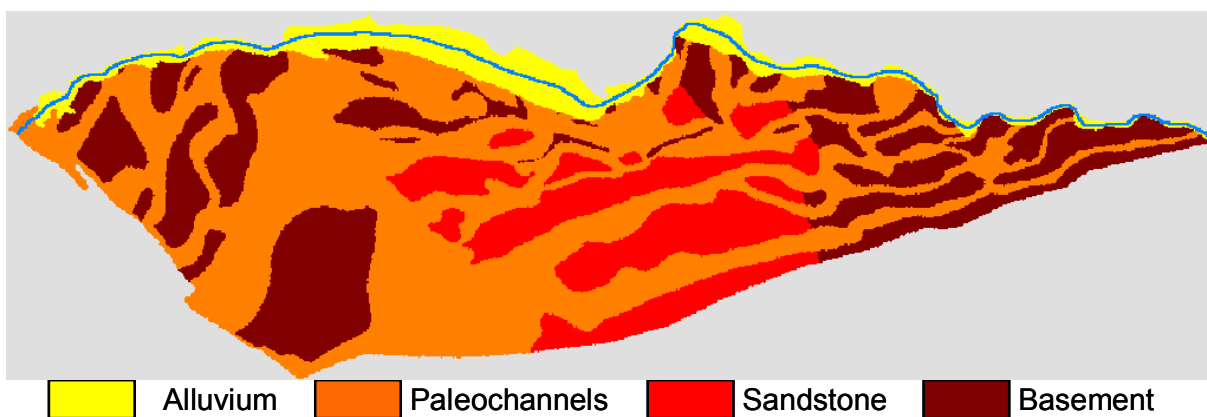


Figure 5.4: Geological subdivisions of the model area.

- c) **Paleochannels:** The Kuiseb incised a network of paleochannels into the basement rocks as well as into the sandstone formation. On the base of the channels, alluvial material was deposited (gravel, calcareous muds and silts). Later, the channels were abandoned and filled with dune sands. The hydraulic conductivity of the paleochannels is not exceptionally high; still they are able to store more water than the sandstone. Their average thickness is set to 105 m.
- d) **Alluvium:** The riverbed of the active Kuiseb consists of highly conductive gravels and sands. It forms the major storage space for groundwater abstraction in the model area and is by far the most productive area concerning groundwater recharge. The average thickness of the alluvium is 30 m.

Table 5.1 resumes the hydraulic properties of the different geological units present in the model area.

Table 5.1: Hydraulic properties of the model area.

	Basement	Sandstone	Paleochannels	Alluvium
Thickness	(100 m)	100 m	105 m	30 m
Horizontal hydraulic conductivity	$1.55 \cdot 10^{-8}$ m/s	$1.00 \cdot 10^{-6}$ m/s	$3.00 \cdot 10^{-6}$ m/s	$4.17 \cdot 10^{-4}$ m/s
Vertical hydraulic conductivity	$1.55 \cdot 10^{-9}$ m/s	$1.00 \cdot 10^{-7}$ m/s	$3.00 \cdot 10^{-7}$ m/s	$4.17 \cdot 10^{-5}$ m/s
Effective porosity	0.1 %	7.0 %	25.0 %	30.0 %
Specific storage	$3.3 \cdot 10^{-6}$	$6.9 \cdot 10^{-5}$	$8.0 \cdot 10^{-4}$	$1.0 \cdot 10^{-4}$
Specific yield	0.09 %	4.00 %	4.40 %	15.00 %

The groundwater model has two layers. The top layer is unconfined; the bottom layer is either confined or unconfined, depending on the groundwater head: if the layer desaturates, vertical leakage from above is limited.

The bottom elevation of the first layer is derived from the thickness of the geological units and the surface elevation:

- 1.) The digital elevation model of the surface was smoothed to get rid of the dune field's sinusoidal waves.
- 2.) The thickness of the respective geological unit was subtracted from the smoothed surface.
- 3.) At places where the basement rocks come to the surface the top layer was assigned an arbitrary thickness (100 m).

The vertical leakance between the two layers was set to the value of the hydraulic conductivity of the basement ($1.55 \cdot 10^{-8}$ m/s).

5.1.4 Recharge

In the steady-state simulations no stream flow routing was used to simulate recharge in the alluvial fill of the Active Kuiseb channel. Instead, the recharge in this area was simulated by adding a constant recharge rate evenly distributed over the whole alluvial surface. The rate of 1.5 million m^3/a was derived from the estimated average annual recharge caused by flash floods. Each of the 10328 cells of the alluvium was assigned a recharge rate of $4.61 \cdot 10^{-10}$ m/s.

5.1.5 Pump wells

The influence of artificial pumping on the groundwater tables is explored in the second steady-state simulation. For this purpose 32 pump wells were inserted at their actual position in the alluvial aquifer of the Kuiseb River (*Figure 5.5*). 5 of the wells are lying within the so-called Dorob South aquifer, close to the downstream end of the alluvium. They are all pumped at a rate of 22.0 m^3/h (with a total of 110.0 m^3/h). 6 wells are located in the Rooibank A aquifer between Rooibank and Ururas. Their pump rates range from 8.7 m^3/h to 32.8 m^3/h with a total abstraction of 138.6 m^3/h . The remaining 21 wells are all situated in the aquifer downstream of Swartbank. The pump rates range from 0.2 m^3/h up to 106.7 m^3/h with a total abstraction rate of 406.1 m^3/h . Summing up all the 32 pump wells leads to an artificial groundwater abstraction of 5.7 million m^3 per year within the model area. The pump rates were provided by DWA (2004). The detailed pump rates are listed in *annex II*.

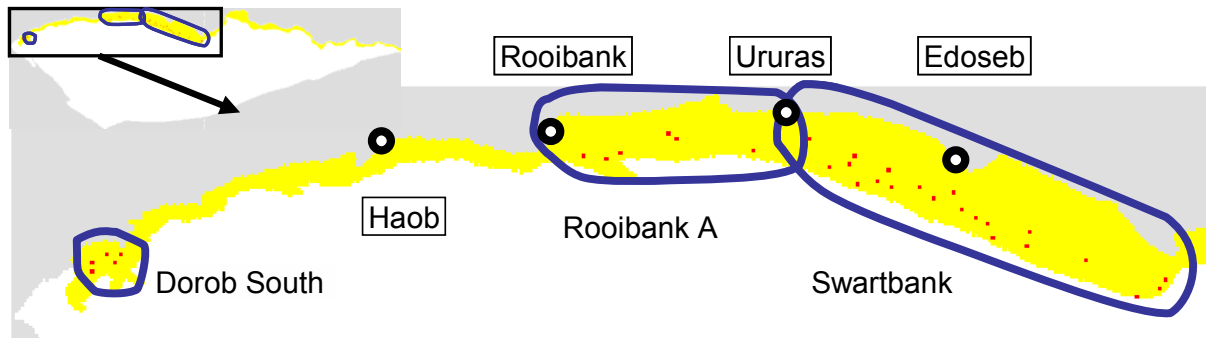


Figure 5.5: The three main groundwater abstraction areas of the Active Kuiseb aquifer: Dorob South, Rooibank A and Swartbank. Location of the pump wells (red dots).

5.1.6 Drain

It was necessary to insert a drain into the model, in order to keep the water table in the alluvium at a reasonable level during the steady-state simulations. The drain has the same position as the river channel and serves as a substitute for water withdrawing processes, including evaporation and water consumption of the vegetation.

5.1.7 Initial conditions

The initial hydraulic heads of the individual simulations build upon each other:

- For the first steady-state natural conditions simulation, the initial hydraulic heads were simply set to the elevation of the top layer surface.
- The steady-state simulation including pump wells used the aquifer heads calculated in the first steady-state simulation. This allows for a closer inspection on how much the pump wells affect the natural groundwater table.
- Finally, the transient simulation was conducted with the aquifer head of the pump wells steady-state simulation. That way, it is possible to quantify the recharge a flood wave adds to the pumped aquifer.

5.2 Input to the hydraulic model

The basis of the hydraulic model is the branch of the Kuiseb which flows along the north-eastern boundary of the model area. No tributaries are considered since they hardly ever

contribute any flow to the area. The branch is divided into 1166 subreaches and has no internal junctions. The bed thickness was set to 1 m and its conductivity to $1.0 \cdot 10^{-4}$ m/s (DAHAN 2006). The slope of the riverbed was extracted from the longitudinal profile of the Kuiseb while it was assured that the transitions between the sections were not too abrupt. The elevation of the riverbed was assumed to be 2 m below the surface of the aquifer cell.

5.2.1 Cross-sections

Cross-sections of the alluvium were available at several points along the Kuiseb. However, only two gauging stations also provide a stage-distribution relation. These are the stations Gobabeb and Rooibank. Unfortunately, the Gobabeb weir cannot be used to determine the hydraulic-geometry parameters since at low to medium flows two distinct channels are present (*Figure 5.6*). Therefore, for the Gobabeb station and the upper part of the model area the following hydraulic-geometry parameters were used:

$$A_0 = 0.0 \quad A_1 = 2.2 \quad A_2 = 0.80$$

$$\text{and} \quad W_1 = 16.0 \quad W_2 = 0.40$$

The values are adjusted to the general shape and flows of the Kuiseb River but not calibrated with a stage-distribution relation.

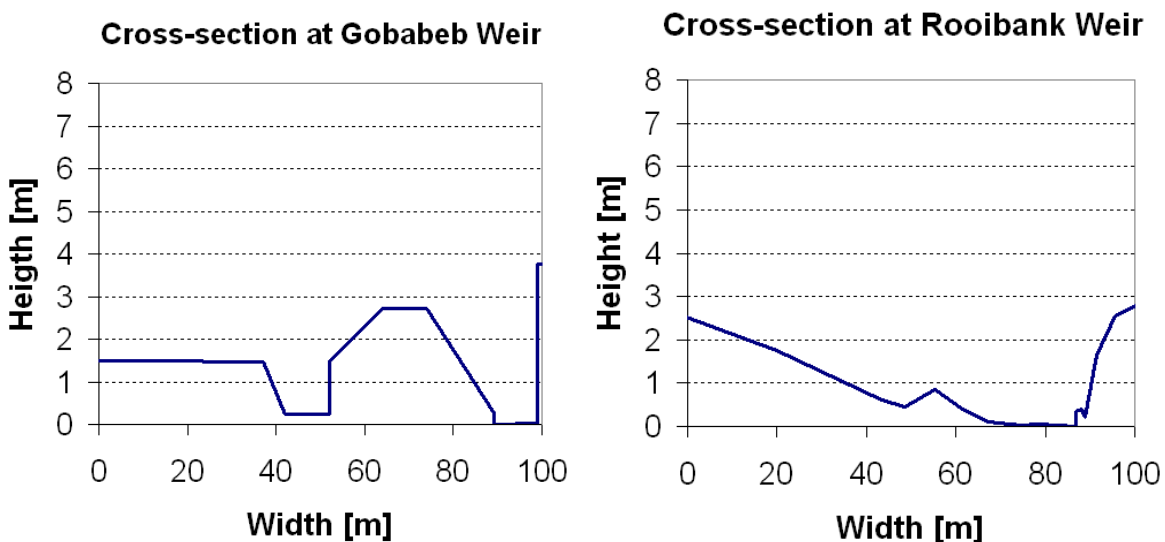


Figure 5.6: Cross-sections of the stream channel at the weirs of Gobabeb and Rooibank.

The Rooibank station allowed for a calibration of the hydraulic-geometry parameters. *Figure 5.7* shows the observed relation of discharge and stream width (respectively cross-sectional area of the stream) as well as the fitted curves along with their equations.

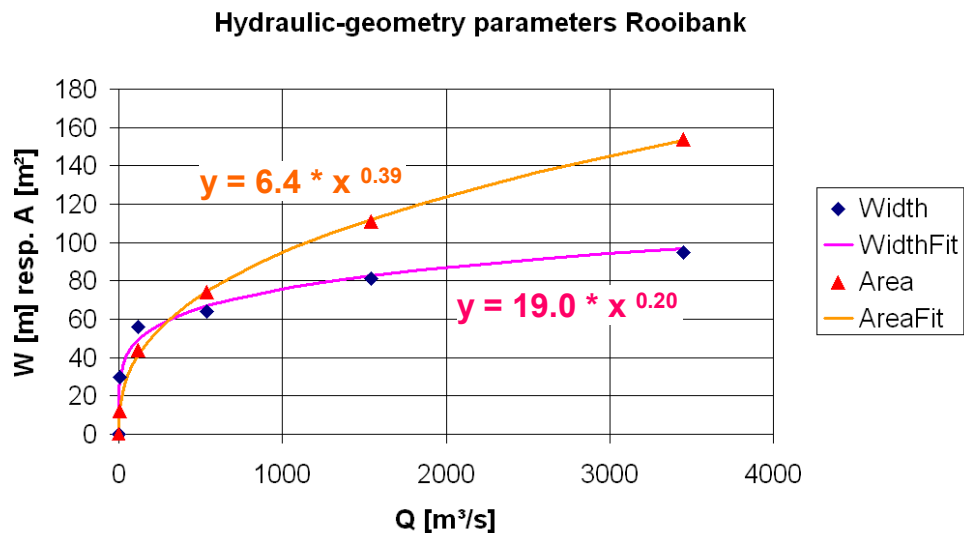


Figure 5.7: Derivation of the hydraulic geometry parameters at Rooibank. Discharge (Q) is plotted against the width (W) and the cross-sectional area (A) of the channel. The fitted curves are labelled with their equations.

Thus, the hydraulic-geometry parameters at Rooibank are:

$$A_0 = 0 \qquad A_1 = 6.4 \qquad A_2 = 0.39$$

and

$$W_1 = 19.0 \qquad W_2 = 0.20$$

The hydraulic-geometry parameters were linearly interpolated along the Kuiseb, from the narrower, deeper channel in the upper part of the area to the wider, flatter channel of the lower part.

5.2.2 Input hydrographs

The floods that were recorded during the years from 1978 until 2000 at Gobabeb were analysed before an input hydrograph was created. The results showed that the median event in this period had a volume of 1.6 million m³, a peak discharge of 24.9 m³/s and a duration of 5 days. The maximum event had a volume of 84.2 million m³, a peak discharge of 595.2 m³/s and a duration of 18 days (KÜLLS & LEISTERT 2006).

The hydrograph in *Figure 5.8* was chosen as input to the flood routing routine. It can be considered a median event with a total volume of 2 million m^3 , a duration of 5 days and a peak discharge of 15 m^3/s .

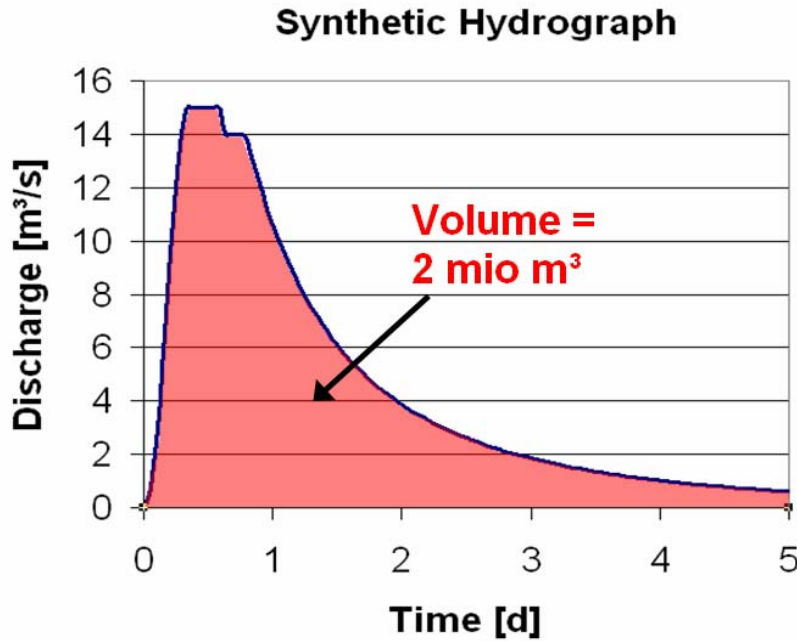


Figure 5.8: Synthetic hydrograph used as input to the routing routine.

Unfortunately, the DAFLOW routing routine was not able to model higher peak discharges in the alluvial channel of the Kuiseb. The gradients of the wave fronts soon became too steep for the diffusion-wave model to work properly. The only possible solution to simulate a bigger discharge volume was to route multiple smaller flood waves in quick succession.

This was accomplished by routing 17 of the aforementioned median floods over a time period of three months (*Figure 5.9*). The accumulated discharge volume equalled 34 million m^3 .

An additional flood wave was routed after 9 months without runoff. This was done to get an impression on how fast the system re-establishes initial conditions after a flood event.

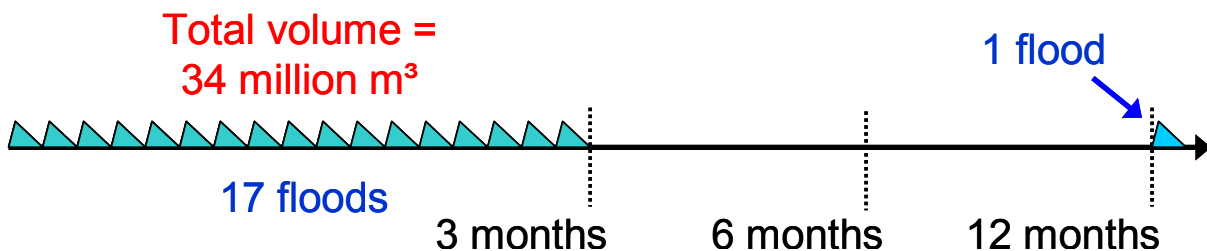


Figure 5.9: Succession of flood waves in the course of the simulation.

The application of this unusual input is an advantage insofar as it indicates the reaction of the system to successive flood waves. However, the routing of a bigger flood wave would add to the overall picture of groundwater recharge in the model area and is recommended for further investigations.

5.3 Conclusion

Three different setups were created for modelling the groundwater situation in the Lower Kuiseb area. The first was a steady-state simulation of the natural system to predict the situation, as it would be without pumping wells. Most of the parameters needed for that, especially the hydraulic aquifer parameters were provided by the GNGEP. Prior to the second model run, the pump wells were added with their respective current pumping rates. And finally the flood routing was set up to monitor the effect that flash floods have on the groundwater system.

6 Results

The simulation of the natural-steady state system, the simulation of the pumped steady-state system and the simulation of the transient system build upon each other. Therefore, especially the examination of the respective differences between the modified versions yields valuable information on the groundwater processes of the Lower Kuiseb.

6.1 Natural steady-state

The simulation of the natural system was accomplished to provide the basic knowledge of the fundamental processes in the model area. The results represent a state of the system that was present before the groundwater abstraction intensified. Of particular interest is the situation in the Kuiseb alluvium. At which place is the groundwater close to the surface or even discharging out of the aquifer? *Figure 6.1* depicts the depths to water table in the alluvium.

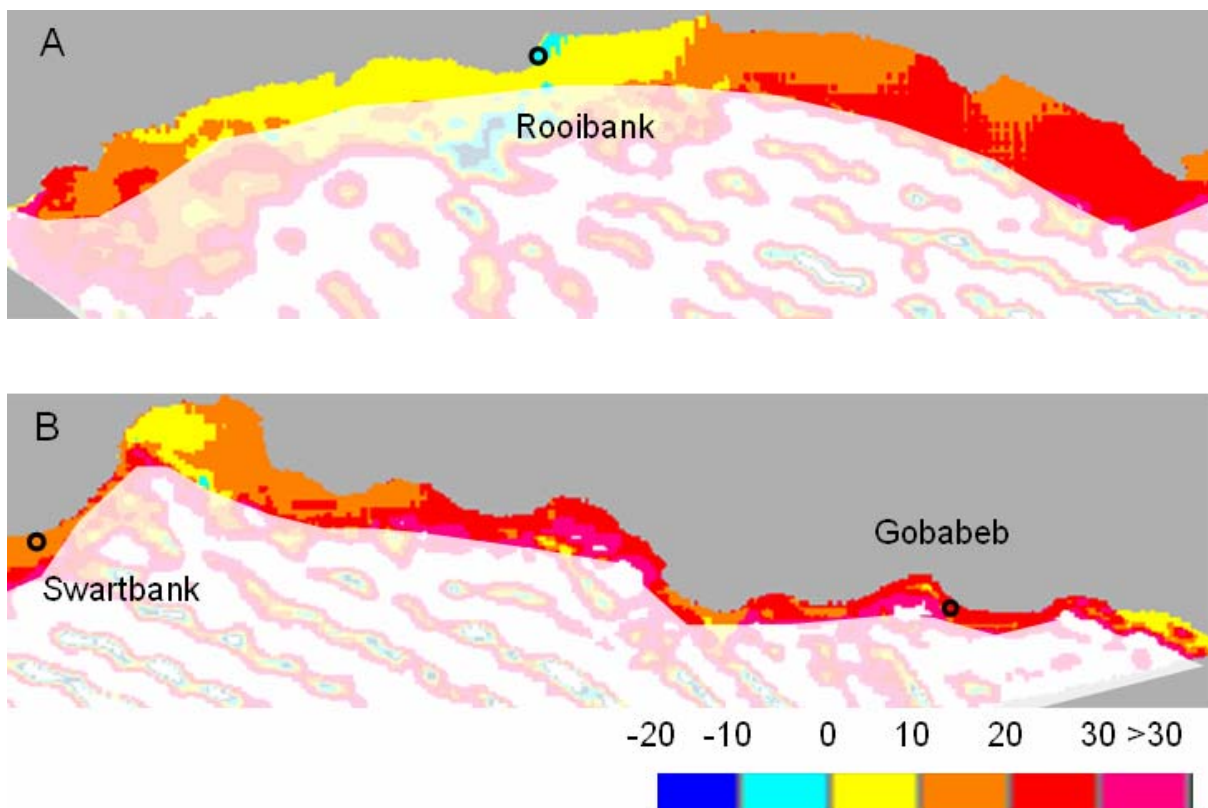


Figure 6.1: Depth to water table (in meters below surface) in the alluvial aquifer of the Lower Kuiseb. A: Lower part of the model area around Rooibank; B: upper part of the model area between Gobabeb and Swartbank.

In the upper part of the model area around Gobabeb, the groundwater tables are rather low, 20 to 30 m below the surface. One has to keep in mind that the alluvium is only 30 m deep, i.e. most of the upper alluvial aquifer is empty by nature. This causes a high potential for infiltration and may serve as an explanation why the bulk of transmission losses already occurs in the narrow channel between Gobabeb and Swartbank. As it is expectable, the depth to water table decreases before the alluvial channel turns eastward some kilometres upstream of Swartbank. There, the width of the alluvium is reduced to a mere 350 m and the groundwater impounds for it cannot maintain its flow intensity in the less conductive geological units below and to the sides.

Downstream of Swartbank, the channel width increases to 2000 m and the water tables drop again to the bottom of the alluvium. Around Rooibank, the depth to water table is considerably small. This is caused by three factors:

- The relatively large alluvial recharge area between Swartbank and Rooibank
- The constriction of the alluvial channel downstream of Rooibank to 800 m
- The short decrease in hydraulic gradient downstream of Rooibank

Approaching the sea, the depth to water table increases again, what is most probably due to the rising hydraulic gradient.

Looking at a cross-section that cuts the model area from south-east to north-west, a trend becomes obvious (see *Figure 6.2*). In the upper parts of the Lower Kuiseb region, the saturated thickness of the top layer is rather small ranging from 35 m to 70 m, whereas in the lower parts the saturated thickness ranges from 70 m up to 105 m. Conversely, the average depth to water table decreases. Thus, the aquifers in the upper part of the model area offer more storage space for infiltration than the aquifers downstream of Swartbank.

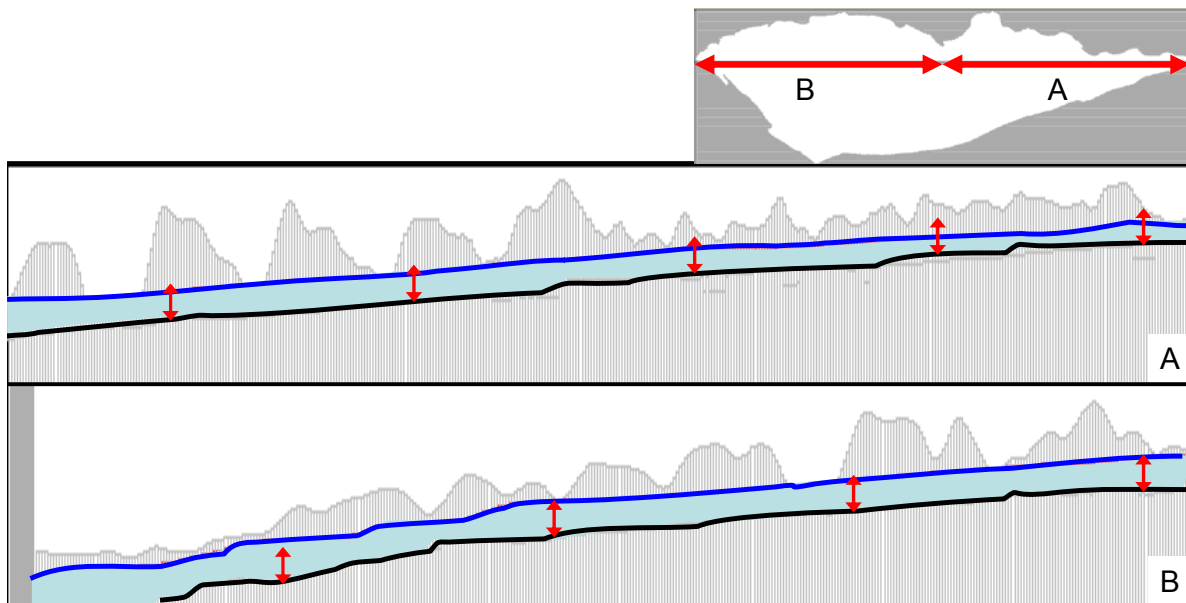


Figure 6.2: Longitudinal cross-section of the model area. Between the bottom of the upper layer (black line) and the groundwater table (blue line) lies the saturated aquifer. The red arrows are approx. 35 m long and show the rising saturated aquifer thickness from the upper (A) to the lower (B) part of the model area.

In order to determine the main flow paths of the Lower Kuiseb area, particle tracking was performed. A grid with the dimensions of 2.5 km times 10 km was superimposed onto the area. The cross points of the grid formed the starting points for the particles (Figure 6.3). The particles were placed on the surface of the top layer.

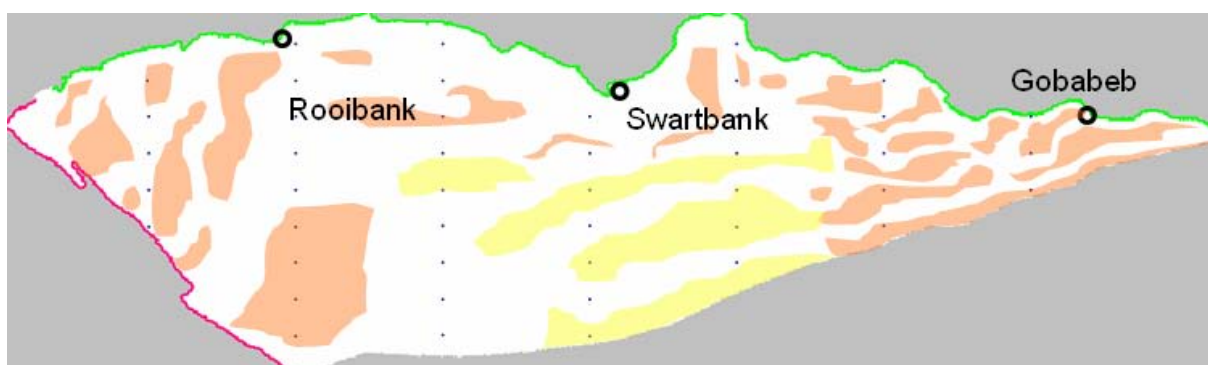


Figure 6.3: Starting point grid for the particle tracking (blue dots). The grid has the dimensions 2.5 km times 10 km.

The flow paths are shown in Figure 6.4. It is obvious that the paleochannels are the main water transport routes inside the aquifer. Once a particle entered one of the paleochannels it is very unlikely that it leaves it again. Three main flow paths can be distinguished that conduct the biggest part of water out of the model area:

- The first flow path is the Active Kuiseb channel in the north of the area.

- The second one is located in the area approximately 10 km north of Anichab, where the model area directly borders the sea
- The third flow path is situated at the southern end of the western border, close to the settlement of Anichab and Sandwich Harbour.

The vast majority of the particles stays in the top layer flowing down the aquifer in either the paleochannels or the alluvium without entering the basement rock.

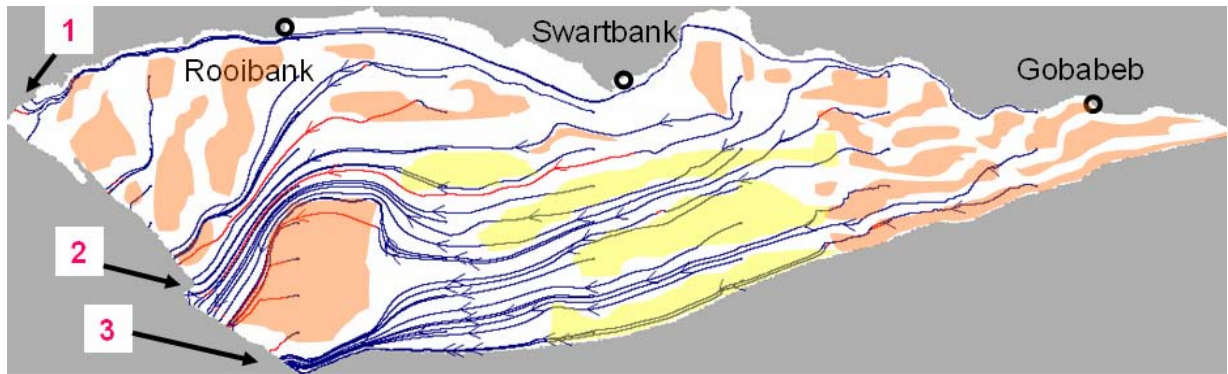


Figure 6.4: Preferred flow paths in the Lower Kuiseb model area. Blue arrows indicate flow in the upper layer, red arrows flow in the bottom layer. 1, 2 and 3 are the main outlets of the modelled aquifer.

Since the recharge to the groundwater is supposed to take place mainly linearly along the Kuiseb and not evenly distributed over the whole area, it was necessary to take a closer look at the flow paths in the alluvial aquifer. In the second simulation of the particle tracking the particles all were placed in the middle of the alluvium just next to a river cell. The results indicate that most of the water that infiltrates into the alluvium stays there until the end (Figure 6.5). Only a small proportion of the particles enters the paleochannels. By far the majority is transported inside the highly conductive alluvial channel. Interestingly, between Swartbank and Rooibank not a single particle leaves to the paleochannel which, in this section, has the largest inlet through a gap in the basement rocks.

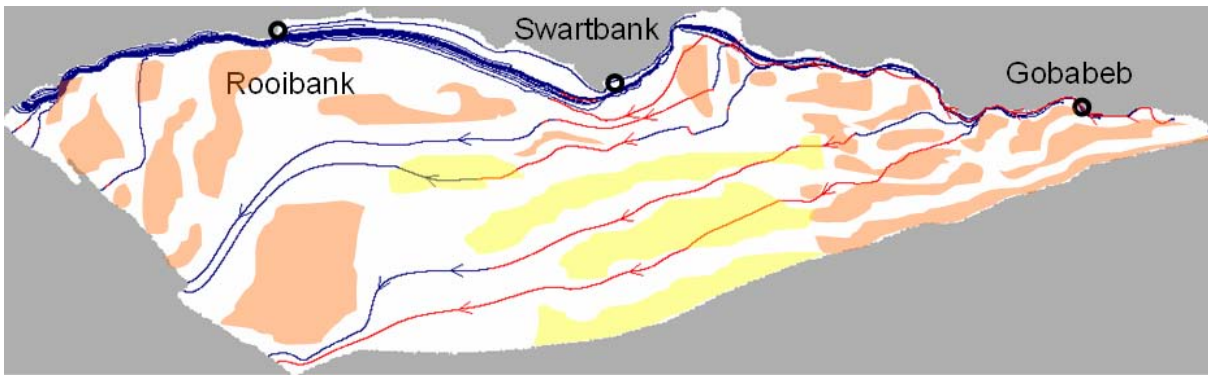


Figure 6.5: Flow paths originating in the alluvial aquifer. Blue arrows indicate flow in the upper layer, red arrows flow in the bottom layer.

6.2 Pumped steady-state

At the moment, the alluvial aquifer between Swartbank and Rooibank is the main source area for the extraction of water for domestic and industrial use in the region. To receive an impression of the impact that the current abstraction rate will have on the future groundwater levels, the model of the natural system was extended. The current pump rates of the 32 discharge wells were added to the top layer while all the other parameters were maintained.

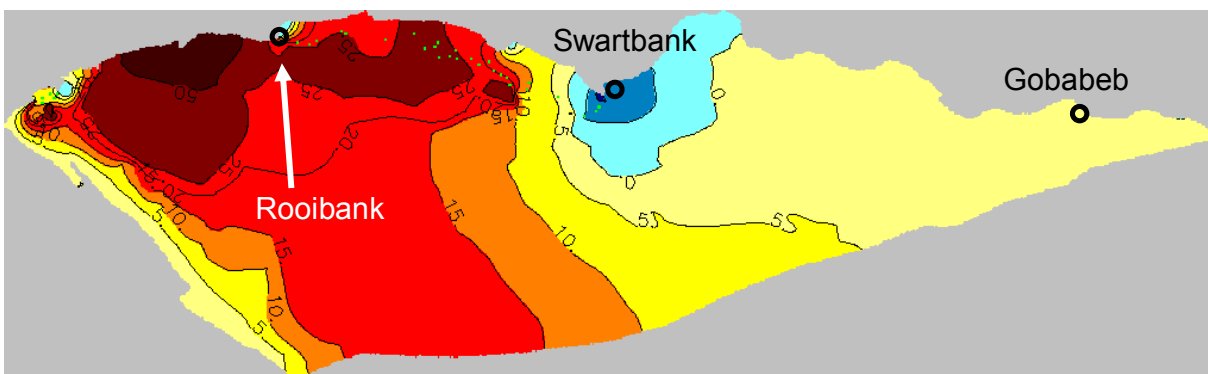


Figure 6.6: Simulation of drawdowns caused by water abstraction from pump wells (green dots) in the Kuiseb alluvial aquifer.

The drawdown of the water levels in the model area caused by artificial groundwater abstraction is shown in *Figure 6.6*. The upper part of the area is only affected to a small extent by slightly lower water tables whereas the lower part suffers up to 50 m of drawdown and more. The whole aquifer downstream of Swartbank is pumped until depletion (see *Figure 6.7*). Between Swartbank and Rooibank the water tables just stop falling because the pump wells do not penetrate below the top aquifer. The largest drop of groundwater levels can be observed downstream of Rooibank. Interestingly, it is the only area where the water levels

drop below the alluvial aquifer, although there are not even pump wells in the direct vicinity. This happens due to the convex profile of the area. Here, the water table between the two pumped areas cuts more or less straight through the aquifer.

The groundwater abstraction also affects the parts of the area which are situated to the south of the pump wells. Groundwater levels drop 15 to 20 m there.

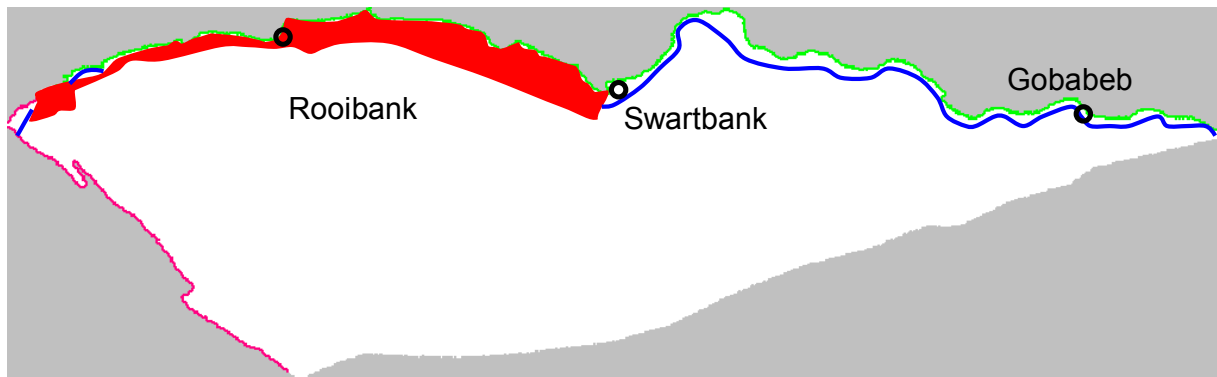


Figure 6.7: Total depletion of the aquifer downstream of Swartbank (red area).

According to the simulation, there are also three areas along the alluvial channel which experience a groundwater table rise as a result of the pumping. They are located around the settlements of Swartbank, Rooibank and just upstream of Dorob. This observation can be ascribed to the fact that around the pump well areas, the groundwater levels drop. That causes the reduction of the aquifer's hydraulic cross-section. Hence, the transmissivity of the alluvial aquifer decreases. The water flowing in from the upper part of the model area dams up in front of these groundwater flow constrictions.

6.3 Pumped transient

The transient simulation was run for 9480 time steps, each 1 hour long. That added up to 13 months in total. In the first three months, flood water entered the model area through the Kuiseb River channel from south-west. The total volume of 34 million m³ inflow was subdivided into 17 separate flood waves with median flood properties (peak discharge: 15 m³/s, volume: 2 million m³, duration: 5 days). While all the boundary conditions (such as pump rates and constant flux boundaries) were held steady throughout the simulation, the inflow in the channel ended after three months. That way, it was possible to first monitor the instantaneous effects of flood waves on groundwater recharge and then have a closer look at the processes taking place after the flood has passed.

Figure 6.8 shows the situation after 5 days, that is, after the first flood wave has fully entered the model area.

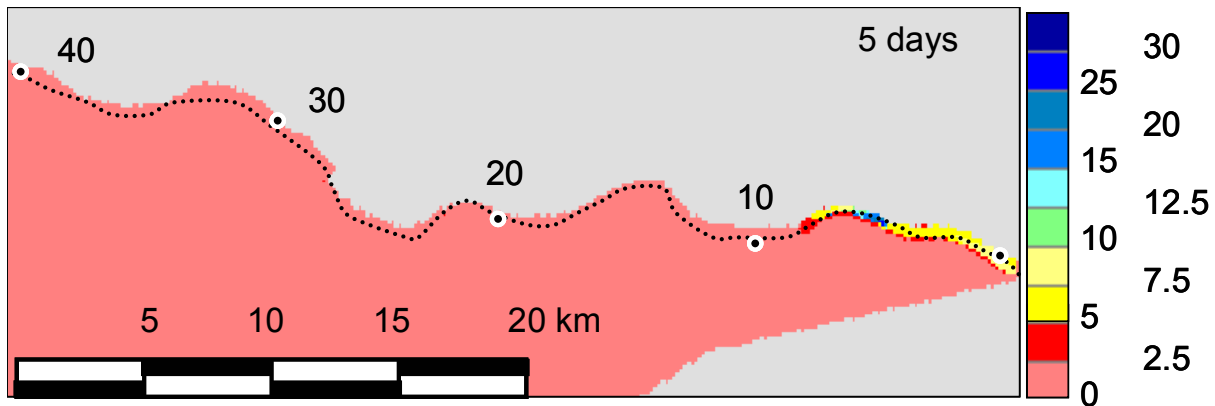


Figure 6.8: Rise of groundwater table (in meters) after a flood event with a duration of 5 days. The white circles indicate the river kilometers from the inflow to the model area.

The flood wave does not reach the 10 km point in the riverbed. Instead, all the water infiltrates into the alluvium raising the water table in this section up to the riverbed elevation. After 10 days and 2 flood waves the process of filling up the aquifer continues further downstream. Now the flood wave passes the 10 km point and successively saturates the whole alluvium (see Figure 6.9).

It is remarkable that the flood wave is not able to proceed before the water table in the alluvium reaches ground level. Needless to say, that this behaviour would change once the peak discharge of the flood wave rose above the maximum infiltration rate. Unfortunately, this scenario cannot be simulated with the applied diffusion-wave routing model since it causes the rising limb of the flood wave to steepen until stability problems lead to the abortion of the simulation.

Nevertheless, what can be stated is that median floods fill the aquifer in the upper part of the model area more or less completely down to the point where they finally disappear.

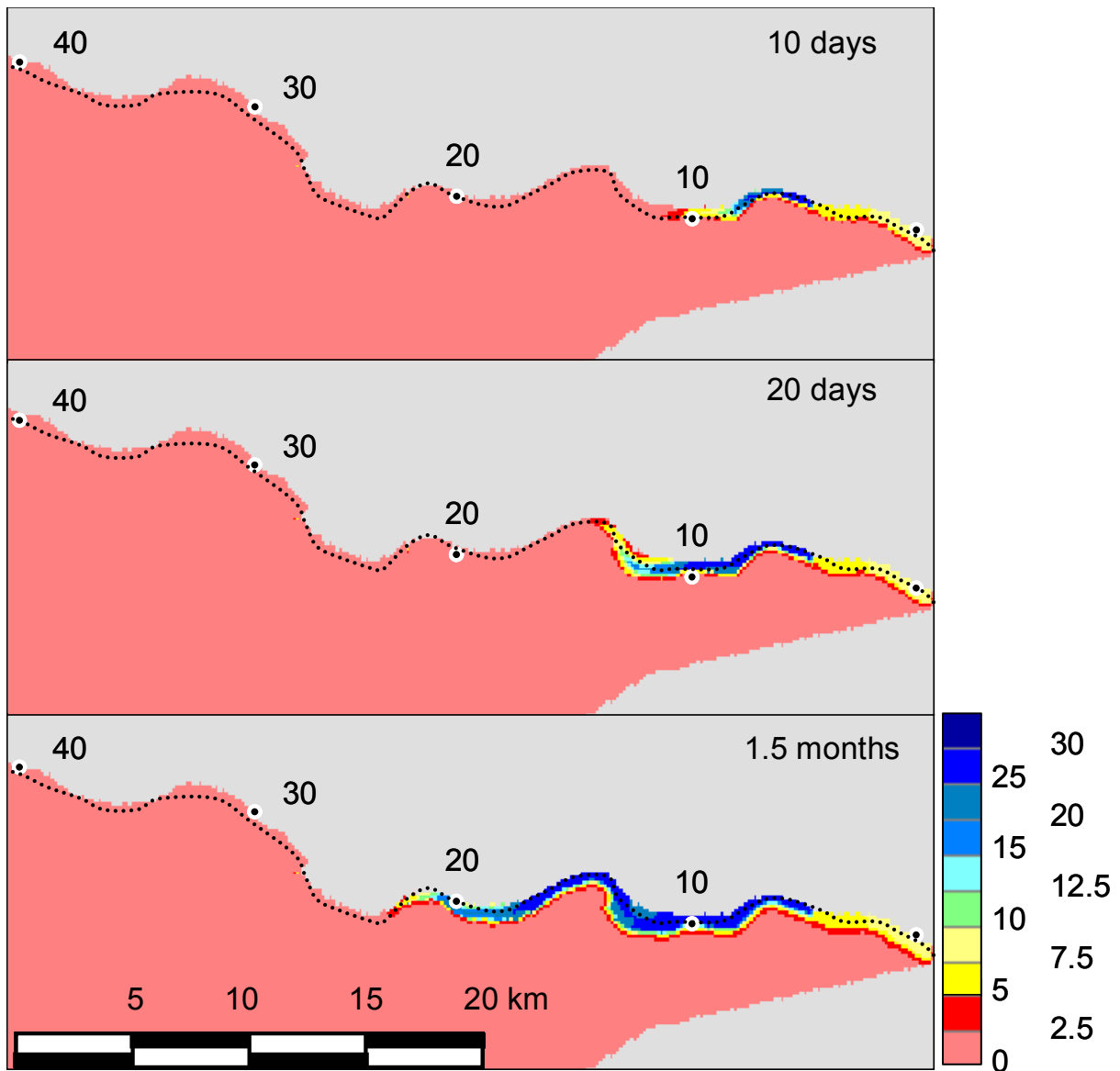


Figure 6.9: Progression of the recharge front in the Active Kuiseb alluvium after 10, 20 and 46 days. Rise of water tables in meters.

The saturation of the aquifer reaches km 15 after 20 days and km 22 after 1.5 months. These observations of temporal-spatial relations can be used to give approximate values of groundwater recharge in the respective river sections as will be explained in the following example:

The discharges of the successive flood waves at the different points along the river are plotted against the time in *Figure 6.10*. It takes around 0.7 months until a flood wave flows past the point at km 10 without losing water due to infiltration. This indicates that from this moment on, the alluvial aquifer is saturated upstream of km 10. Now, as far as the hydrograph of the point at km 20 is concerned, it is not influenced anymore after 1.8 months. Therefore, it needs 1.1 months to fill the aquifer between km 10 and km 20. Within 1.1 months 7 floods enter the aquifer section, each with a volume of 2 million m³. That means the groundwater recharge in

this section of the river is about 14 million m³. In comparison to this, the recharge between km 20 and 30 only amounts to 8 million m³ (0.6 months to fill → 4 floods → 8 million m³).

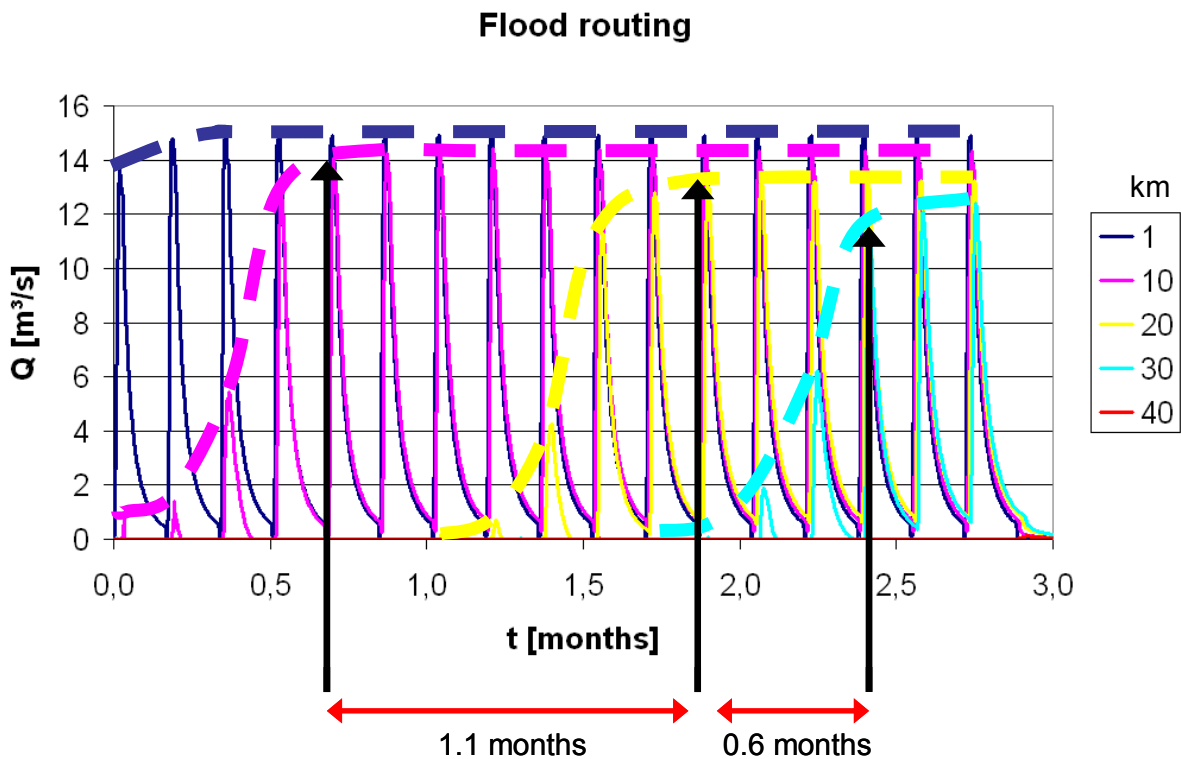


Figure 6.10: Flood hydrographs from the transient flood routing at 5 points along the river. The black arrows mark the time when the aquifer is filled and water no longer infiltrates. For example, the aquifer section between 10 and 20 km needs 1.1 months to fill up completely.

The last of the 17 floods still does not flow further than 35 km into the model area. After 3 months of quasi-constant stream flow in the channel almost the whole alluvium of the upper part of the Lower Kuiseb is saturated.

What happens now that the infiltration from the ephemeral stream stops? Do the paleochannels that branch off the Active Kuiseb play an important role in distributing the water away from the alluvium? The model was run another 9 months after the last flood wave contributed to the groundwater recharge. *Figure 6.11* presents the results of the simulation.

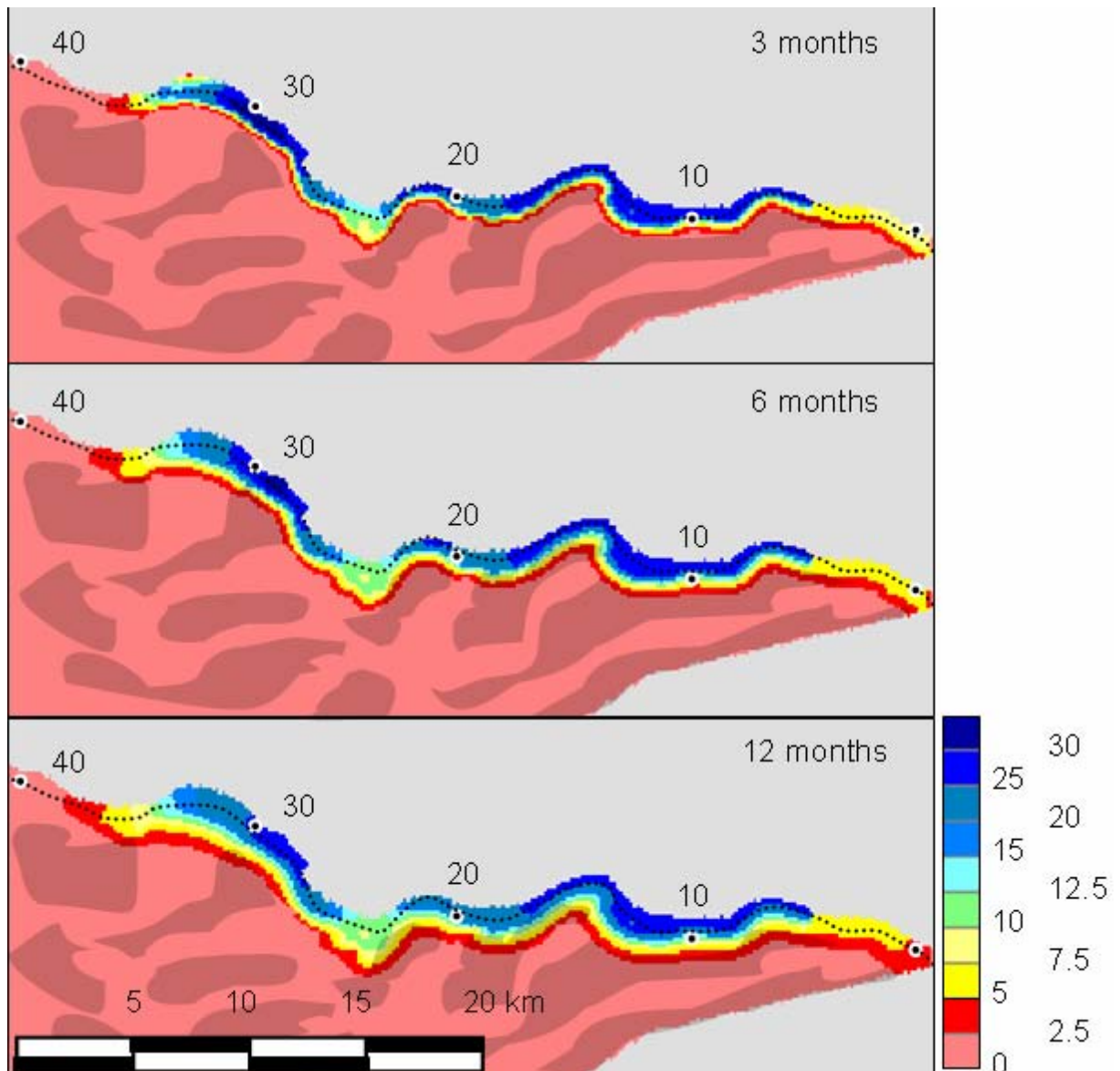


Figure 6.11: Behaviour of the aquifer after the flooding ended. Redistribution of infiltrated water. Rise of water tables in meters.

Surprisingly, the high groundwater table rests relatively stable in the alluvial aquifer. It does not flow much further downstream in the aquifer, as one could have expected. It only shifts about 1.5 km down in the alluvial channel. Instead, it starts diffusing to the area that surrounds it. The paleochannels are not recognisable as preferred flow paths after one year. However, this changes, once longer periods of time are modelled. Since the water maintains the relatively high hydraulic gradient from the alluvial aquifer to the paleochannels, there is a good chance they serve as paths to transport water away from the Active Kuiseb channel. In this case, the rather small inclination and aquifer cross-section of the Active Kuiseb in the upper part of the model area between Gobabeb and Swartbank would compensate for the two orders of magnitude difference in hydraulic conductivity between the alluvium and the paleochannels.

Further down the Kuseb, between Swartbank and Rooibank, the slope of the alluvium is higher. Therefore, the groundwater tends to flow down the aquifer of the Active Kuseb instead of entering the paleochannel system at the widest inlet which is situated halfway in between Swartbank and Rooibank.

An additional flood wave was routed in the Kuseb after the 12th month of the simulation, i.e. after 9 months of no-flow conditions in the channel. This was done to compare the differences of:

- the first flood wave that enters the area after a long period of no-flow (initial conditions from the steady-state simulation),
- the flood wave that enters the area as the last of a number of consecutive flood waves (the last of the 17 floods) and
- the flood wave that appears 9 months after the last big flood event.

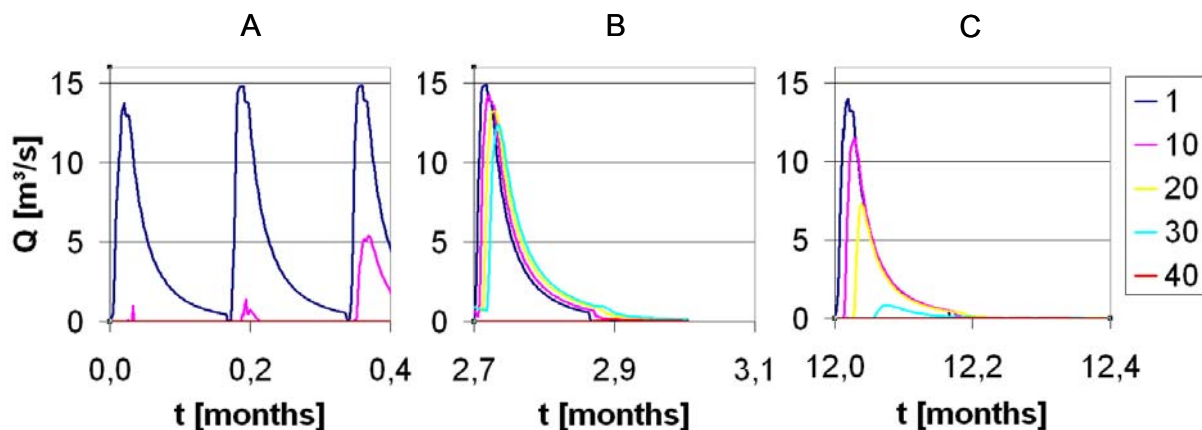


Figure 6.12: Comparison of three sets of hydrographs. A: very first floods from the beginning of the simulation; B: last of the 17 flood waves in straight succession; C: flood wave after 9 months of no-flow in the channel. The different colours of the hydrographs represent the points along the river where they are recorded (in km from the inflow point).

Figure 6.12 presents the result. The hydrographs from flood C prove that the alluvium between km 1 and km 30 still is saturated to a large extent. Just like flood B, flood C continues to pass the 30 km point, whereas flood A only managed to flow 10 km before it infiltrated completely into the aquifer.

Given the fact that flood C has a volume of 2 million m³ and fills up the aquifer again on a 30 km stretch, it can be stated that in the course of the preceding 9 months approximately 2 million m³ of water flew out of the alluvial channel section between km 1 and km 30. This transport was directed both down the Active Kuseb channel and towards the paleochannels.

6.4 Conclusion

The natural steady-state simulation confirmed the shallow water tables in parts of the alluvial aquifer of the Kuiseb. It also showed the general trend of decreasing depth to water table from the upper part of the model area towards the lower part.

Particle tracking determined the main flow paths in the system and proved that the paleochannels, along with the Kuiseb alluvium, are the preferred groundwater flow regions within the aquifer. It also supported the assumption that water which infiltrates into the Kuiseb alluvium is likely to remain there on its way downstream. Only a minor proportion of the groundwater recharge from flash floods actually enters the paleochannels.

It was found, that a continued pumping of the Kuiseb alluvium will finally lead to the depletion of most parts of the aquifer section downstream of Swartbank.

Median-sized flash floods fill the alluvium in the upper part of the area completely before they manage to pass on to the next aquifer section. The alluvium reacts very quickly to these floods. However, after the flooding ended, the high water levels remain very stable, more diffusing into the surrounding area than moving down the alluvium. This allows for at least some recharge to the paleochannels.

7 Validation and Uncertainty

The best, most reliable way to validate simulation results of a groundwater model is to compare the calculated hydraulic heads of the groundwater to actual measured data. In case, major discrepancies are discovered, it is attempted to calibrate certain model parameters until consistency is achieved. Unfortunately, no such data was available within the scope of this thesis.

Instead of this, the modelling results were compared with existing knowledge on the processes and conditions in the system of the model area. For example:

- It is well-known that the groundwater tables in the upper part of the model area between Gobabeb and Swartbank are extremely stable during periods of no-flow. Once filled up by a periodically occurring flash flood, they drop only very slowly (DAHAN 2007).
 - This behaviour was also observed in the MODFLOW/DAFLOW simulation of groundwater – surface water interaction.

Further down the Lower Kuiseb area, within the sand dunes of the paleochannel section, other observations validate the quality of the modelling:

- At the bottom of some of the interdune valleys, there is vegetation present, which benefits from extremely shallow groundwater levels. The sand is saturated already in a depth of 1 to 2 m in some of those valleys.
 - The same situation occurs when the area is explored with the applied groundwater model. In some interdune valleys, the water table even rises above surface elevation.
- Along the whole coast line, with a higher frequency around Sandwich Harbour, groundwater reaches the surface and feeds numerous wells.
 - Not surprisingly, this area was identified as one of the main outlets of the paleochannel aquifer.
- Lately, the wells at the coast line are less productive; some of them even stopped discharging.
 - This can be associated with the intensified pumping in the Active Kuiseb alluvium that is supposed to cause a significant drop of water tables (around 15 m) even on the south-western border.

The depletion of the alluvial aquifer of the Kuiseb due to excessive groundwater abstraction is a prediction that has already been made by other researchers (DWA 1987, SCHMIDT & PLÖTHNER 1999).

The results obtained from the coupled modelling approach are expected to adequately represent the hydrological system of the Lower Kuiseb. It is an advantage of the coupled approach that it produces as output both simulated hydrographs and groundwater tables. This way, the modeller is provided with more complex information to compare with the real situation.

The data used to set up the model can be considered of sufficiently good quality.

- Especially the parameters defined by the German-Namibian Groundwater Exploration Project (GNREP) are based on extensive field work (including pump tests and geophysics). These parameters include the hydraulic aquifer properties and the general aquifer geometry.
- The boundary conditions could be determined with high accuracy. Earlier research confirmed the inflow from the northern basement. Both the southern and western boundaries are clearly defined (by a geological fault line and the Atlantic Ocean).
- The digital elevation model proved to be less precise. No correct elevation data exists of the dune field to the south of the Kuiseb River. Obviously due to radar shadow, the interdune valleys could not be captured. Therefore, the elevation of this area was derived from an algorithm that simulates the dune undulations from similar dune regions. However, the average elevation of the dune area is correct and moreover, the exact elevation of the aquifer surface is not required since the sandy dunes do not play an important role for the groundwater system.
- The pump rates of the wells in the Active Kuiseb alluvium are approved and fairly up-to-date (from 2004).
- The assumptions on the general flood properties (annualities of duration, peak discharge and volume) stand on a firm basis of statistical analysis.
- The lack of more detailed information on the channel geometry is probably the factor adding most uncertainty to the results. Although there is a multitude of measured channel cross-sections, only the two at Gobabeb and Rooibank also provide a stage-distribution relation (but the one at Gobabeb is not useable for determining the hydraulic geometry parameters).

To sum up, although some uncertainties remain, the overall quality of the results should be assured.

8 Overall Conclusions

The two main objectives of this thesis were to contribute to the understanding of indirect groundwater recharge in general and to add to the knowledge on the groundwater system and groundwater recharge in the Lower Kuiseb area.

Concerning the general understanding of indirect recharge from flash floods, the following conclusions can be drawn:

- The depth to water table has a major influence on groundwater recharge. It determines the space that is available for infiltrating water. The recharge volume is linearly dependent on the depth to water table.
- The aquifer thickness influences groundwater recharge insofar as thicker aquifers have the ability to transport more water in the saturated zone away from the point of infiltration. The recharge volume is also linearly dependent on aquifer thickness.
 - An increase of depth to water table of 1 m has roughly the same effect on recharge volumes as an increase of aquifer thickness of 100 m.
- The hydraulic conductivity of the aquifer is important for the recharge process as long as it does not exceed the hydraulic conductivity of the riverbed.
 - In most cases it restricts the velocity of water transport away from the point of infiltration.
 - However, it is of no importance if the riverbed conductivity restricts the infiltration.
- Two main recharge behaviours could be specified:
 - 1) In case the hydraulic conductivity of the riverbed is lower than the one of the aquifer:
 - Water infiltrates straight down to the groundwater table and is distributed evenly over the whole aquifer. Aquifer heads rise more or less simultaneously in the alluvial cross-section.
 - 2) In case the hydraulic conductivity decreases with distance from the channel:
 - The groundwater table mounts directly below the stream channel, restricting further infiltration. Large parts of the aquifer remain uninfluenced.
 - The front of a flash flood tends to steepen because infiltration rates decrease with time.
- The recharge volume depends more on the duration of a flood wave than on its peak discharge or volume.

-
- The influence of the hydraulic gradient is rather small, since both the flood duration and the discharge stay the same for all the points along the river.
 - The recharge behaviour of successive flash floods can differ considerably. If the first flood raises the groundwater table directly below the channel, the second flood may not have the possibility to infiltrate anymore. That way, a flash flood can pass an aquifer which is dry in most parts on top of a small strip of mounted groundwater.

For the Lower Kuiseb catchment the results include:

- The depth to water table is generally greater in the upper part of the model area and decreases downstream. This is valid both for the dune area and for the Active Kuiseb alluvium.
- Most of the water that infiltrates into the Active Kuiseb alluvium remains there on its way downstream. Only a small proportion enters the paleochannels.
- Since the bulk of groundwater recharge takes place in the alluvial channel of the Active Kuiseb, it constitutes the main flow path for groundwater in the model area.
- The paleochannels serve as preferred flow paths within the model area.
- Water tables in the alluvium of the upper part of the model area rise quickly during a flood event but remain relatively stable afterwards.
- A median flood event with a peak flow of 15 m³/s fills the alluvium between Gobabeb and Swartbank completely up to the point where it finally infiltrates.
- Continuing the abstraction of water with the current pump rates will eventually lead to a total depletion of the alluvial aquifer downstream of Swartbank.

Regarding the general applicability of MODFLOW/DAFLOW:

- The DAFLOW stream routing routine proved to be very sensitive concerning the flood wave input. Especially the increase of slope of the rising limb often led to a sudden abortion of the program.
- Since the steepening of the wave front is one of the main characteristics of a flash flood, important aspects of groundwater recharge cannot always be simulated properly by MODFLOW/DAFLOW.
 - This includes waves of short duration but high peak flows that flow past a stream section before they have filled up the cell below the stream channel.
- Higher hydraulic conductivities of the aquifer are more difficult to simulate.

- Apart from these problems, MODFLOW/DAFLOW can be considered a useful tool for simulating flash floods in ephemeral streams.

Bibliography

- ABBOTT, M.B. ET AL. (1986): An introduction to the European Hydrological System – Système Hydrologique Européen, “SHE”, 2: Structure of a physically-based, distributed modelling system. In: *Journal of Hydrology*, 87: pp. 61-77. Elsevier, Amsterdam.
- AIN (ASSESSMENT INTERCONSULT NAMIBIA LTD) (1999): Preliminary Environmental Assessment of proposed development at the Gobabeb Training and Research Centre, March 1999.
- BEVEN, K. & KIRKBY, M.J. (1993): Channel Network Hydrology, p. 91. John Wiley & Sons, New York.
- BLOM, L. (1978): A report on the ground water investigations of the Lower Kuiseb River. Geohydrological Report 2990/1, DWA-Archive No. 89/1316. Department of Water Affairs, Windhoek.
- CHIANG, W.-H. & KINZELBACH, W. (1998): Processing MODFLOW: A simulation system for modeling groundwater flow and pollution. User’s Manual. Scientific Software Group, Washington.
- DAHAN, O. (2006, 2007): Personal communication.
- DEPARTMENT OF WATER AFFAIRS (1987): The Kuiseb Environment Project – An update of the hydrological, geohydrological and plant ecological aspects. Report Nr: W87/7. Department of Water Affairs, Windhoek.
- DEPARTMENT OF WATER AFFAIRS (2004): Personal Communication with J. Mareis, NamWater, Rooibank.
- FREEZE, R.A. (1972): Role of Subsurface Flow in Generating Surface Runoff 1. Base Flow Contributions to Channel Flow. In: *Water Resources Research*, 8 (3): pp. 609-623. American Geophysical Union, Washington.
- HENDRICKX, M.H. & WALKER, G.R. (1997): Recharge from precipitation. In: *Simmers, I. (Editor): Recharge of phreatic aquifers in (semi-) arid areas*, p. 21. Balkema, Rotterdam.
- JOBSON, H.E. (1989): Users manual for an open-channel streamflow model based on the diffusion analogy. In: *Water-Resources Investigations*, 89-4133. USGS, Reston.
- JOBSON, H.E. & HARBAUGH, A.W. (1999): Modifications to the Diffusion Analogy Surface-Water Flow Model (DAFLOW) for Coupling to the Modular Finite-Difference Ground-Water Flow Model (MODFLOW). In: *U.S. Geological Survey, Open-file Report 99-217*. USGS, Reston.
- KLAUS, J. (2007): Personal Communication.

- KÜLLS, C. & LEISTERT, H. (2006): Statistical analysis of runoff events – Results for the River Kuiseb, Namibia. Interim Report for WADE, GOCE-CT-2003-506680-WADE. 17 p, 15 fig., 7 tab. Institute of Hydrology, Freiburg.
- LENZ, R., GROBBELAAR, H. & DJAMA, M. (1995): Groundwater Exploration in the Kuiseb Dune Area. Report of the German-Namibian Groundwater Exploration Project (GNAGEP), Volume D-1. Windhoek (DWA) and Hannover (BGR).
- LEOPOLD, L.B. & MADDOCK, T. (1953): The hydraulic geometry of stream channels and some physiographic implications. In: *U.S. Geological Survey Professional Paper 252*. USGS, Reston.
- MCDONALD, M.G. & HARBAUGH, A.W. (1988): A modular three-dimensional finite-difference ground-water flow model. In: *Water-Resources Investigations*, Book 6. USGS, Denver.
- MUINJO, K. (1998): Groundwater modelling of the Lower Kuiseb River between Rooibank and Gobabeb gauging stations. M.Sc. degree project. Department of Civil and Environmental Engineering, Land and Water Resources. Thesis report series 1998, 8. Royal Institute of Technology, Stockholm.
- NAMWATER (1998): The impact of the 1997 flood events in the Lower Kuiseb river on the recharge to the Lower Kuiseb aquifers. Compiled by Geohydrology Division, Ref: NWC-WR-7/1/6/3-REP.
- NEMETH, M.S., WILCOX, W.M. & SOLO-GABRIELE, H.M. (2003): Evaluation of the Use of Reach Transmissivity to Quantify Exchange between Groundwater and Surface Water. In: *Journal of Hydrology*, 274: pp. 145-159. Elsevier, Amsterdam.
- NISWONGER, R.G. & PRUDIC, D.E. (2004): Modeling Variably Saturated Flow Using Kinematic Waves in MODFLOW. In: *Groundwater Recharge in a Desert Environment: The Southwestern United States*. Water Science and Application 9. American Geophysical Union, Washington, DC.
- PERKINS, S.P. & KOUSSIS, A.D. (1996): Stream-aquifer interaction model with diffusive wave routing. In: *Journal of Hydraulic Engineering*, 122 (4): pp. 4-12. American Society of Civil Engineers, New York.
- SCHMIDT, G. (1995): Geohydraulical investigations and groundwater modelling, Kuiseb Dune Area. Report of the German-Namibian Groundwater Exploration Project (GNAGEP), Volume E-1. Windhoek (DWA) and Hannover (BGR).
- SCHMIDT, G. & PLÖTHNER, D. (1999): Abschätzung der Grundwasservorräte im Fluß- und Dünengebiet des Unteren Kuiseb, Namibia. In: *Zeitschrift für angewandte Geologie*, 45 (3). Bundesanstalt für Geowissenschaften und Rohstoffe, Stuttgart.
- SCHMITZ, A. (2004): Transmission losses and soil moisture dynamics in the alluvial fill of the Kuiseb river, Namibia. Diploma Thesis at the Institute of Hydrology, Freiburg.

- STALL, J.B. & YANG, C.T. (1970): Hydraulic geometry of 12 selected stream systems of the United States. In: *Illinois State Water Survey Research Report*, No. 32, July. University of Illinois, Water Resources Center, Urbana.
- SWAIN, E.D. & WEXLER, E.J. (1996): A coupled surface-water and groundwater model (MODBRANCH) for simulation of stream-aquifer interaction. In: *Techniques of Water-Resources Investigations of the United States Geological Survey*, Book 6, Chapter A6. USGS, Washington.
- THOMS, R.B. (2003): Simulating fully coupled overland and variably saturated subsurface flow using MODFLOW. Master Thesis. Oregon Health and Science University.
- VANDERKWAAK, J.E. (1999): Numerical simulation of flow and chemical transport in integrated surface-subsurface hydrologic systems. PhD Dissertation. University of Waterloo, Waterloo.
- WNNR (WETENSKAPLIKE EN NYWERHEID NAVORSINGS RAAD) (1984): Sintese van fisies prosesse in en om Walvisbaai-strandmeer. WNNR Verlag 8424, Nasionale Navorsingsinstituut vir Oseanografie, afdeling Sedimentdinamika.

Annex I

List of abbreviations and symbols:

1-D		One-dimensional
2-D		Two-dimensional
3-D		Three-dimensional
DAFLOW		Diffusion analogy surface-water flow model
MODFLOW		Modular finite-difference groundwater flow model
m a.s.l.	[m]	Meters above sea level
Q	[m ³ /s]	Discharge
X	[m]	Distance along channel
A	[m ²]	Cross-sectional area
t	[s]	Time
U	[m/s]	Velocity
g	[m ² /s]	Acceleration of gravity
Y	[m]	Depth
S _f	[-]	Friction slope
S _o	[-]	Streambed slope
D _f	[-]	Wave diffusion coefficient
Q _s	[m ³ /s]	Flow under steady uniform conditions
C	[m/s]	Celerity of moving wave
A ₀	[m ²]	Average cross-sectional area at zero flow
A ₁	[-]	Hydraulic geometry coefficient for area
A ₂	[-]	Hydraulic geometry exponent for area
W	[m]	Top width of channel
W ₁	[-]	Hydraulic geometry coefficient for width
W ₂	[-]	Hydraulic geometry exponent for width
K _{be}	[m/s]	Hydraulic conductivity of riverbed
K _{aq}	[m/s]	Hydraulic conductivity of aquifer
H or h	[m]	Head of aquifer
B _e	[m]	Average elevation of riverbed
B _t	[m]	Thickness of streambed
S _{ep}	[]	Seepage flow
V	[m ³]	Volume
i	[m]	Additional change in aquifer head due to infiltration
Depth to WTable or DWT	[m]	Depth to water table
AqTh or AT	[m]	Aquifer thickness
Inf	[m ³ /s]	Rate of infiltration / rate of exfiltration

Annex II

Location and pump rates of the abstraction wells in the Kuiseb alluvium:

Well Number	Easting	Northing	Pump rate [m ³ /h]	Abstraction total [m ³ /a]
Rooibank				
22129	465420	7435329	32.6	
27745	465902	7434702	24.9	
16592	466432	7434461	32.8	
10786	468552	7432774	17.7	
29412	468263	7433690	22.0	
35847	468311	7433642	8.7	1,215,137
Swartbank				
10657	471781	7430509	15.4	
20151	471733	7429256	25.9	
20149	472311	7428919	3.4	
20150	472600	7429015	28.1	
20165	472070	7428196	13.4	
20152	472600	7427811	16.8	
20170	472889	7427280	106.7	
21518	473227	7427811	9.5	
21606	473709	7426027	14.1	
20196	473661	7426076	22.0	
20184	474383	7425690	4.1	
20200	474191	7425064	33.8	
21520	474383	7424533	0.2	
21615	474601	7424069	3.7	
21527	474457	7423635	8.3	
20143	475131	7422575	41.0	
20145	475565	7422912	4.4	
20171	476336	7420840	17.6	
20146	476963	7418719	22.1	
20147	477734	7418093	10.9	
36795	478167	7418093	3.7	3,560,154
Dorob				
36786	449819	7443939	22.0	
36787	449628	7443713	22.0	
36780	450465	7443747	22.0	
36777	450691	7443468	22.0	
36781	450395	7443434	22.0	964,260

Ehrenwörtliche Erklärung:

Hiermit erkläre ich, dass die Arbeit selbständig und nur unter Verwendung der angegebenen Hilfsmittel angefertigt wurde.

Freiburg, den 11.05.2007

Ingo Heidbüchel